

Composite topological solitons consisting of domain walls, strings, and monopoles in $O(N)$ models

Minoru Eto, ^{a,b} Yu Hamada, ^{b,c} and Muneto Nitta, ^{b,d,e}

^a*Department of Physics, Yamagata University, Kojirakawa-machi 1-4-12, Yamagata, Yamagata 990-8560, Japan*

^b*Research and Education Center for Natural Sciences, Keio University, 4-1-1 Hiyoshi, Yokohama, Kanagawa 223-8521, Japan*

^c*KEK Theory Center, Tsukuba 305-0801, Japan*

^d*Department of Physics, Keio University, 4-1-1 Hiyoshi, Kanagawa 223-8521, Japan*

^e*International Institute for Sustainability with Knotted Chiral Meta Matter(SKCM²), Hiroshima University, 1-3-2 Kagamiyama, Higashi-Hiroshima, Hiroshima 739-8511, Japan*

E-mail: meto@sci.kj.yamagata-u.ac.jp, yuhamada@post.kek.jp, nitta@phys-h.keio.ac.jp

ABSTRACT: We study various composites of global solitons consisting of domain walls, strings, and monopoles in linear $O(N)$ models with $N = 2$ and 3 . Spontaneous symmetry breaking (SSB) of the $O(N)$ symmetry down to $O(N - 1)$ results in the vacuum manifold S^{N-1} , together with a perturbed scalar potential in the presence of a small explicit symmetry breaking (ESB) interaction. The $O(2)$ model is equivalent to the axion model admitting topological global (axion) strings attached by N_{DW} domain walls. We point out for the $N_{\text{DW}} = 2$ case that the topological stability of the string with two domain walls is ensured by sequential SSBs $(\mathbb{Z}_2)^2 \rightarrow \mathbb{Z}_2 \rightarrow 1$, where the first SSB occurs in the vacuum leading to the topological domain wall as a mother soliton, only inside which the second SSB occurs giving rise to a subsequent kink inside the mother wall. From the bulk viewpoint, this kink is identical to a global string as a daughter soliton. This observation can be naturally extended to the $O(3)$ model, where a global monopole as a daughter soliton appears as a kink in a mother string or as a vortex on a mother domain wall, depending on ESB interactions. In the most generic case, the stability of the composite system consisting of the monopole, string, and domain wall is understood by the SSB $(\mathbb{Z}_2)^3 \rightarrow (\mathbb{Z}_2)^2 \rightarrow \mathbb{Z}_2 \rightarrow 1$, in which the first SSB at the vacuum gives rise to the domain wall triggering the second one, so that the daughter string appears as a domain wall inside the mother wall triggering the third SSB, which leads to a granddaughter monopole as a kink inside the daughter vortex. We demonstrate numerical simulations for the dynamical evolution of the composite solitons.

Contents

1	Introduction	1
2	String-wall composites	3
2.1	Linear $O(2)$ model	3
2.2	Topological solitons for $N = 0$	5
2.3	Non-topological string-wall composite for $N = 1$	6
2.4	Topological string-wall composite for $N = 2$	7
2.5	Dynamics of vortex-wall composites	13
3	Monopole-string composites and monopole-wall composites	14
3.1	Linear $O(3)$ model	14
3.2	Topological solitons for $N = 0$	16
3.3	Non-topological monopole-string composite soliton for $N = 1$	17
3.4	Topological monopole-string composite for $N = 2$ with $\alpha > 0$	19
3.5	Topological monopole-wall composite for $N = 2$ with $\alpha < 0$	27
3.6	Relations to spherical monopoles	31
4	Monopole-string-wall composites	31
5	Summary and discussion	37
A	Classifying composite solitons	40
A.1	Classification	40
A.2	Domain-wall vortex composites	41
A.3	Vortex monopole composites	45
A.4	Domain-wall monopoles	47
B	$N = 2$ axion string-wall composite: An effective Lagrangian approach	47

1 Introduction

Topological solitons such as monopoles, vortices and domain walls ubiquitously appear in nature and play crucial roles. Not only in quantum field theories [1–7] including supersymmetric gauge theories [8–12] and quantum chromodynamics(QCD) [13], they also appear in cosmology [14–19] and various condensed matter systems [20]: superfluids [21, 22], Josephson junctions [23], quantum Hall effects [24], ultracold atomic gasses [25], nonlinear media [26, 27], liquid crystals [28–30] and active matter [31].

In particular, composite solitons composed of different topological solitons attract attentions in field theory [32] (see also references therein), cosmology [19], and condensed

matter physics. For instance, domain-wall Skyrmions in QCD [33] and in chiral magnets [34–38] (see also [39]), and composite solitons in ${}^3\text{He}$ superfluids [40, 41]. On the theoretical side, by using the most general composite soliton consisting of kinks, vortices, monopoles and Yang-Mills instantons, all possible relations among topological solitons are exhausted [32]. On the experimental side, domain-wall Skyrmions in chiral magnets are expected to be useful for a racetrack memory. In addition, in cosmology, cosmic strings (vortex strings) attached by domain walls [42, 43], such as axion strings with axion domain walls [19, 44, 45], exhibit non-trivial dynamics driven by the tensions of the strings and domain walls and have been studied for decades.

In this paper, we focus on composite solitons consisting of global monopoles, global vortices and domain walls, motivated by the fact that most of topological solitons in condensed matter physics are in fact global solitons. Monopoles can be attached by vortices, or can be immersed into a domain wall. The former and latter are called vortex monopoles and domain-wall monopoles, respectively. As a lower dimensional analogue, a vortex can be attached by one (two or more) domain wall(s), as axion strings. This can be called domain-wall vortices. All previously known domain-wall vortices, vortex monopoles and domain-wall monopoles are summarized in Appendix A. More specifically, here we study composite solitons in linear $O(N)$ models ($N = 2, 3$) with a spontaneous symmetry breaking (SSB) $O(N) \rightarrow O(N - 1)$ together with small explicit symmetry breaking (ESB) terms that are linear or quadratic with respect to the fields.

In the $O(2)$ model, we consider composites consisting of domain walls and vortices, which are the same as the so-called axion strings attached with the $N_{\text{DW}} = 1$ or 2 domain walls. In the literature, such composites have been understood in terms of an approximate $SO(2)$ and exact $\mathbb{Z}_{N_{\text{DW}}}$ symmetries spontaneously broken into $\mathbb{1}$. We however present another understanding of these composites. Firstly we find that the proper exact SSB at the vacuum is $\mathbb{Z}_2 \times \mathbb{Z}_2 \rightarrow \mathbb{Z}_2$ for $N_{\text{DW}} = 2$. This correct understanding for the SSB leads to a novel picture that the composite soliton is stabilized by two sequent SSBs; $G = \mathbb{Z}_2 \times \mathbb{Z}_2 \rightarrow H = \mathbb{Z}_2$ at the vacuum producing the topological domain wall as a mother soliton, inside which $H = \mathbb{Z}_2$ is spontaneously broken further into $\mathbb{1}$, resulting in production of a subsequent kink in the mother domain wall. This can be regarded as a daughter vortex of the mother domain wall from the bulk perspective. This composite soliton is a global counterpart of an Abrikosov-Nielsen-Olesen (ANO) vortex [46, 47] inside a domain wall [48–52], or local non-Abelian vortex [53–56] realized as non-Abelian sine-Gordon solitons [57, 58] inside a non-Abelian domain wall [59–61].

We also consider global-monopole analogues of vortex monopoles and domain wall monopoles in the linear $O(3)$ model. Depending on the ESB terms and the sign of their coefficients, there can be a global monopole as a daughter soliton attached with one or two strings and a daughter monopole localized on a domain wall. While the monopole attached with one string is not stable, that with two strings is topologically stable, as can be understood by sequential SSBs: $O(2) \times \mathbb{Z}_2 \rightarrow \mathbb{Z}_2 \times \mathbb{Z}_2$ in the vacuum, producing the topological strings, and $\mathbb{Z}_2 \times \mathbb{Z}_2 \rightarrow \mathbb{1}$ inside the strings. This monopole is regarded as a kink connecting the two strings. This composite soliton is a global counterpart of a local monopole (‘t Hooft-Polyakov monopole [62, 63]) attached by two non-Abelian vortex

strings [64–68].

On the other hand, a monopole localized on the wall is associated with $O(2) \times \mathbb{Z}_2 \rightarrow O(2)$ at the vacuum, producing the topological domain wall, and $O(2) \rightarrow \mathbb{Z}_2$ inside the domain wall, which implies that the daughter monopole is a vortex inside the mother domain wall. Again, this composite soliton is a global counterpart of a local (‘t Hooft-Polyakov) monopole immersed into a non-Abelian domain wall [69]. These composite solitons appear only when the subsequent (second-step) SSB takes place inside the mother solitons. We also observe the phase transition between the broken and symmetric phases varying the coefficients of the ESB terms. This phase transition inside the mother solitons can provide interesting phenomena as discussed in Sec. 5.

Furthermore, when the ESB terms in the potential of the $O(3)$ model take more general forms, a composite soliton consisting of the domain wall, vortex string and monopole can exist. This topological stability can be understood by the sequential SSBs of $(\mathbb{Z}_2)^3 \rightarrow (\mathbb{Z}_2)^2$ at the vacuum leading to the domain wall, $(\mathbb{Z}_2)^2 \rightarrow (\mathbb{Z}_2)^1$ inside the wall leading to a wall (daughter string from the bulk perspective) on the mother wall, and $(\mathbb{Z}_2)^1 \rightarrow \mathbb{1}$ inside the daughter wall, leading to a kink inside the daughter vortex. This kink is nothing but a monopole as a granddaughter soliton from the bulk perspective. We also investigate the real-time dynamics of these composite solitons.

This paper is organized as follows. In Sec. 2, we study the topological strings attached with one or two domain walls in the $O(2)$ model. In Sec. 3, we study, in the $O(3)$ model, a global monopole attached with one (or two) string(s), and a monopole localized on a domain wall. In sec. 4, we study the composite soliton consisting of the domain wall, vortex string and monopole. We present the summary and discussion in Sec. 5. In Appendix A, we classify composite solitons and summarize known composite solitons composed of vortices and domain walls, and those composed of monopoles and vortices. In Appendix B, we give a comment on the effective Lagrangian approach.

2 String-wall composites

In this section, we study string-domain wall composites in the linear $O(2)$ model with the small ESB potential term.

2.1 Linear $O(2)$ model

Let us consider an axion model or an $O(2)$ linear sigma model consisting of a two-component real scalar field $\phi = (\phi_1, \phi_2)$ in (2+1) and (3+1) dimensions in this section. The Lagrangian we will study is

$$\mathcal{L}_N = \frac{1}{2}(\partial_\mu \phi)^2 - \frac{\lambda}{4}(\phi^2 - v^2)^2 - \alpha V_N, \quad (2.1)$$

where the ESB potential V_N is given by

$$V_N = (\phi_2)^N \quad (2.2)$$

with $N \leq 4$ for stable vacua. In this work we will focus on $N = 0, 1,$ and 2 . A (global) symmetry G of the model and an unbroken subgroup H in the vacuum depend on N .

$N = 0$ **case:** The symmetries are $G = O(2)$ and $H = \mathbb{Z}_2$. For example, $\begin{pmatrix} 1 & 0 \\ 0 & -1 \end{pmatrix} \in O(2)$ is unbroken for a specific vacuum $\phi = (v, 0)$. Thus, the vacuum manifold is $G/H = S^1$.

$N = 1$ **case:** $O(2)$ is explicitly broken into $G = \mathbb{Z}_2^{(1)}$ which acts only on ϕ_1 as $(\phi_1, \phi_2) \rightarrow (\pm\phi_1, \phi_2)$. We set $\alpha < 0$ without loss of generality. There is a unique vacuum on the positive side of the ϕ_2 axis, as shown in Fig. 1 (b1) and (b2). The symmetry G is not spontaneously broken, so that we have $H = \mathbb{Z}_2^{(1)}$.

$N = 2$ **case:** We have $G = \mathbb{Z}_2^{(1)} \times \mathbb{Z}_2^{(2)}$ where $\mathbb{Z}_2^{(2)}$ acts as $(\phi_1, \phi_2) \rightarrow (\phi_1, \pm\phi_2)$. Again we set $\alpha < 0$. The vacuum manifold consists of two discrete points on the ϕ_2 axis as shown in Fig. 1 (c1) and (c2). Only $\mathbb{Z}_2^{(2)}$ is spontaneously broken, so that we have $H = \mathbb{Z}_2^{(1)}$. The vacuum manifold is $G/H \simeq \mathbb{Z}_2$. These symmetry breaking patterns are summarized in Table. 1. The rows of “single soliton” and “composite soliton” will be discussed in more detail in the following sections.

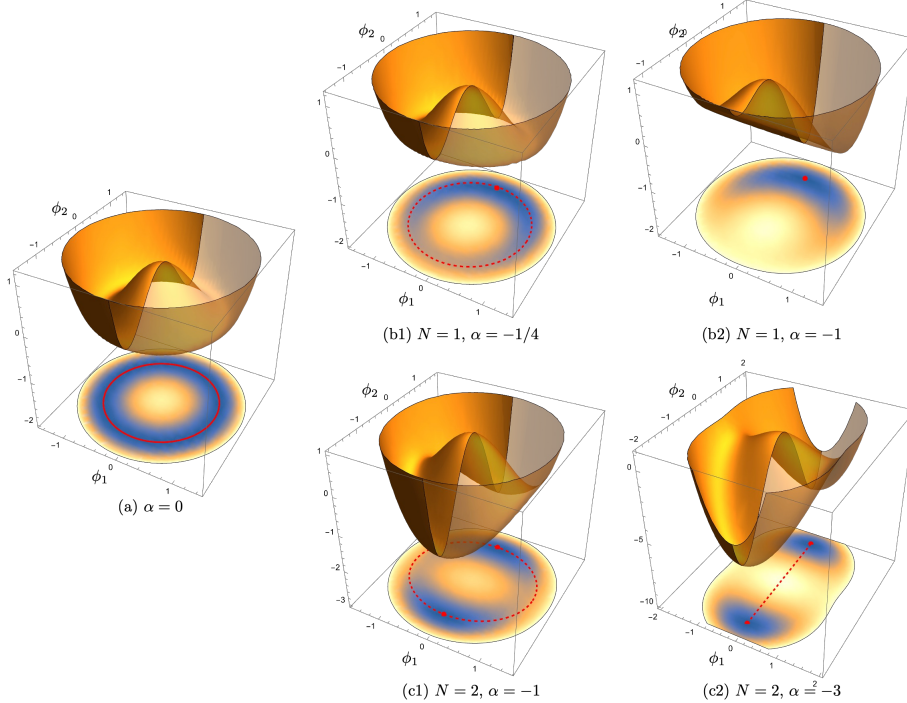


Figure 1: The total scalar potential including V_N as a function of (ϕ_1, ϕ_2) . The parameters are set as $(\lambda, v) = (4, 1)$ for concreteness.

This model (2.1) is identical to the well known axion(-like) model with the “domain wall number” $N_{\text{DW}} = N$,

$$\mathcal{L}^{(\text{axion})} = \frac{1}{2} |\partial_\mu \varphi|^2 - \frac{\lambda}{4} (|\varphi|^2 - v^2)^2 - \frac{2\alpha v^2}{N^2} (\cos N\Theta - 1), \quad (2.3)$$

with a complex scalar $\varphi = v f e^{i\Theta}$. The Lagrangian (2.3) is essentially equivalent to our Lagrangian (2.1) with $V_N = (\phi_2)^N$ (up to some overall and additive constants), as is

	$N = 0$	$N = 1$	$N = 2$
G	$O(2)$	$\mathbb{Z}_2^{(1)}$	$\mathbb{Z}_2^{(1)} \times \mathbb{Z}_2^{(2)}$
H	\mathbb{Z}_2	$\mathbb{Z}_2^{(1)}$	$\mathbb{Z}_2^{(1)}$
vacuum manifold	S^1	1 point	2 points
single soliton	vortex	none	domain wall
composite soliton	none	VW	VW ²

Table 1: Solitons in the linear $O(2)$ model. The description “VW” (“VW²”) represents the composite solitons consisting of one vortex and one (two) domain wall(s).

understood by rewriting $\varphi = \phi_2 + i\phi_1$. If one takes the limit of $\lambda \rightarrow \infty$, the model reduces to a sine-Gordon model with the $2\pi/N$ periodicity for $N \neq 0$ or the XY model for $N = 0$.

In this paper, we are mostly interested in the case that the ESB term is small,

$$\lambda v^4 \gg |\alpha|v^N. \quad (2.4)$$

(Note that the mass dimension of α is $d+1-N(d-1)/2$ in $d+1$ dimensions.) This condition ensures that the structure of the minimum of the potential for $N = 0$ is not significantly deformed by αV_N ($N = 1, 2$). Namely, the potential V_N does not largely affect the original ($N = 0$) vacuum manifold, which consists of continuously degenerated minima forming S^1 , but slightly resolves the continuous degeneracy leaving N points as the true minima. Thus, the original ($N = 0$) vacuum manifold S^1 is still approximately realized as the minimum of the deformed potential, and hence we call this S^1 the quasi-vacuum manifold. This quasi-vacuum manifold is parameterized by a pseudo-Nambu-Goldstone boson appearing as a consequence of the SSB of the approximate symmetry $O(2)$ into \mathbb{Z}_2 .

2.2 Topological solitons for $N = 0$

In the case of $N = 0$, the vacuum manifold is S^1 of the radius v , which is not simply connected. Therefore it gives rise to topological solitons characterized by the fundamental homotopy group $\pi_1(S^1) = \mathbb{Z}$, the so-called global vortices. Since no analytic solutions even for a single winding vortex are available, we need a numerical analysis to obtain the solutions. A suitable ansatz for a static vortex solution that is axially symmetric about the z axis is given by

$$\phi = v f(\rho) \hat{\rho}, \quad (2.5)$$

with $\rho = \sqrt{x^2 + y^2}$, and $\hat{\rho} = (x, y)/\rho$. The equation of motion (EOM) reads

$$\frac{d^2 f}{d\rho^2} + \frac{1}{\rho} \frac{df}{d\rho} - \frac{f}{\rho^2} - \lambda v^2 f (f^2 - 1) = 0. \quad (2.6)$$

The profile function $f(\rho)$ should satisfy the boundary condition

$$f(0) = 0, \quad f(\infty) = 1. \quad (2.7)$$

Fig. 2 shows a numerical solution for $\lambda v^2 = 4$.

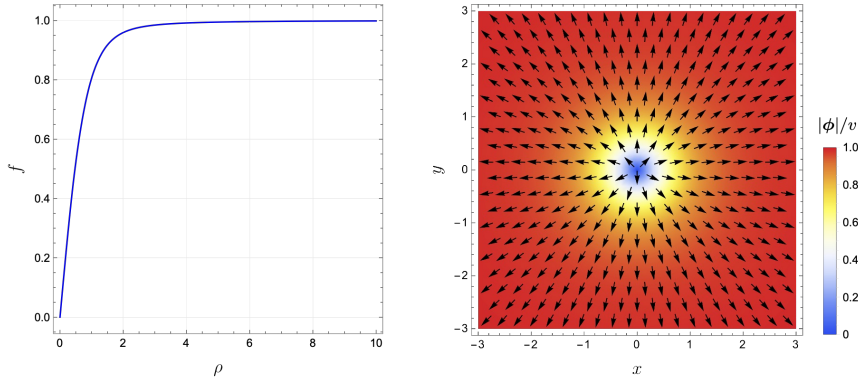


Figure 2: The numerical solution of a global vortex for $v = 1$ and $\lambda = 4$. The left figure shows the amplitude $f(\rho)$. In the right figure the color density corresponds to the amplitude $|\phi|/v$ and the arrows are the vector plot of the normalized field $\hat{\phi}$.

2.3 Non-topological string-wall composite for $N = 1$

Here we briefly explain a vortex-wall composite for $N = 1$. As explained previously, the model has only $\mathbb{Z}_2^{(1)}$ symmetry which is not spontaneously broken. Consequently, there is the unique vacuum. Therefore, there are no topologically stable objects under the presence of V_1 . Nevertheless, if the effect of the additional potential V_1 is sufficiently small, namely the condition (2.4) is satisfied, the quasi-vacuum manifold S^1 shown in Fig. 1(b1) allows solitonic objects, that is global vortices winding the quasi-vacuum manifold S^1 . The soliton looks like a global vortex on one side, but at the same time it also looks like a domain wall on the other side. This is because the S^1 is not the flat bottom of the potential but the sine-Gordon-like potential appears, $V_1 \simeq v \cos \Theta$, where Θ is the phase of $\phi_1 + i\phi_2$. Hence, when one goes around the vortex, one inevitably passes the sine-Gordon-like potential once. This explains that the global vortex is necessarily attached by the domain wall. This kind of “soliton-attached solitons” are called composite solitons in this paper, and the description “VW” in Table. 1 represents the composite soliton consisting of the one vortex and one domain wall.

In order to construct a numerical solution of the vortex-wall composite in two dimensional plane, we set the boundary condition as follows. At an edge of box, say $x = -L$, we set $\Theta(L, y)$ to be an anti-sine-Gordon-like soliton, $\Theta(L, y) \simeq 4 \arctan \exp(-\sqrt{\alpha}y) + \pi/2$ behaving $\Theta(L, y \rightarrow -L) \rightarrow \pi/2$ and $\Theta(L, y \rightarrow L) \rightarrow -3\pi/2$. On the remaining three edges, we set Θ as a constant $\Theta = \pi/2$. A numerical solution obtained by making use of a standard relaxation technique is shown in Fig. 3. The solution is not topologically stable in the sense that it cannot be static since the domain wall continuously pulls the vortex.

The sine-Gordon domain wall can also terminate with an anti-global vortex at the opposite end. The resulting configuration is a sort of confined pair of vortex and anti-vortex connected by the domain wall. A numerical solution is shown in Fig. 4. Again, this is not stable. Because of the domain wall tension, the vortex and anti-vortex are pulled and eventually pair annihilate to decay into the vacuum.

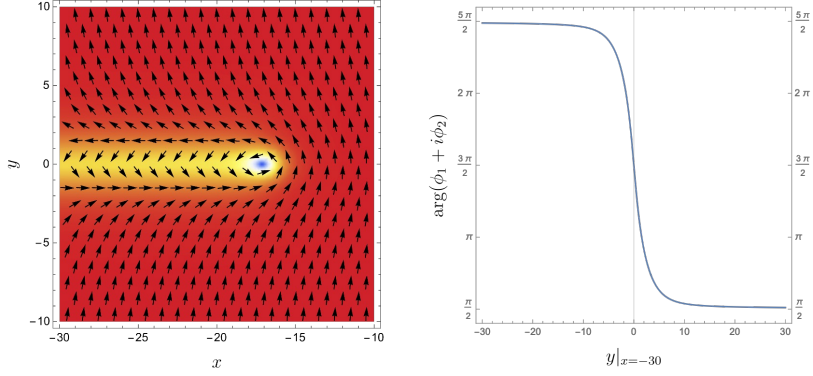


Figure 3: The vortex-wall composite in $N = 1$ model. The color shows the amplitude and the vectors show the phase of ϕ in the left panel. The right panel shows the sine-Gordon-like soliton in the phase $\Theta = \arg(\phi_1 + i\phi_2)$ on the slice $x = -30$.

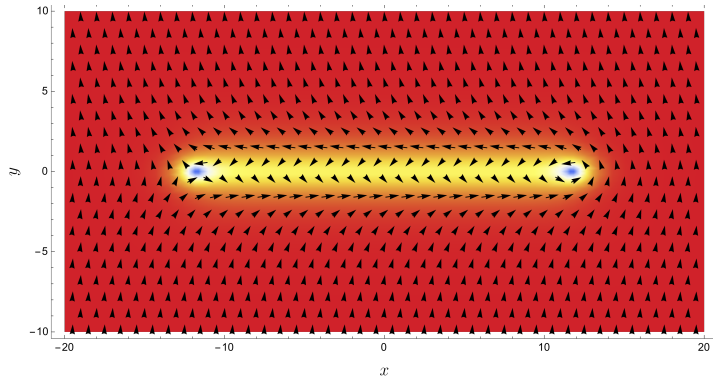


Figure 4: The confined pair of vortex and anti-vortex connected by the sine-Gordon-like domain wall.

2.4 Topological string-wall composite for $N = 2$

As stated above, our model is identical to the axion(-like) model (2.3). However, there is a point that is not fully emphasized in the literature. It is said that in the axion model, a global $U(1)$ symmetry associated with the phase rotation of φ (called the Peccei-Quinn symmetry) is explicitly broken into \mathbb{Z}_N due to the cosine potential, $G = \mathbb{Z}_N : \varphi \rightarrow e^{i2\pi k/N} \varphi$ with $k = 0, 1, \dots, N - 1$. In particular, $G = \mathbb{Z}_2$ for $N = 2$. However, we emphasize that the Lagrangian (2.3) is also invariant under the CP symmetry, $\varphi \rightarrow \varphi^*$, and hence the true symmetry is $G = \mathbb{Z}_2 \times \mathbb{Z}_2^{\text{CP}}$, where the action of the former \mathbb{Z}_2 is equivalent to $\mathbb{Z}_2^{(1+2)} : (\phi_1, \phi_2) \rightarrow -(\phi_1, \phi_2)$ in our model while the latter \mathbb{Z}_2^{CP} acts as $\mathbb{Z}_2^{(1)}$. Hence, the genuine symmetry is $\mathbb{Z}_2^{(1)} \times \mathbb{Z}_2^{(2)}$ instead of $\mathbb{Z}_2^{(1+2)}$. The presence of two \mathbb{Z}_2 's is crucial for the arguments below.

2.4.1 Topological domain wall with $\mathbb{Z}_2^{(2)}$ charge

We first explain topological domain walls in the case of $N = 2$. As is shown in Table 1, the $\mathbb{Z}_2^{(2)}$ symmetry is spontaneously broken, and it gives rise to topologically stable domain walls. Note that there are two phases for the domain walls corresponding to whether or not the $\mathbb{Z}_2^{(1)}$ symmetry is further broken *inside the walls*. If the condition (2.4) is satisfied, the S^1 structure remains as the quasi vacuum manifold as indicated by the red-dashed curve in Fig. 1 (c1). Therefore, for the field configuration connecting $(0, v)$ and $(0, -v)$, the straight path in the field space is shorter but energetically higher than detours around the potential barrier at $|\phi| = 0$. The field configuration tends to lie along the low-lying S^1 locus. Now, there are two possibilities, the field configuration goes around either clockwise or counterclockwise. These can be distinguished by whether ϕ_1 takes positive or negative value on the way. In other words, ϕ_1 positively or negatively condenses near the core of the domain wall. Namely, the $\mathbb{Z}_2^{(1)}$ symmetry is spontaneously broken near the domain wall core, which is schematically expressed as

$$\mathbb{Z}_2^{(1)} \times \mathbb{Z}_2^{(2)} \xrightarrow{\text{vac}} \mathbb{Z}_2^{(1)} \xrightarrow{\text{wall}} 1. \quad (2.8)$$

The SSB at the vacuum corresponds to the first SSB indicated by the solid-line arrow. It gives rise to the domain wall, inside which the second SSB indicated by the dashed-line arrow takes place. Hence, the domain wall has the $\mathbb{Z}_2^{(1)}$ charge (or the $\mathbb{Z}_2^{(1)}$ modulus like Ising spin). One should carefully distinguish the solid and dashed arrows.

The topological nature of the domain wall is associated with the first SSB,

$$\pi_0 \left((\mathbb{Z}_2^{(1)} \times \mathbb{Z}_2^{(2)}) / \mathbb{Z}_2^{(1)} \right) \simeq \mathbb{Z}_2 \neq 1. \quad (2.9)$$

We show numerical solutions for the topological domain wall perpendicular to the x axis in Fig. 5. The panel (a) shows the scalar fields $\phi_{1,2}$ as the function of x , and (c) shows the corresponding parametric plot in the field space. The orbits are half ovals reflecting the small deformation by αV_2 . The panels (d) and (e) show $|\phi|/v_{\text{max}}$ and the phase of $\phi_2 + i\phi_1$ in the xy plane. While the genuine topological charge is associated with the spontaneously broken $\mathbb{Z}_2^{(2)}$, the domain walls can also be characterized by a quasi-topological quantity, the winding number of the low-lying S^1 (oval) locus. Clearly, this winding number is quantized in a half integer in comparison with the topological global vortices for $N = 0$.

There is another type of domain wall, when the additional potential V_2 has such a large coupling constant $|\alpha|$ as the condition (2.4) is not met. Since the original S^1 structure completely disappears, the field configuration corresponding to the domain wall forms an orbit in the $\phi_1\phi_2$ plane as a straight segment connecting $(0, \pm\tilde{v})$, the red-dashed line in Fig. 1(c2). For this domain wall, ϕ_1 is kept to be zero everywhere, so that the $\mathbb{Z}_2^{(1)}$ symmetry is unbroken everywhere. As a result, there is only a unique domain wall without the $\mathbb{Z}_2^{(1)}$ charge, which means that it is neutral under the $\mathbb{Z}_2^{(1)}$ symmetry. The relevant symmetry breaking in this case is

$$\mathbb{Z}_2^{(1)} \times \mathbb{Z}_2^{(2)} \xrightarrow{\text{vac}} \mathbb{Z}_2^{(1)}. \quad (2.10)$$

The numerical solution is shown in Fig. 5(b) and (f).

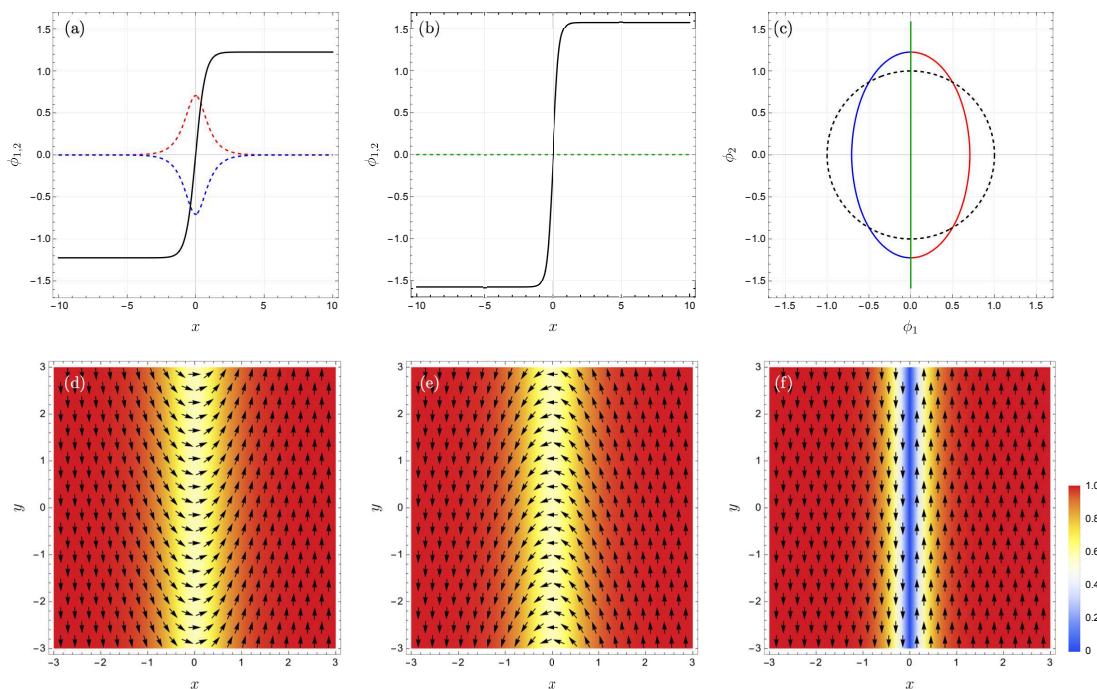


Figure 5: The topological domain wall solutions in the case with $N = 2$ in the linear $O(2)$ model. The parameter combinations are chosen as $(\lambda, v) = (4, 1)$. (a): The $\mathbb{Z}_2^{(1)}$ charged domain wall solutions for $\alpha = -1$. The black curve stands for $\phi_2(x)$, and the dashed curves show $\phi_1(x)$. The color (red and blue) of the dashed curves indicates the $\mathbb{Z}_2^{(1)}$ charge. (b): The $\mathbb{Z}_2^{(1)}$ neutral domain wall for $\alpha = -3$. ϕ_2 is the black curve and the green-dashed line stands for $\phi_1 = 0$. (c): The orbits corresponding to the solutions in (a) and (b) expressed in the $\phi_1\phi_2$ plane. (d), (e), and (f) show the vector plot of ϕ and the density plot of $|\phi|/v_{\max}$ in the xy plane for the domain wall solutions of (a) with the blue-dashed, red-dashed, and (b), respectively (v_{\max} is the maximum value of $|\phi|$).

The transition between the $\mathbb{Z}_2^{(1)}$ neutral domain wall and charged one is shown in Fig. 6. We plot the value of ϕ_1 at the center of domain wall ($x = 0$) which is an order parameter for the $\mathbb{Z}_2^{(1)}$ symmetry as a function of α while the other parameters are fixed as $(\lambda, v) = (4, 1)$. The domain wall is neutral if $\phi_1(0) = 0$ while charged if $\phi_1(0) \neq 0$.

2.4.2 Topological wall-string composite: a kink in a domain wall

Let us next consider composite solitons for the small α satisfying the condition (2.4). Hereafter, we will refer the $\mathbb{Z}_2^{(1)}$ -charged domain wall associated with the spontaneously broken $\mathbb{Z}_2^{(2)}$ to the mother domain wall. The composite soliton we are going to study consists of the global vortex attached by the two domain walls.

When the $\mathbb{Z}_2^{(2)}$ symmetry is spontaneously broken in the vacuum, it gives rise to the

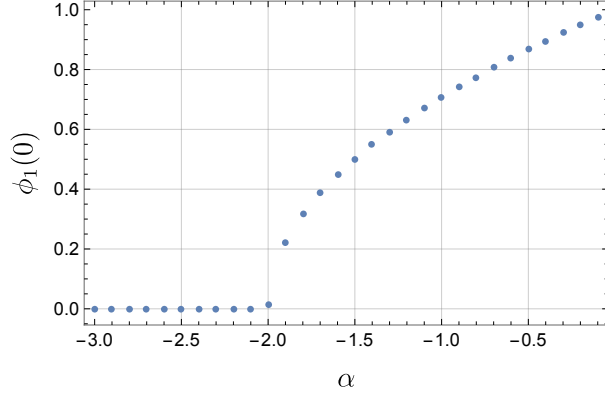


Figure 6: The transition of the $\mathbb{Z}_2^{(1)}$ neutral and charged domain wall for the case of $N = 2$. The domain wall is $\mathbb{Z}_2^{(1)}$ charged for $\phi_1(0) \neq 0$ while is neutral for $\phi_1(0) = 0$. The parameters are taken as $(\lambda, v) = (4, 1)$.

mother domain walls in the vacuum. Similarly, when the $\mathbb{Z}_2^{(1)}$ symmetry is spontaneously broken in the mother domain wall, it gives rise to a kink inside the mother domain wall. Namely, this kink connects two domain walls with different $\mathbb{Z}_2^{(1)}$ charges. Below we will identify this kink as a global vortex from the bulk point of view, which we call a daughter vortex.

A concrete field configuration which illustrates the above properties is realized by a product ansatz

$$\phi = v \begin{pmatrix} \tanh \alpha y \cos \Theta(x) \\ \gamma \sin \Theta(x) \end{pmatrix}, \quad \Theta(x) = 2 \arctan e^{-\beta x} + \frac{\pi}{2}, \quad (2.11)$$

with α, β and γ are constants. Θ is the sine-Gordon soliton with a half period which embodies the mother domain wall, and $\tanh \alpha y$ corresponds to the inner kink (daughter vortex). In Appendix B we derive this ansatz by making use of an effective theory approach. Indeed, taking $y \gg 0$ or $y \ll 0$, (i.e., far from the inner kink,) it reduces to the half-sine Gordon soliton going around the left or right half of the quasi-vacuum manifold S^1 as

$$\phi|_{y \gg 0} = v \begin{pmatrix} \cos \Theta(x) \\ \gamma \sin \Theta(x) \end{pmatrix}, \quad \phi|_{y \ll 0} = v \begin{pmatrix} -\cos \Theta(x) \\ \gamma \sin \Theta(x) \end{pmatrix}. \quad (2.12)$$

On the mother domain wall at $x = 0$, we have $\Theta = \pi$ and the configuration reduces to

$$\phi|_{x=0} = v \begin{pmatrix} -\tanh \alpha y \\ 0 \end{pmatrix}. \quad (2.13)$$

This exhibits the inner kink at which the ϕ_1 condensation flips its sign.

The product ansatz (2.11) is also useful for constructing a numerical solution by a relaxation method. We can adopt it as an initial configuration, and it quickly converges. Fig. 7 shows numerical solutions. Clearly, these are made by joining the two \mathbb{Z}_2 charged

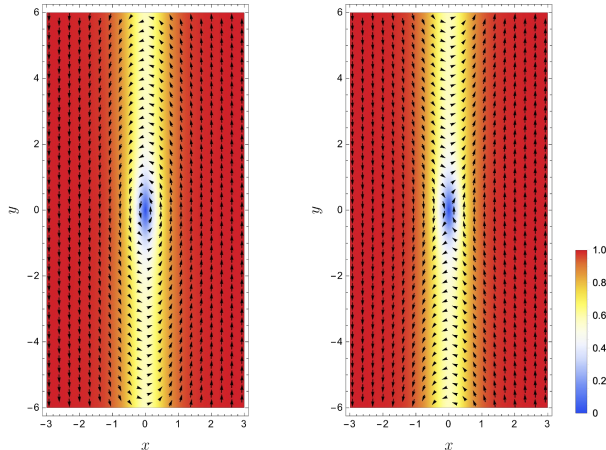


Figure 7: Topological vortex-wall composites in the $N = 2$ model. The upper part of the mother wall in the left (right) panel has a negative (positive) ϕ_1 condensation whereas that for the lower part is opposite. Hence, the inner kinks correspond to the vortex and the anti-vortex on the left and right panels, respectively.

domain walls given in the panels (d) and (e) of Fig. 5. The junction point, corresponding to the guest domain wall, can also be seen as the global vortex. Indeed, one observes that the black arrow counterclockwise (clockwise) rotates once as we counterclockwise go around the boundary of the left (right) panel of Fig. 7. The phase $\Theta = \arg(\phi_1 + i\phi_2)$ rotates by π only on the upper and lower edges while it is constant at the left and right edges. In total, the phase rotate by 2π . Moreover, $|\phi|$ vanishes at the junction point, which is necessary to avoid a singularity.

The topological origin of the composite system can be understood in the following way. Firstly, we quickly review the conventional way given by Preskil-Vilenkin's work [70]. For $\alpha = 0$, the model has a symmetry $SO(2)$, which spontaneously breaks due to the VEV of ϕ . This symmetry breaking gives rise to the global vortex associated with the first homotopy group $\pi_1(S^1) \simeq \mathbb{Z}$. Switching on $\alpha \neq 0$ with small $|\alpha|$, the original $SO(2)$ symmetry is only an approximate symmetry and the exact symmetry is \mathbb{Z}_2 . It is spontaneously spontaneously broken, leading to the non-trivial zeroth homotopy group of the vacuum manifold and hence the topological domain wall. In Ref. [70], this is expressed schematically as follows:

$$\begin{array}{ccc}
 G_{\text{approx}} = SO(2) & \rightarrow & 1 \\
 \cup & & \cup \\
 G_{\text{exact}} = \mathbb{Z}_2 & \rightarrow & 1
 \end{array} \tag{2.14}$$

The approximate SSB in the top row implies the global vortex while the exact SSB in the bottom row ensures the topological domain walls.

We can improve this sequence by correcting the symmetries, leading to another interpretation of the composite system: a wall in a wall. As stated above, the SSB of $\mathbb{Z}_2^{(2)}$ in the vacuum gives rise to the host domain walls in the vacuum. In the host domain walls, the

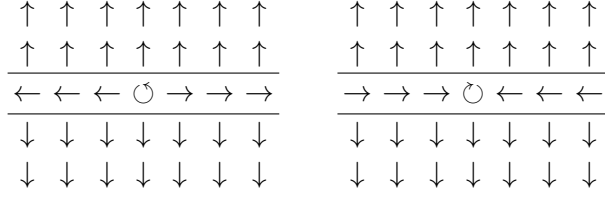


Figure 8: Schematic pictures of the composite solitons of a domain wall and vortices. The small arrows represent configurations of ϕ . The horizontal lines denote a domain wall. The left (right) represent a (anti-)kink which is regarded as a (anti)vortex.

$\mathbb{Z}_2^{(1)}$ symmetry is spontaneously broken, leading to the guest domain wall inside the host. Therefore, the topological stability of the composite soliton owes the SSBs summarized as follows:

$$\begin{array}{ccc}
G_{\text{approx}} = O(2) & \xrightarrow[\text{vortex}]{\text{vac}} & \mathbb{Z}_2 \\
\cup & & \cup \\
G_{\text{exact}} = \mathbb{Z}_2^{(1)} \times \mathbb{Z}_2^{(2)} & \xrightarrow[\text{mother wall}]{\text{vac}} & \mathbb{Z}_2^{(1)} \xrightarrow[\text{kink}]{\text{mother wall}} 1. \quad (2.15)
\end{array}$$

The words above the arrows correspond to the triggers of the SSBs, and those below to the topological solitons generated by the corresponding SSBs. It endows the genuine topologically nontrivial property to the composite solitons. This is a clear distinction of the topological composite soliton for $N = 2$ from the non-topological composite soliton for $N = 1$.

We here give an intuitive explanation which can connect the original global vortex for the $O(2)$ symmetry and the string-wall composite for the $\mathbb{Z}_2^{(1)} \times \mathbb{Z}_2^{(2)}$. The $SO(2)$ symmetry rotates a two dimensional arrow “ \rightarrow ” which corresponds to a vector $\phi = (\phi_1, \phi_2)$ in the field space. For example, when we go around the string, the arrow spins along the path as $\rightarrow \nearrow \uparrow \nwarrow \leftarrow \swarrow \downarrow \searrow \rightarrow$. How many times the arrow rotates is counted by $\pi_1[SO(2)] \simeq \mathbb{Z}$. On the other hand, the $\mathbb{Z}_2^{(2)}$ symmetry flips \uparrow into \downarrow and *vice versa*, and it gives rise to the mother domain wall. Inside the mother domain wall, the arrow points either \leftarrow or \rightarrow associated with the $\mathbb{Z}_2^{(1)}$ charge. Thus, when the inner kink is generated, the distribution of the arrows on the xy plane is either of those depicted in Fig. 8. When we go around the boundary counterclockwise, the arrows rotates counterclockwise on the left figure and clockwise on the right figure. This clearly explains that the string-wall composite with respect to $\mathbb{Z}_2^{(1)} \times \mathbb{Z}_2^{(2)}$ has the non-trivial topology and is homotopic to the genuine $SO(2)$ global vortex characterized by $\pi_1[SO(2)]$.

A local-soliton counterpart of this composite soliton is an ANO vortex inside a domain wall [48, 49, 51] in which the ESB was introduced for a global symmetry. A texture version is a domain-wall Skyrmions in 2+1 dimensions [49, 50] (see also [71–75]) and also those in chiral magnets [34–38] (see also [39]).

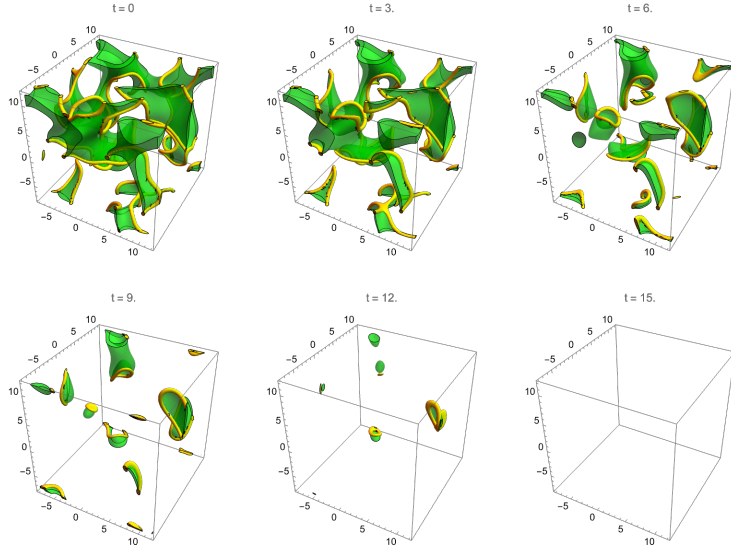


Figure 9: A numerical evolution of $N = 1$ vortex-wall composites.

2.5 Dynamics of vortex-wall composites

We numerically investigate dynamics of both the $N = 1$ non-topological composite solitons and the $N = 2$ topological composite solitons in $(3+1)$ dimensions. In this dimensionality, vortices are string and domain walls are sheets. A domain-wall sheet can stretch inside a closed string. See, e.g., Ref. [76] for three-dimensional configurations of a domain-wall disk bounded by a circular vortex loop. We firstly show a dynamical evolution of a randomly chosen initial configuration ($t = 0$) in the model of $N = 1$ in Fig. 9. The global strings (yellow) are attached by single green domain walls. The composite decays quite fast in comparison with the $N = 2$ case shown below.

Next, we show time evolution with a randomly chosen initial configuration ($t = 0$) in the $N = 2$ model in Fig. 10. The global strings (the guest domain walls corresponding the yellow objects) are attached by a pair of green and orange host domain walls. The topological composite solitons are quite long-lived in comparison with the non-topological one.

In cosmological contexts, long-lived domain walls should be ruled out because they are inconsistent with cosmological and astrophysical observations. Hence, the $N = 2$ model would have the domain wall problem whereas the $N = 1$ case would be safe, as is well known in the context of the axion strings and domain walls.

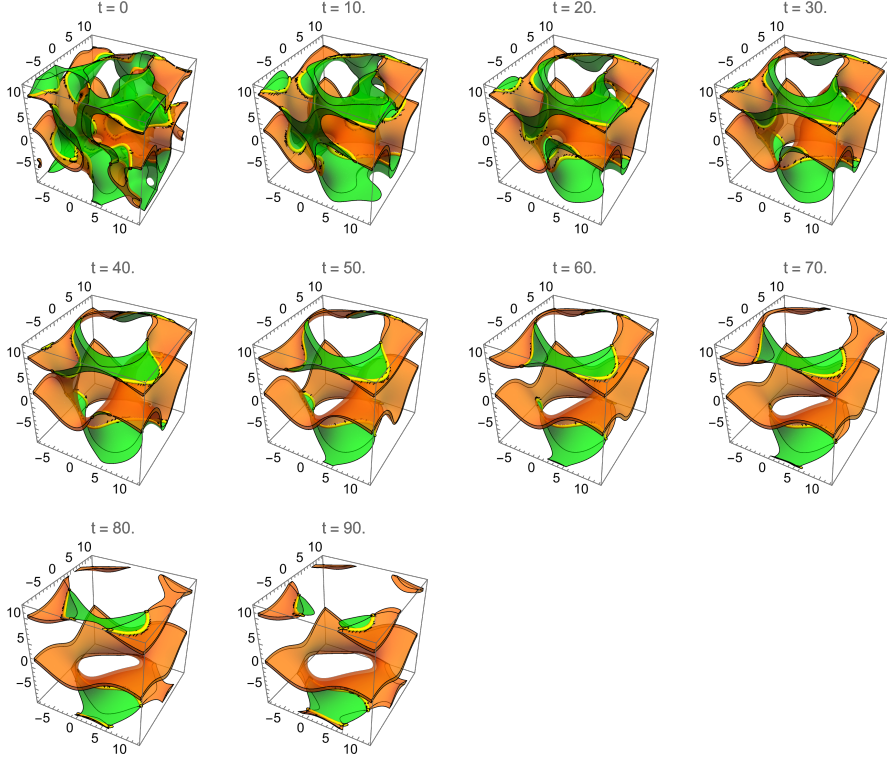


Figure 10: A numerical evolution of $N = 2$ vortex-wall composites.

3 Monopole-string composites and monopole-wall composites

3.1 Linear $O(3)$ model

In this section, we are going to investigate composite solitons in the model with a three-component scalar field $\phi = (\phi_1, \phi_2, \phi_3)$ in $(3+1)$ dimensions. We will study the Lagrangian

$$\mathcal{L} = \frac{1}{2}(\partial_\mu \phi)^2 - \frac{\lambda}{4}(\phi^2 - v^2)^2 - \alpha V_N, \quad (3.1)$$

where V_N is an ESB term given by

$$V_N = (\phi_3)^N. \quad (3.2)$$

This Lagrangian has a similar form to the one given in Eq. (2.1). In the limit of $\lambda \rightarrow \infty$, the model reduces to the $O(3)$ nonlinear sigma model.

As before, we will study $N = 0, 1, 2$. The symmetry G of the Lagrangian and H of the vacua depend on N .

The $N = 0$ case: The symmetries are $G = O(3)$ and $H = O(2)$, which leads to the vacuum manifold $G/H \simeq S^2$;

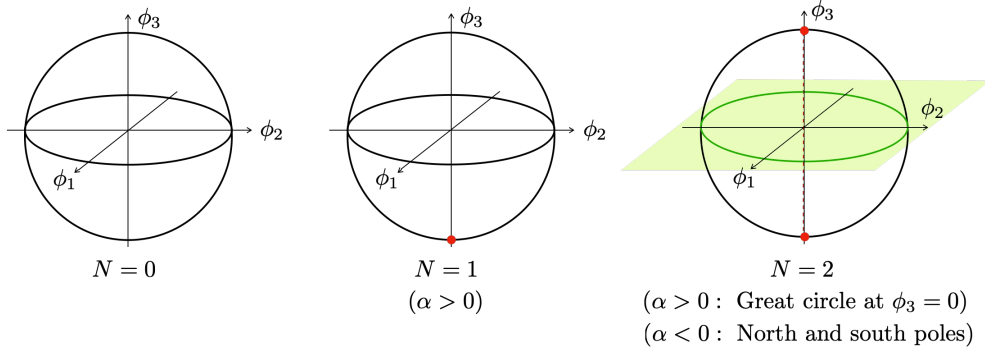


Figure 11: The vacua of the three-component model.

	$N = 0$	$N = 1$	$N = 2$	
G	$O(3)$	$O(2)^{(12)}$	$O(2)^{(12)} \times \mathbb{Z}_2^{(3)}$	
H	$O(2)$	$O(2)^{(12)}$	$\alpha > 0$ $\mathbb{Z}_2^{(12)} \times \mathbb{Z}_2^{(3)}$	$\alpha < 0$ $O(2)^{(12)}$
Vacuum manifold	S^2	1 point	S^1	2 points
Single soliton	monopole	none	vortex	domain wall
Composite soliton	none	MS	MS ²	WM

Table 2: The patterns of the symmetry breaking and possible solitons in the linear $O(3)$ models. The composite solitons “MS” and “MS²” indicate a global monopole attached by one and two strings, respectively, while “MW” indicates a monopole localized on a domain wall.

The $N = 1$ case: We have $G = O(2)^{(12)}$ which acts on the first two components of (ϕ_1, ϕ_2, ϕ_3) . We set, without loss of generality, $\alpha > 0$. There is a unique vacuum on the negative side of the ϕ_3 axis, as shown in the middle panel of Fig. 11. The symmetry G is unbroken in the vacuum, leading to $H = O(2)^{(12)}$.

The $N = 2$ case: We have $G = O(2)^{(12)} \times \mathbb{Z}_2^{(3)}$ where $\mathbb{Z}_2^{(3)}$ acts as $\phi_3 \rightarrow -\phi_3$ while $\phi_{1,2}$ is not changed. The vacuum manifold and the unbroken subgroup H depend on the sign of α as shown in the rightmost panel in Fig. 11. For $\alpha > 0$, the vacuum manifold is a great circle with $\phi_3 = 0$ (called the easy-plane potential), and $H = \mathbb{Z}_2^{(12)} \times \mathbb{Z}_2^{(3)}$. On the other hand, for $\alpha < 0$, the vacuum manifold consists of two discrete points on the ϕ_3 axis (called the easy-axis potential) and we have $H = O(2)^{(12)}$. These are summarized in Table. 2.

Again, we assume that the ESB potential V_N in (2.4) is small. Thus, the vacuum manifold S^2 in the case of $N = 0$ is not largely deformed even for $N = 1, 2$ but is approximately realized as the quasi-vacuum manifold.

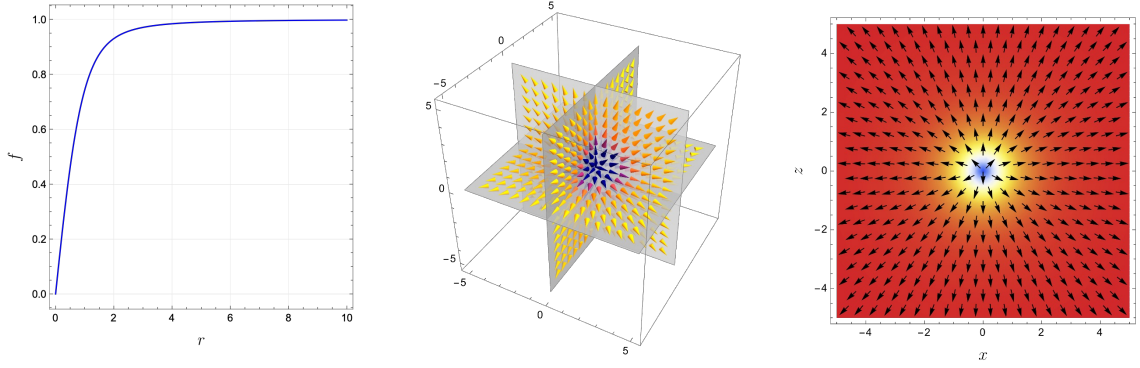


Figure 12: The numerical solution of a spherical global monopole for $(\lambda, v) = (4, 1)$. In the middle and right panels, the arrows and the colors indicate the vector plot for ϕ and the amplitude $|\phi|/v = f(r)$, respectively.

3.2 Topological solitons for $N = 0$

Let us begin with the simplest case of $N = 0$ where the vacuum manifold is $SO(3)/SO(2) \simeq S^2$. The nontrivial second homotopy group $\pi_2(S^2) \simeq \mathbb{Z}$ ensures the existence of the global monopoles. Similarly to the global vortices, no analytic solutions even for a single winding monopole have been obtained, so that we need a numerical analysis to have a concrete solution. The hedgehog ansatz for an radially symmetric monopole solution is given by

$$\phi = v f(r) \hat{r}, \quad (3.3)$$

with $r = \sqrt{x^2 + y^2 + z^2}$, and $\hat{r} = (x, y, z)/r$. The EOM for $f(r)$ reads

$$\frac{d^2 f}{dr^2} + \frac{2}{r} \frac{df}{dr} - \frac{2f}{r^2} - \lambda v^2 f (f^2 - 1) = 0. \quad (3.4)$$

The amplitude $f(r)$ should satisfy the boundary condition

$$f(0) = 0, \quad f(\infty) = 1. \quad (3.5)$$

We show a typical numerical solution in Fig. 12.

For later convenience, let us introduce the monopole charge density by

$$\mathcal{M}_0 = \frac{1}{3!} \epsilon_{ijk} \epsilon_{abc} \partial_i \phi_a \partial_j \phi_b \partial_k \phi_c, \quad (i, j, k = 1, 2, 3; a, b, c = 1, 2, 3). \quad (3.6)$$

We will use this to detect the monopoles in the subsequent sections. The topological charge of monopole is then given by

$$M = \int d^3x \mathcal{M}_0 = \frac{4\pi v^3}{3} n, \quad (3.7)$$

with $n \in \pi_2(S^2) \simeq \mathbb{Z}$.

3.3 Non-topological monopole-string composite soliton for $N = 1$

We next study the $N = 1$ case with $\alpha > 0$. The global minimum of the potential reads $\phi = (0, 0, -\tilde{v})$, where $\tilde{v} (> 0)$ is the solution of $\lambda\tilde{v}(\tilde{v}^2 - v^2) = \alpha$. The vacuum corresponds to the south pole of the quasi vacuum manifold S^2 , see Fig. 11 (middle). The exact symmetry $G = O(2)^{(12)}$ of the Lagrangian is not spontaneously broken and the above vacuum is topologically trivial. Therefore, there is no stable topological soliton. However, when the smallness condition (2.4) is satisfied, the S^2 structure remains as the quasi vacuum manifold as mentioned. Then, there exist quasi-topological composite solitons which winds the quasi vacuum manifold S^2 .

We construct a numerical solution in a box of the size $(2L)^3$. We should set $\phi = (0, 0, -\tilde{v})$ on the five faces of the numerical box. On the remaining boundary, say the top face at $z = L$, we should set $\phi(x, y, L)$ to be an $O(3)$ lump-like configuration,

$$\phi|_{z=L} = v \left(\frac{a(x + iy) + a^*(x - iy)}{\rho^2 + |a|^2}, \frac{a(x + iy) - a^*(x - iy)}{i(\rho^2 + |a|^2)}, \gamma \frac{|a|^2 - x^2 - y^2}{\rho^2 + |a|^2} \right), \quad (3.8)$$

with a and γ are constants. This satisfies the algebraic equation for an ellipsoid $(\phi_1)^2 + (\phi_2)^2 + \gamma^{-2}(\phi_3)^2 = v^2$. It is, however, not easy to prepare a suitable initial configuration for the standard relaxation scheme. Therefore, we adopt the spherical hedgehog configuration as the initial configuration and evolve it with the Neumann boundary condition by the relaxation scheme. The result is shown in Fig. 13. The monopole can easily be detected by drawing the charge density \mathcal{M}_0 . It is largely deformed to be a droplet shape and attached by a single string on the upper side. We emphasize that the string is not similar to a global vortex but to a $O(3)$ sigma model lump. Indeed, on the plane normal to the sting, ϕ points down at the boundary of the plane whereas it points up at the center of the string, see the right-upper panel of Fig. 13. This is of course not stable since the string pulls the monopole.

The string can also be terminated by anti-monopole. We show a pair of monopole and anti-monopole connected by the string, a dumbbell, in Fig. 14. Again, this is not stable. The monopole and anti-monopole are pulled by the string and eventually annihilate in pair. This configuration is called a toron in condensed matter physics [30].

3.3.1 Dynamical simulations for monopole-string composites for $N = 1$

We numerically simulate the real time dynamics of the monopole-string composites in the $N = 1$ case. We prepare random and periodic configurations as initial configurations for the real time dynamics (we smear the random configuration a little by using the relaxation scheme). The field ϕ evolves from the initial configurations with zero velocity $\dot{\phi}(t = 0) = \mathbf{0}$. We impose the periodic boundary conditions in the x , y , and z directions. Therefore, the numbers of the monopoles and anti-monopoles in the initial states are precisely identical.

A typical evolution of the $N = 1$ non-topological monopole-string composites is shown in Fig. 15. The top-leftmost panel shows the initial state which is quite cluttered with many monopoles (red lumps) and anti-monopoles (blue lumps). The strings correspond to the yellow objects but they are not initially so stringy. As soon as the time evolves, however,

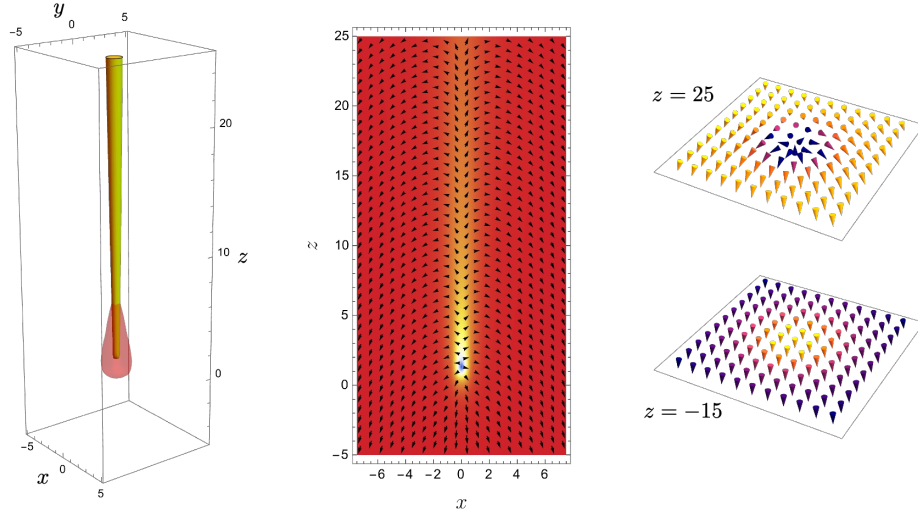


Figure 13: A numerical solution of the non-topological string-monopole composite soliton for $(v, \lambda, \alpha) = (1, 4, 1/4)$. (left) The red surface shows the isosurface of monopole charge density $\mathcal{M}_0 = 1/18$ and the yellow surface shows the isosurface of $|\phi_1 + i\phi_2| = 1/2$. (middle) The vector plot of ϕ at $y = 0$. (right) The vector plots of ϕ at $z = 25$ and $z = -15$ for $x \in [-15, 15]$ and $y \in [-15, 15]$.

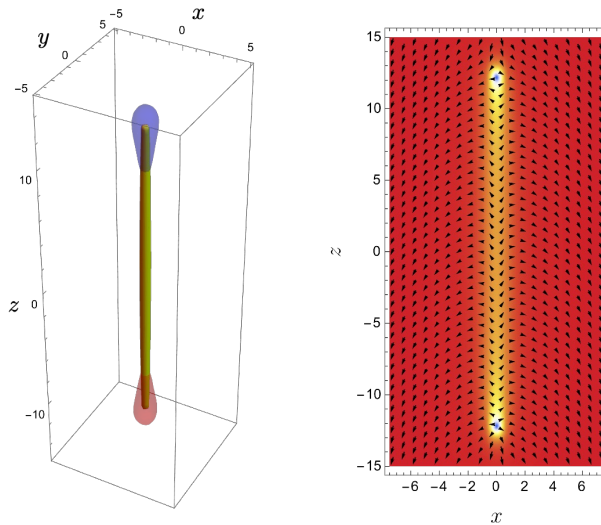


Figure 14: The non-topological antimonopole-string-monopole composite soliton for $(v, \lambda, \alpha) = (1, 4, 1/4)$.

the yellow objects transform into the stringy stuffs connecting one (red) monopole and one (blue) anti-monopoles. The pairs of monopole and anti-monopole with the string annihilate very fast, and soon disappear from the numerical box. The cosmological monopole problem

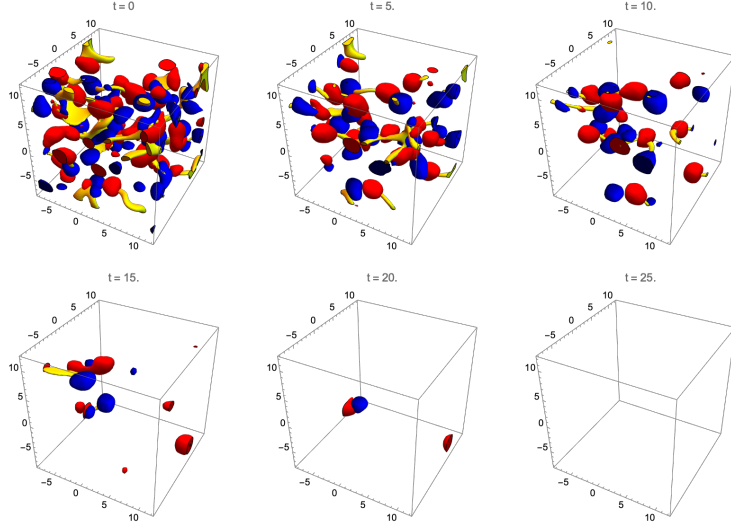


Figure 15: A real time dynamics of the $N = 1$ non-topological monopole-string composites for $(v, \lambda, \alpha) = (1, 4, 1/4)$. The red (blue) surface shows the isosurface of the monopole charge density $\mathcal{M}_0 = 1/24$ ($-1/24$), representing (anti-)monopoles. The yellow surface shows the isosurface of $|\phi_1 + i\phi_2| = 1/2$, representing non-topological strings. The initial configuration is shown in the top-leftmost panel, and we show the five snapshots at every $\delta t = 5$ time with the unit v .

does not exist in this case.

3.4 Topological monopole-string composite for $N = 2$ with $\alpha > 0$

In this subsection, we study the $N = 2$ cases with $\alpha > 0$.

3.4.1 Topological string with $\mathbb{Z}_2^{(3)}$ charge

We first focus on topological strings in the $N = 2$ case with $\alpha > 0$ (the easy-plane potential). The vacuum manifold is S^1 of the radius v in the $\phi_1\phi_2$ plane which corresponds to the equator of the unperturbed S^2 with $\alpha = 0$, see Fig. 11 (right panel with $\alpha > 0$). As is summarized in Table 2, the exact symmetry of the Lagrangian $G = O(2)^{(12)} \times \mathbb{Z}_2^{(3)}$ is spontaneously broken to $H = \mathbb{Z}_2^{(12)} \times \mathbb{Z}_2^{(3)}$. Therefore, it gives rise to a sort of global strings characterized by $\pi_1(G/H) = \pi_1(SO(2)^{(12)}) = \mathbb{Z}$.

Let us consider a straight global string extending along the z axis. Namely, we impose $\partial_0\phi_{1,2,3} = \partial_3\phi_{1,2,3} = 0$ and set the following boundary condition

$$\phi_1 + i\phi_2 \rightarrow ve^{i\theta}, \quad \phi_3 \rightarrow 0, \quad \text{as } \rho \rightarrow \infty, \quad (3.9)$$

which describes a map with the winding number unity from a loop on the xy plane, $\theta \in [0, 2\pi)$, to a loop in the field internal space, $\arg(\phi_1 + i\phi_2) \in [0, 2\pi)$. On the other hand, as approaching the origin of the xy plane, $\rho = 0$, the loop in the field space must be contracted for regularity, i.e., $\phi_1 = \phi_2 = 0$. Since the S^2 structure remains as the quasi

vacuum manifold of the potential due to the small coupling condition (2.4), ϕ energetically prefers to leave off from the $\phi_3 = 0$ plane at $\rho = 0$, resulting in that the contraction can take place at two points: the north pole ($\phi_3 > 0$) or the south pole ($\phi_3 < 0$) of S^2 . For the former (latter) case, as ρ varying from $\rho \rightarrow \infty$ to $\rho = 0$, the loop in the internal space sweeps the upper (lower) hemisphere of the quasi vacuum manifold S^2 . In other words, the third component ϕ_3 positively or negatively condenses inside the global string. Consequently, the $\mathbb{Z}_2^{(3)}$ symmetry which is unbroken in the vacuum is spontaneously broken by the global string as

$$O(2)^{(12)} \times \mathbb{Z}_2^{(3)} \xrightarrow{\text{vac}} \mathbb{Z}_2^{(12)} \times \mathbb{Z}_2^{(3)} \xrightarrow{\text{string}} 1. \quad (3.10)$$

Hence, the topological string in the weak coupling regime has the $\mathbb{Z}_2^{(3)}$ charge.

On the contrary, in a regime where $|\alpha|$ is so large that the condition (2.4) is not satisfied, the S^2 structure completely disappears in the scalar potential. Then the contraction of the loop can occur without leaving the $\phi_3 = 0$ plane. Therefore, $\mathbb{Z}_2^{(3)}$ is unbroken and the global string with large $|\alpha|$ is neutral under the $\mathbb{Z}_2^{(3)}$ transformation.

Let us make an appropriate ansatz for the axially symmetric string with the minimal winding number

$$\phi_1 + i\phi_2 = vf(\rho)e^{i\theta}, \quad \phi_3 = vg(\rho). \quad (3.11)$$

Then, the EOMs read

$$\frac{d^2 f}{d\rho^2} + \frac{1}{\rho} \frac{df}{d\rho} - \frac{f}{\rho^2} - \lambda v^2 f(f^2 + g^2 - 1) = 0, \quad (3.12)$$

$$\frac{d^2 g}{d\rho^2} + \frac{1}{\rho} \frac{dg}{d\rho} - \lambda v^2 g(f^2 + g^2 - 1) - 2\alpha_2 g = 0. \quad (3.13)$$

Note that $g = 0$ solves the second equation, and the first one with $g = 0$ is identical to that we studied in Eq. (2.6) for the global vortices. However, of course, we should not assume $g = 0$ from the beginning when it is an unstable solution. We numerically solve these with the boundary condition

$$f(0) = 0, \quad f(\infty) = 1, \quad \left. \frac{dg}{d\rho} \right|_{\rho=0} = 0, \quad g(\infty) = 0. \quad (3.14)$$

Fig. 16(a) shows numerical solutions in the weak coupling regime, and (b) shows the $\mathbb{Z}_2^{(3)}$ neutral string in the strong coupling regime. (c) shows the solutions represented in the $\phi_1\phi_3$ plane. The red (blue) curve does not lie on the upper (lower) hemisphere (black-dashed curve) but it lies on a slightly squashed upper (lower) hemisphere, namely the quasi vacuum manifold S^2 . On the contrary, the green curve corresponds to the solution with large $|\alpha|$ and has $\phi_3 = 0$ everywhere. As can be seen in (d), (e), (f), it is common among the three string solutions that ϕ radially spreads as the 2 dimensional hedgehog in asymptotic far region, namely $(\phi_1, \phi_2) \rightarrow v(\cos\theta, \sin\theta)$ with $\phi_3 \rightarrow 0$. This ensures the winding number $n = 1$ around the vacuum manifold S^1 . On the other hand, they show different behaviors near the center of string: ϕ points down and up for (d) and (e) whereas

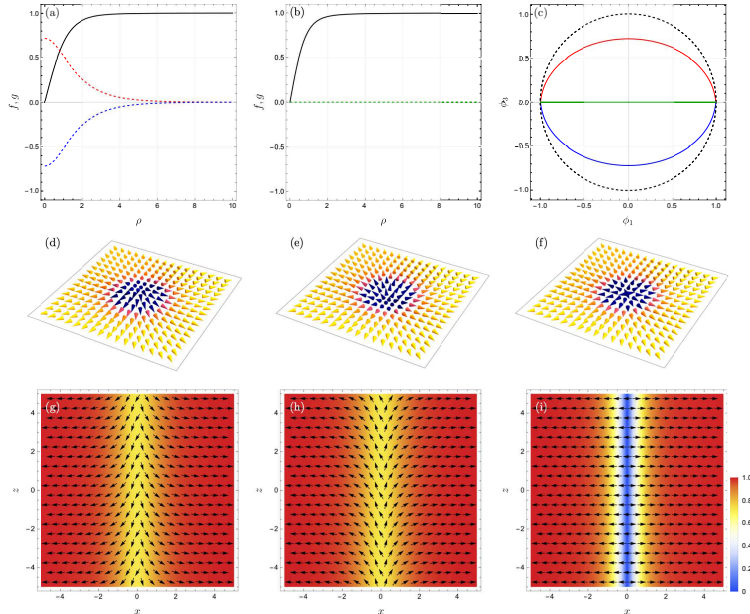


Figure 16: The axially symmetric string solutions for $(\lambda, v) = (4, 1)$ and $\alpha = 1/4$ for (a) and $\alpha = 1$ for (b). (a) The $\mathbb{Z}_2^{(3)}$ charged global strings. The black-solid curve shows $f(\rho)$ and the red-dashed and blue-dashed curves corresponds to $g(\rho)$. (b) The $\mathbb{Z}_2^{(3)}$ neutral global string. The black-solid curve corresponds to $f(\rho)$ and the green-dashed line shows $g(\rho) = 0$. (c) The parametric plots of the solutions given in (a) and (b) in the $\phi_1\phi_3$ plane ($\phi_2 = 0$). The black-dashed curve indicates the unperturbed order parameter space S^2 at $\alpha = 0$. (d), (e), (f) show the 3d vector plot of ϕ on the xy plane for the sting solutions of (a) with the blue-dashed curve, red-dashed curve, and (b), respectively. (g) [(h)] shows the 3d vector plot on the slices $x = 0$, $y = 0$, and $z = 0$ corresponding to (d) [(e)].

ϕ_3 for (f) is everywhere zero. This reflects the $\mathbb{Z}_2^{(3)}$ charge of the strings; (d) and (e) are charged whereas (f) is neutral.

The $\mathbb{Z}_2^{(3)}$ charged strings can be also interpreted as textures (half-lumps) wrapping the quasi vacuum manifold S^2 whose winding number is half quantized because they cover a half of the quasi vacuum manifold S^2 . Such half lumps are also called merons in condensed matter physics. However, note that the wrapping number as the texture is not a conserved topological charge but an approximate charge. The topological nature comes from $\pi_1(S^1) \simeq \mathbb{Z}$ together with the $\mathbb{Z}_2^{(3)}$ charge.

In order to determine when the global strings become $\mathbb{Z}_2^{(3)}$ charged, we measure $g|_{\rho=0}$ by varying α while v and λ are fixed. The result is shown in Fig. 17. As is consistent with Eq. (2.4), the $\mathbb{Z}_2^{(3)}$ charged string appears in the weak coupling regime. Therefore this figure shows the phase transition (of Ising spins) inside the vortex.

In the limit of $\lambda \rightarrow \infty$, the model reduces to the $O(3)$ nonlinear sigma model with an easy-plane potential. In this limit, a lump charge of $\pi_2(S^2) \simeq \mathbb{Z}$ becomes exact in contrast to the linear model for which the lump charge is only approximate. If we add four-derivative

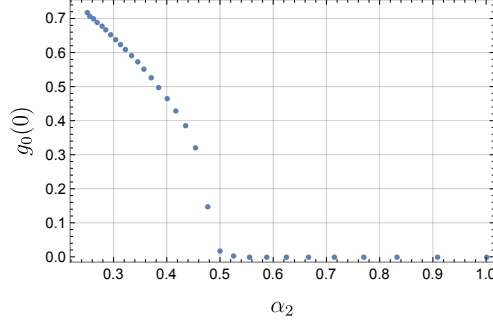


Figure 17: The value of $g_0(0)$ as the function of α_2 . The string is coreless in the sense of $|\phi| \neq 0$ if $g_0(0) \neq 0$, otherwise it has a core. The other parameters are fixed as $(v, \lambda) = (1, 4)$.

Skyrme terms, the model is a baby-Skyrme model with an easy-plane potential, admitting stable half-baby Skyrmions (merons) [77–79].

3.4.2 Topological monopole-string composite: a kink inside a string

Now we are ready to study the global monopoles in the presence of a perturbation V_2 with positive and small α . An important clue is that the spontaneous breaking of $\mathbb{Z}_2^{(3)}$ inside the string. Just as a usual \mathbb{Z}_2 breaking in 1 + 1 dimensions gives rise to a topological domain wall, the domain wall is spontaneously generated on the string. This domain wall is a point-like object from the perspective of 3+1 dimensions in the bulk, and it is a junction point which connects the two strings with the different $\mathbb{Z}_2^{(3)}$ charges. It is nothing but a global monopole, which is deformed by V_2 , attached by the two strings on the opposite sides. Notice that $\pi_2(S^2)$ is only approximately meaningful for characterizing the composite solitons since S^2 is not the exact vacuum manifold. Alternatively, the combination of $\pi_1(S^1) \simeq \mathbb{Z}$ for the mother strings and $\mathbb{Z}_2^{(3)}$ for the domain wall inside it is more appropriate to characterize the composite soliton. This is summarized by the sequential symmetry breaking

$$\begin{array}{ccc}
 G_{\text{approx}} = O(3) & \xrightarrow[\text{monopole}]{\text{vac}} & O(2) \\
 \cup & & \cup \\
 G_{\text{exct}} = O(2)^{(12)} \times \mathbb{Z}_2^{(3)} & \xrightarrow[\text{mother string}]{\text{vac}} & \mathbb{Z}_2^{(12)} \times \mathbb{Z}_2^{(3)} \xrightarrow[\text{kink}]{\text{mother string}} 1. \quad (3.15)
 \end{array}$$

With the picture that the monopole is the kink in the string at hand, we are lead to a natural product ansatz

$$\phi = v \left(\begin{array}{c} \frac{x}{\sqrt{\rho^2 + a^2}} \\ \frac{y}{\sqrt{\rho^2 + a^2}} \\ \frac{ca}{\sqrt{\rho^2 + a^2}} \tanh bz \end{array} \right), \quad (3.16)$$

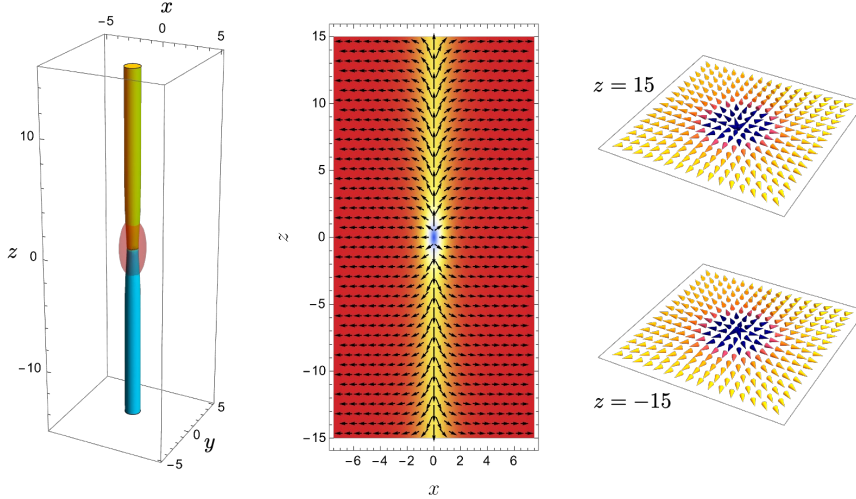


Figure 18: A numerical solution of the topological monopole-string composite for $(v, \lambda, \alpha_2) = (1, 4, 1/4)$. (left) The red surface is the isosurface of $\mathcal{M}_0 = 1/24$. The yellow and cyan surfaces show $|\phi_1 + i\phi_2| = 1/2$ with $\phi_3 > 0$ and $\phi_3 < 0$, respectively. (middle) The vector plot of ϕ at $y = 0$. (right) The vector plot of ϕ at $z = \pm 15$.

with a , b and c are constants. See Appendix B for the validity of this ansatz. The z dependence comes from the kink while the x, y dependence exhibits the $\mathbb{Z}_2^{(3)}$ charged string. In fact, for $z \gg 0$ and $z \ll 0$, we have

$$\phi|_{z \gg 0} = v \begin{pmatrix} \frac{x}{\sqrt{\rho^2 + a^2}} \\ \frac{y}{\sqrt{\rho^2 + a^2}} \\ \frac{ca}{\sqrt{\rho^2 + a^2}} \end{pmatrix}, \quad \phi|_{z \ll 0} = v \begin{pmatrix} \frac{x}{\sqrt{\rho^2 + a^2}} \\ \frac{y}{\sqrt{\rho^2 + a^2}} \\ -\frac{ca}{\sqrt{\rho^2 + a^2}} \end{pmatrix}. \quad (3.17)$$

These are nothing but the $\mathbb{Z}_2^{(2)}$ charged mother strings which wrap the upper- and lower-half hemispheres of the quasi-vacuum manifold S^2 (ellipsoid). On the other hand, at the center of string ($x = y = 0$) we have

$$\phi|_{x=y=0} = v \begin{pmatrix} 0 \\ 0 \\ \frac{ca}{\sqrt{\rho^2 + a^2}} \tanh bz \end{pmatrix}. \quad (3.18)$$

This is clearly the inner kink which embodies the flip of the ϕ_3 condensation.

We can make use of the above ansatz as an initial configuration for the relaxation scheme. The numerical solution obtained at the convergence of relaxation scheme is shown in Fig. 18. Note that the final state is independent of the parameters of the initial configurations.

So far, we have considered the ESB potentials which includes only linear or quadratic terms. The linear potential leads to the non-topological composite solitons while the

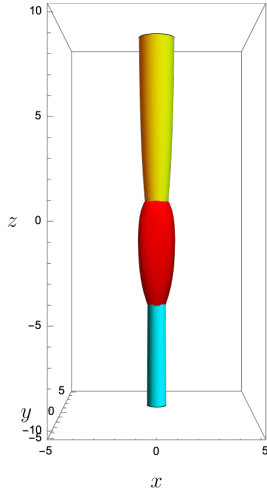


Figure 19: Asymmetric monopole-string composite. The tension of strings are different. This configuration is unstable since the string with larger tension continuously pulls the monopole.

quadratic one allows the topologically nontrivial composite solitons. If we mix the linear and quadratic terms, some symmetries are explicitly broken and it leads to imbalance of tension of the constituent solitons. Here, we give only one example:

$$V_{1+2} = \alpha_1 \phi_3 + \alpha_2 (\phi_3)^2, \quad (3.19)$$

For the parameter $(v, \lambda, \alpha_1, \alpha_2) = (1, 4, -1/10, 1/4)$, we have found the monopole-string composite but the two strings have different tensions, see Fig. 19. Thus, the monopole cannot be static. This resembles the unstable Nambu monopole in the two Higgs doublet model [80]. If we consider more generic ESB potential beyond the quadratic order in the fields, more complicated composite solitons should emerge. We will report the details elsewhere.

As mentioned in introduction, a local-soliton version of this composite soliton is a local monopole (’t Hooft-Polyakov monopole [62, 63]) attached by two non-Abelian vortex strings, in which monopoles are realized as kinks on the vortex [64–68]. This is realized by introducing an ESB term for a global symmetry that is locked with the gauge symmetry in the vacuum. As a version of textures, Skyrmions inside a vortex string as sine-Gordon solitons were also studied in Refs. [81, 82].

3.4.3 Dynamical simulations for monopole-string composites for $N = 2$

We numerically simulate the real time dynamics of the monopole-string composites in the $N = 2$ case. As the case of $N = 1$, We prepare random and periodic configurations as initial configurations for the real time dynamics and smear it by using the relaxation scheme. Again, We impose the periodic boundary conditions in the x , y , and z directions.

A numerical simulation for the $N = 2$ topological monopole-string composites is shown in Fig. 20. The top-leftmost panel shows an initial configuration with random distributions

of the monopoles and anti-monopoles, and the $\mathbb{Z}_2^{(3)}$ charged strings. We keep the initial number of monopoles to be the same order both for Figs. 15 and 20. In comparison with Fig. 15, the life time of the (anti-)monopoles is relatively long. The life time of the strings is as long as that of monopoles. This is due to the $\mathbb{Z}_2^{(3)}$ symmetry which ensures that the tensions of the strings with different $\mathbb{Z}_2^{(3)}$ charged are exactly equal. The cosmological monopole problem may exist in this case.

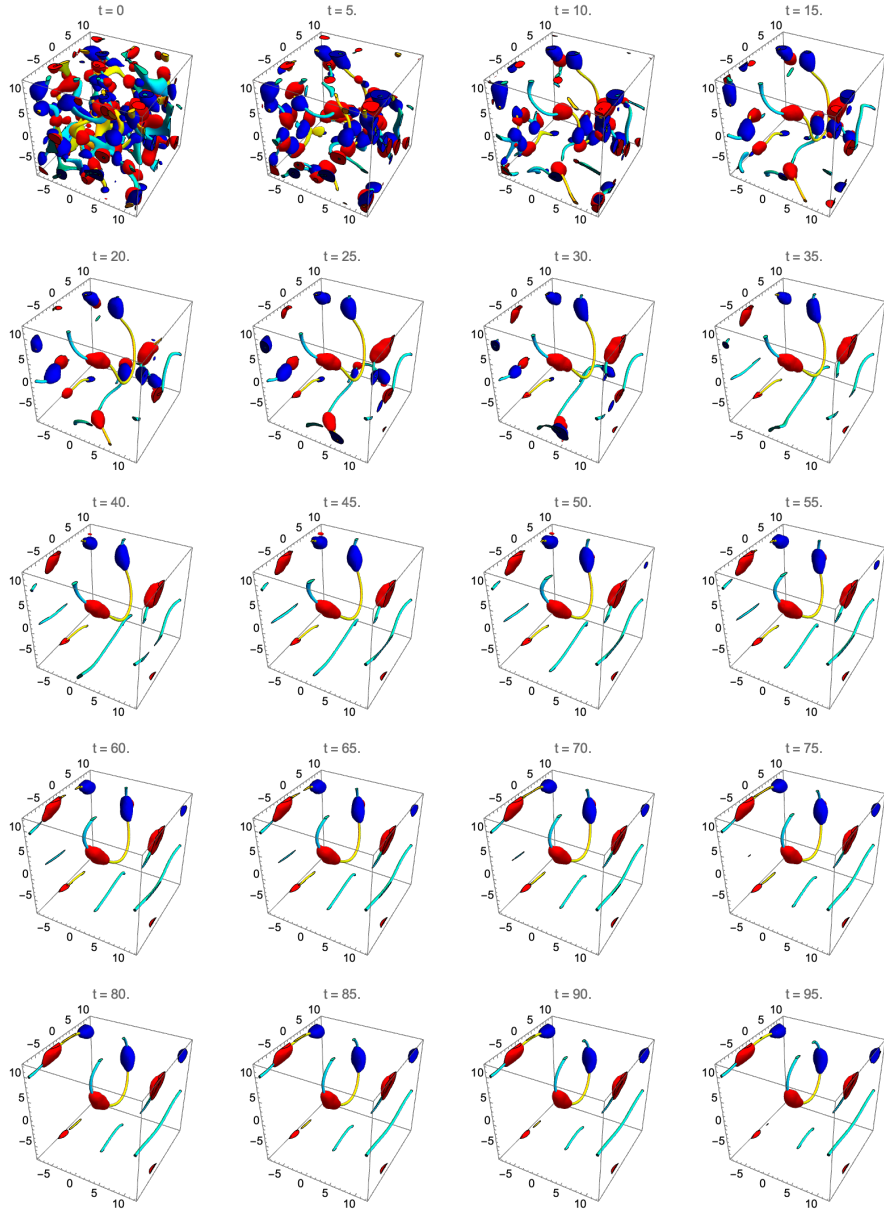


Figure 20: $(v, \lambda, \alpha) = (1, 4, 1/4)$. The red (blue) surface shows the isosurface of the monopole charge density $\mathcal{M}_0 = 1/24$ ($-1/24$), representing (anti-)monopoles. The yellow and cyan surfaces show the isosurface of $|\phi_1 + i\phi_2| = 1/2$ with $\phi_3 > 0$ and $\phi_3 < 0$, respectively, representing topological strings with up and down spins, respectively.

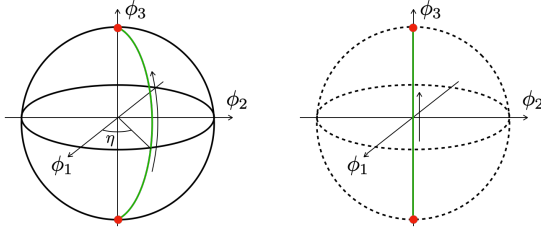


Figure 21: The left figure shows a domain wall with $SO(2)$ moduli whereas the right one corresponds to the domain wall without internal moduli.

3.5 Topological monopole-wall composite for $N = 2$ with $\alpha < 0$

In this subsection, we study the $N = 2$ cases with $\alpha < 0$ (the easy-axis potential).

3.5.1 The topological domain wall with $SO(2)^{(12)}$ moduli

Let us consider the Lagrangian with V_2 for $\alpha < 0$. As before, the S^2 structure remains as the quasi vacuum manifold of the potential in the weak coupling regime satisfying Eq. (2.4). The genuine vacuum manifold consists of the two points as shown in Fig. 11 (the right panel with $\alpha < 0$). As is summarized in Table 2, the discrete symmetry $\mathbb{Z}_2^{(3)}$ is spontaneously broken so that there exist topologically stable domain walls.

If we impose $\phi_2 = 0$ which is consistent with EOMs, the three component field reduces to the two components as $\phi \rightarrow (\phi_1, 0, \phi_3)$. Then, the EOMs for (ϕ_1, ϕ_3) are the same as those studied in Sec. 2.4.1 replacing ϕ_3 by ϕ_2 . Hence, the domain wall solution shown in Fig. 5 (a) in the linear $O(2)$ model can be embedded without any change.

There is an important difference between the $O(2)$ and $O(3)$ models. In the former case, the spontaneously broken symmetry in the presence of the domain wall is $\mathbb{Z}_2^{(2)}$, whereas it is $O(2)^{(12)}$ which breaks down into $\mathbb{Z}_2^{(12)}$ in the latter as

$$O(2)^{(12)} \times \mathbb{Z}_2^{(3)} \xrightarrow{\text{vac}} O(2)^{(12)} \xrightarrow{\text{wall}} \mathbb{Z}_2^{(12)}. \quad (3.20)$$

Hence, the domain wall carries the continuous moduli $O(2)^{(12)}/\mathbb{Z}_2^{(12)} = SO(2)^{(12)} \simeq S^1$. This is intuitively understood as follows. When one connects the two vacua, the path passes through a point on the equator (great circle with $\phi_3 = 0$, which is parameterized by an azimuth angle $\eta \in [0, 2\pi)$ as shown in Fig. 21 (left). η is nothing but the Nambu-Goldstone mode localized on the domain wall.

On the contrary, the domain wall does not have any moduli in the strong coupling regime where the original S^2 structure completely disappears. The domain wall solution corresponds to a straight segment along the ϕ_3 axis connecting the two vacua with $\phi_1 + i\phi_2 = 0$ as illustrated in Fig. 21 (right). This is neutral under $SO(2)^{(12)}$. The numerical solution is the same as those given in Fig. 5 (b).

In the limit of $\lambda \rightarrow \infty$, the model reduces to the $O(3)$ nonlinear sigma model with an easy-axis potential, equivalent to the so-called massive $\mathbb{C}P^1$ model [83–86]. It admits a domain wall with a $U(1)$ modulus.

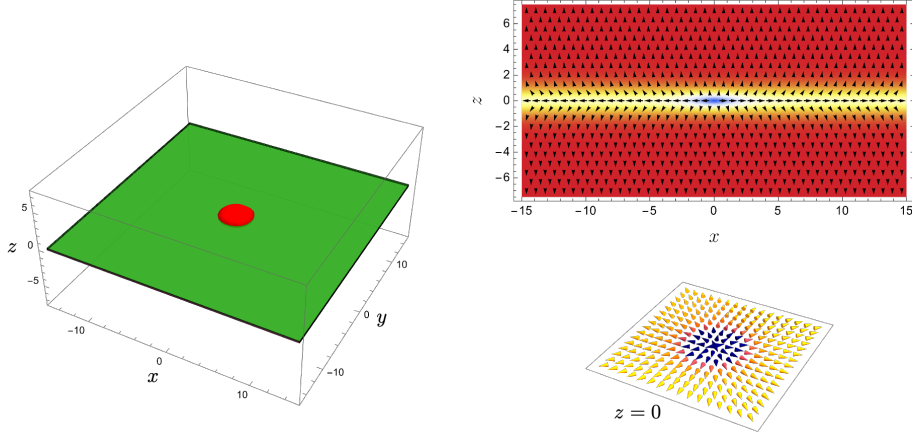


Figure 22: A numerical solution of an $N = 2$ topological monopole-wall composite for $(v, \lambda, \alpha) = (1, 2, -1/2)$. (left) The red surface corresponds to the monopole charge density $\mathcal{M}_0 = 1/24$. The green (head) and purple (tail) surfaces corresponds to $0 < \phi_3 < 0.15$ and $-0.15 < \phi_3 < 0$, respectively. (up-right) The vector plot of ϕ at the $y = 0$ plane. (lower-right) The vector plot of ϕ on the domain wall at $z = 0$ for $x \in [-15, 15]$ and $y \in [-15, 15]$.

3.5.2 Topological monopole-wall composite: a vortex inside a domain wall

Let us next study a global monopole in the presence V_2 with negative α in the weak coupling regime. As is given in Eq. (3.20), the $SO(2)^{(12)}$ symmetry of the vacuum is spontaneously broken by the topological domain wall whose world volume is a $2 + 1$ dimensional surface. This SSB inside the domain wall gives rise to a topological vortex, which is localized on the wall and looks a point-like object from the $3+1$ dimensional bulk perspective. This is nothing but a global monopole in the bulk. One can also regard this as the global monopole deformed by V_2 and immersed into a domain wall. As before, the homotopy group $\pi_2(S^2) \simeq \mathbb{Z}$ for monopoles is only approximately meaningful for characterizing the composite solitons. Alternatively, the combination of $\mathbb{Z}_2^{(3)}$ for the mother domain wall and $\pi_1(SO(2)^{(12)}) = \mathbb{Z}$ for the vortices inside it is more appropriate to characterize it. This can be briefly summarized by a sequence of symmetry breaking of the system

$$\begin{array}{ccc}
 G_{\text{approx}} = O(3) & \xrightarrow[\text{monopole}]{\text{vac}} & O(2) \\
 \cup & & \cup \\
 G_{\text{exact}} = O(2)^{(12)} \times \mathbb{Z}_2^{(3)} & \xrightarrow[\text{mother wall}]{\text{vac}} & O(2)^{(12)} \xrightarrow[\text{vortex}]{\text{mother wall}} 1.
 \end{array} \quad (3.21)$$

With these observations at hand, we are lead to a product ansatz

$$\phi = v \begin{pmatrix} \frac{x}{\sqrt{\rho^2 + a^2}} \cos \Theta \\ \frac{y}{\sqrt{\rho^2 + a^2}} \cos \Theta \\ c \sin \Theta \end{pmatrix}, \quad \Theta = 2 \arctan e^{bz} - \frac{\pi}{2}, \quad (3.22)$$

with a , b and c are constants. For large $\rho \gg 0$, we have

$$\phi|_{\rho \gg 0} = v \begin{pmatrix} \cos \theta \cos \Theta \\ \sin \theta \cos \Theta \\ c \sin \Theta \end{pmatrix}, \quad \tan \theta = \frac{y}{x}, \quad (3.23)$$

which can be understood as the mother domain wall with the orientational moduli θ . On the $z = 0$ plane, this behaves as a vortex

$$\phi|_{z=0} = v \begin{pmatrix} \frac{x}{\sqrt{\rho^2 + a^2}} \\ \frac{y}{\sqrt{\rho^2 + a^2}} \\ 0 \end{pmatrix}. \quad (3.24)$$

The $|\phi|$ vanishes only at the origin, which implies the presence of the point-like defect, namely a monopole, at the origin.

We can utilize the above product ansatz as an initial configuration for the relaxation scheme. The numerical solution is shown in Fig. 22. Note that the converged final configuration is independent of the initial configurations. The monopole as a daughter is squashed, looking like a flat pancake inside the mother domain wall.

Let us discuss the case that two vacua are not degenerated, replacing the scalar potential V_2 by V_{1+2} given in Eq. (3.19). Then, the $\mathbb{Z}_2^{(3)}$ symmetry is only an approximate symmetry whereas the $O(2)^{(12)}$ symmetry remains as a genuine symmetry, leading to an imbalance between energies of vacua. One remains as a true vacuum and the other is lifted as a false vacuum. The domain wall connects the true and false vacua and is no longer static. Nevertheless, once it is created, the $O(2)^{(12)}$ symmetry is spontaneously broken inside it, yielding daughter monopoles. We provide a numerical simulation of an imbalanced monopole-wall composite in Fig. 23. One can see that the domain wall bends around the daughter monopole. The domain wall moves down in the figure but it is stacked by the monopole behaving as an impurity. This situation may affect bubble nucleation in the early universe.

As mentioned in introduction, a local version of this composite soliton is a local ('t Hooft-Polyakov) monopole immersed into a non-Abelian domain wall [69]. A texture version of this composite configuration is a domain-wall Skyrmions in which Skyrmions are realized as lumps (or baby Skyrmions) inside the domain wall [33, 58, 87, 88] (see also Ref.[89]).

3.5.3 Dynamical simulations for monopole-wall composites

Fig. 24 shows a numerical simulation for the real time dynamics evolving from a random and periodic initial configuration for $(v, \lambda, \alpha) = (1, 4, -1/4)$. All the monopoles and anti-monopoles appear on domain walls. The domain walls are in general closed surfaces under the periodic boundary condition, they shrink by their tension. Which of the north or south vacuum is left is determined by chance with the probability 1/2. (In Fig. 24, the final vacuum is accidentally the north vacuum.)

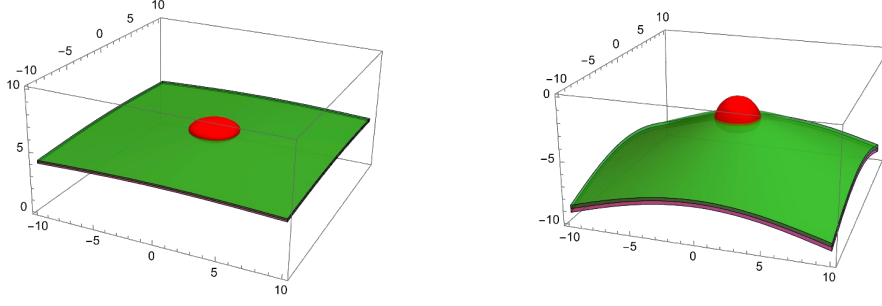


Figure 23: Asymmetric monopole-wall composite. The vacuum energies above and below the domain wall are different. This configuration is unstable since the vacuum with larger energy continuously push the domain wall. In the figure, the domain wall moves down, but the monopole behaves as an impurity. The parameters are chosen as $(v, \lambda, \alpha_1, \alpha_2) = (1, 2, -1/2, -1/4)$ for the left panel, and $(1, 4, -1/4, -1/2)$ for the right panel.

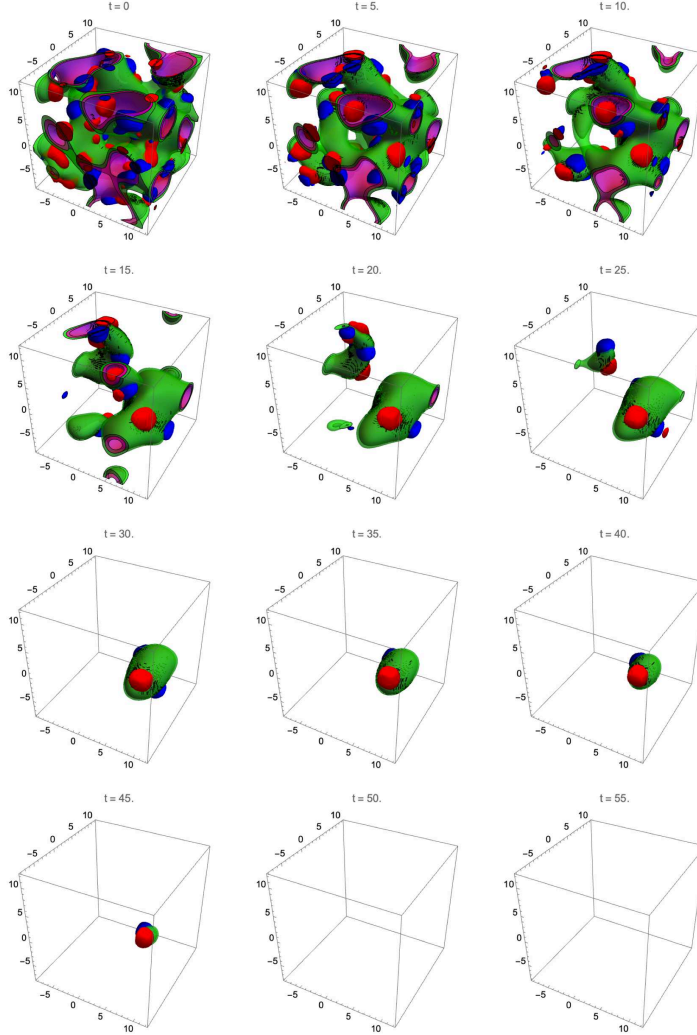


Figure 24: $(v, \lambda, \alpha) = (1, 4, -1/4)$. The red (blue) surfaces are the isosurfaces of the monopole charge density $\mathcal{M}_0 = 1/24$ ($-1/24$), representing (anti-)monopoles. The green (head) and purple (tail) surfaces correspond to $0 < \phi_3 < 0.15$ and $-0.15 < \phi_3 < 0$, respectively, representing domain walls.

Compared with stable monopoles on strings, one can observe that the life time is shorter in this case because the domain walls are long lived compared with strings.

3.6 Relations to spherical monopoles

In the both cases of $\alpha > 0$ and $\alpha < 0$, the SSB pattern of the Lagrangian is the same, $SO(2) \times \mathbb{Z}_2 \rightarrow 1$. However, the difference is the order of the SSBs, i.e., which of $SO(2)$ or \mathbb{Z}_2 is broken first, namely at high energy. If $SO(2)$ is broken first, the mother soliton is the global string. On the other hand, the mother soliton is the domain wall when \mathbb{Z}_2 is broken first. For the former case, the subsequent SSB of \mathbb{Z}_2 on the mother string gives rise to the inner kink which is identical to the monopole. In the latter case, the $SO(2)$ SSB on the mother domain wall leads to the inner vortex which is identical to the monopole. These can be visually understood by drawing the distributions of the ϕ as in the middle and right panels in the second row of Fig. 25. For the both configurations, the $SO(2)$ transformation rotates the arrows and is associated with the vortices whereas \mathbb{Z}_2 flips the arrows and is associated with the domain walls.

Another view point is that both the monopole-string and monopole-wall composites can be constructed by a simultaneous rotation of the real space and internal space from the vortex-wall configuration in \mathbb{R}^2 , as illustrated in the first and second rows in Fig. 25. If we rotate the two-dimensional vortex-wall composite along the axis on the domain wall, we obtain the monopole-string composite in \mathbb{R}^3 . On the other hand, if we rotate it along the axis orthogonal to the domain wall, we obtain the monopole-wall composite in \mathbb{R}^3 . Instead of the rotation, if we translate it to the vertical direction, we obtain the string-wall composite in \mathbb{R}^3 in the $O(2)$ model.

Let us compare these monopoles in the linear $O(3)$ model with the spherically symmetric one associated with the usual SSB $SO(3) \rightarrow SO(2)$ whose topology is characterized by $\pi_2(SO(3)/SO(2)) \simeq \mathbb{Z}$. This counts how many times the hypersurface $\phi(\mathbf{x})$ in the field internal space, whose domain is the spacial boundary $\{\mathbf{x} \mid \mathbf{x} \in S^2 = \partial\mathbb{R}^3\}$, wraps the vacuum manifold $S^2 \simeq SO(3)/SO(2)$. In comparison, the relevant SSB, $SO(2) \times \mathbb{Z}_2 \rightarrow 1$, under the presence of the ESB potential V_2 can be seen clearly on a cylindrical boundary as in the bottom row in Fig. 25. The distributions of ϕ on the cylinder surfaces have distinct difference between the monopole-string and monopole-wall. Nevertheless, for the both cases, the hypersurface ϕ on the boundary forms the sphere. Namely, they can be continuously deformed into the spherical hedgehog configuration. Thus, there should exist the monopole inside the cylinder.

4 Monopole-string-wall composites

Finally, we consider the most generic quadratic potential

$$V_2 = (\phi_1)^2 \cos \gamma + (\phi_2)^2 \cos \beta \sin \gamma + (\phi_3)^2 \sin \beta \sin \gamma. \quad (4.1)$$

As before, we are interested in the weak coupling regime where the overall coefficient α satisfies the weak coupling condition (2.4). Note that the above potential can be rewritten as $V_2 = (\phi)^2 \cos \gamma + (\phi_2)^2 (\cos \beta \sin \gamma - \cos \gamma) + (\phi_3)^2 (\sin \beta \sin \gamma - \cos \gamma)$. The first term can

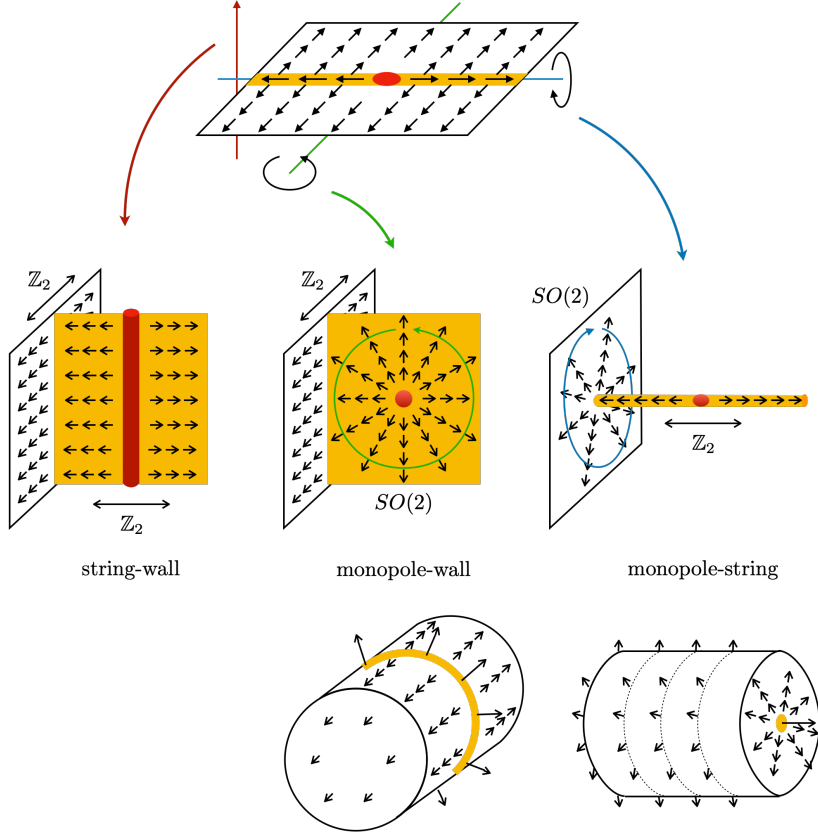


Figure 25: Schematic pictures of the composite solitons of two different solitons. The small arrows represent configurations of ϕ . The top one is the vortex-wall on two dimensional plane. In the second row, the string-wall (left) is made of the two-component scalar field whereas monopole-string (right) and monopole-wall (middle) are made of the three-component scalar field. In the third row, the configuration of ϕ on the cylindrical boundary is shown.

be absorbed into the quadratic potential $\frac{\lambda}{4} (\phi^2 - v^2)^2$. It just shifts the VEV and potential energy by constants leading to no essential changes. Therefore, we can set $\gamma = \pi/2$ without loss of generality and we will adopt the potential with one parameter β

$$V_2(\beta) = (\phi_2)^2 \cos \beta + (\phi_3)^2 \sin \beta. \quad (4.2)$$

For generic β the symmetry of the model is

$$G = \mathbb{Z}_2^{(1)} \times \mathbb{Z}_2^{(2)} \times \mathbb{Z}_2^{(3)}, \quad (4.3)$$

associated with the sign flip of $\phi_{1,2,3}$. The accidental cases are $\beta = \pi/2$ and $3\pi/2$ for which V_2 has the single term $\pm(\phi_3)^2$, respectively. In such a case, the symmetry is enhanced as $G(\beta = \pi/2, 3\pi/2) = O(2)^{(12)} \times \mathbb{Z}_2^{(3)}$ which we have studied in the previous sections. Similarly, we have $G(\beta = 0, \pi) = O(2)^{(13)} \times \mathbb{Z}_2^{(2)}$. In addition $\beta = \pi/4, 5\pi/4$ belongs to the same class. This can be understood by rewriting $V_2(\beta = \pi/4, 5\pi/4) = \pm (\phi^2 - (\phi_1)^2) / \sqrt{2}$.

Again, the first term can be absorbed into the quadratic potential $\frac{\lambda}{4}(\phi^2 - v^2)^2$, so that the potential is essentially $V_2(\beta = \pi/4, 5\pi/4) = \mp(\phi_1)^2/\sqrt{2}$. Therefore, we have $G = O(2)^{(23)} \times \mathbb{Z}_2^{(1)}$.

For illustration, let us take $\beta = \pm\pi/3$ which gives

$$V_2(\pm\pi/3) = \frac{1}{2}(\phi_2)^2 \pm \frac{\sqrt{3}}{2}(\phi_3)^2. \quad (4.4)$$

For $\beta = \pi/3$, the second term has a larger positive coefficient than the first one, so that it enforces $\phi_3 = 0$. Namely, the original vacuum manifold S^2 is restricted to the great circle S^1 perpendicular to the ϕ_3 axis. Subsequently, the first term enforces $\phi_2 = 0$. Namely, the vacuum of the potential is understood by the following three steps; the vacuum is S^2 when $\alpha = 0$, the second term in (4.4) deforms it so that the S^1 submanifold perpendicular to the ϕ_3 axis is the lowest-energy one, and the first term in (4.4) leaves two antipodal points (on the ϕ_1 axis) among the S^1 manifold as the true vacua. We call this potential structure the three-fold structure ($S^2 \supset S^1 \supset S^0$). See Fig. 26 (left).

For $\beta = -\pi/3$, the second term chooses the two points $\phi_3 \sim \pm v$ as the true vacua. In addition, the first term slightly reduces the potential energy on the great circle S^1 perpendicular to the ϕ_2 axis. The structure of the potential is similar to that with $\beta = \pi/3$, and the two cases $\beta = \pm\pi/3$ are identical if we rotate in the internal space by $\pi/2$ as shown in Fig. 26 (middle). The generic β can be straightforwardly understood in a similar manner. In summary, the parameter space $\beta \in [0, 2\pi)$ is divided into 6 regions by the 6 boundaries $\beta = 0, \pi/4, \pi/2, \pi, 5\pi/4, 3\pi/2$ where the symmetry is enhanced.

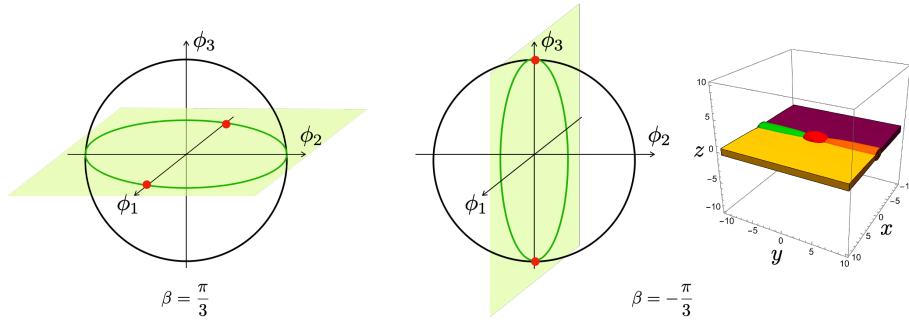


Figure 26: The vacuum manifold under the presence of V_2 and a numerical solution for monopole-string-wall composite.

The three-fold structures S^2 , S^1 , and $S^0 = \mathbb{Z}_2$ of the potential give rise to the monopole, string, and domain wall, respectively. Hence, the resulting soliton is a monopole-string-wall composite. This composite is topologically stable. Note that characterizations of monopoles and strings by the homotopy group $\pi_2(S^2)$ and $\pi_1(S^1)$ are only approximate. Instead, it is exactly characterized by the homotopy group associated with the spontaneous breaking of G .

To be specific, let us consider $\beta = -\pi/3$, see Fig. 26 (middle). The vacua are $\phi = (0, 0, \pm v)$. There, the $\mathbb{Z}_2^{(3)}$ symmetry is spontaneously broken, and the mother domain

wall is generated. In this case, one has to choose a half circle on either positive or negative side of ϕ_1 as the domain wall configuration in the broken phase. Namely, the $\mathbb{Z}_2^{(1)}$ symmetry is spontaneously broken on the mother domain wall. This gives rise to an inner domain wall inside the mother domain wall, namely a daughter string from the 3+1 dimensional bulk perspective. In the daughter vortex core, $\phi_1 = \phi_3 = 0$ and ϕ_2 can be either positive or negative (since it does not lie on the origin $\phi = 0$ due to the quasi vacuum manifold S^2). Namely, the $\mathbb{Z}_2^{(2)}$ symmetry is spontaneously broken inside the daughter vortex localized inside the mother domain wall. This gives rise to an inner kink inside the daughter vortex, which is nothing but a granddaughter monopole from the 3+1 dimensional bulk perspectives. This can be briefly summarized by a sequence of the symmetry breakings of G for $\beta = -\pi/3$

$$\begin{array}{ccc}
G_{\text{approx}} = O(3) & \xrightarrow[\text{monopole}]{\text{vac}} & O(2) \\
\cup & & \cup \\
G_{\text{exact}} = \mathbb{Z}_2^{(1)} \times \mathbb{Z}_2^{(2)} \times \mathbb{Z}_2^{(3)} & \xrightarrow[\text{mother wall}]{\text{vac}} \mathbb{Z}_2^{(1)} \times \mathbb{Z}_2^{(2)} \xrightarrow[\text{daughter vortex}]{\text{mother wall}} \mathbb{Z}_2^{(2)} \xrightarrow[\text{granddaughter monopole}]{\text{daughter vortex}} 1. &
\end{array} \quad (4.5)$$

The composite soliton can be well captured by the following ansatz for $\beta = -\pi/3$

$$\phi = v \begin{pmatrix} \cos \Theta \sin \Phi \\ \delta \tanh \gamma y \cos \Theta \cos \Phi \\ \kappa \sin \Theta \end{pmatrix}, \quad \Theta = 2 \arctan e^{\xi z} - \frac{\pi}{2}, \quad \Phi = 2 \arctan e^{\chi x} - \frac{\pi}{2}, \quad (4.6)$$

with parameters $\xi, \chi, \gamma, \delta$, and κ . The presence of the mother wall can be seen by taking $\Phi = \pi/2$ for $x \gg 0$ and $\Phi = -\pi/2$ for $x \ll 0$

$$\phi|_{x \gg 0} = v \begin{pmatrix} \cos \Theta \\ 0 \\ \kappa \sin \Theta \end{pmatrix}, \quad \phi|_{x \ll 0} = v \begin{pmatrix} -\cos \Theta \\ 0 \\ \kappa \sin \Theta \end{pmatrix}. \quad (4.7)$$

These are the $\mathbb{Z}_2^{(1)}$ -charged domain wall perpendicular to the z -axis. On the domain wall at $\Theta = 0$ ($z = 0$), we have

$$\phi|_{z=0} = v \begin{pmatrix} \sin \Phi \\ \delta \tanh \gamma y \cos \Phi \\ 0 \end{pmatrix}. \quad (4.8)$$

This is essentially the same as Eq. (2.11) for the string-wall composite in the $O(2)$ model. We find the inner walls by taking $y \gg 0$ and $y \ll 0$ as

$$\phi|_{z=0, y \gg 0} = v \begin{pmatrix} \sin \Phi \\ \delta \cos \Phi \\ 0 \end{pmatrix}, \quad \phi|_{z=0, y \ll 0} = v \begin{pmatrix} \sin \Phi \\ -\delta \cos \Phi \\ 0 \end{pmatrix}. \quad (4.9)$$

These are $\mathbb{Z}_2^{(2)}$ -charged domain walls perpendicular to the y -axis. Finally, the inner kink inside the daughter vortex (granddaughter monopole) can be found for $(\Theta, \Phi) = (0, 0)$ at $z = x = 0$ as

$$\phi|_{z=x=0} = v \begin{pmatrix} 0 \\ \delta \tanh \gamma y \\ 0 \end{pmatrix}. \quad (4.10)$$

We present a numerical solution for $\beta = -\pi/3$ in Fig. 26 (right) which is obtained by evolving the above ansatz by the standard relaxation scheme. Since the ansatz is appropriate as the initial configuration, the relaxation process quickly converges and the final state is independent of the parameters of the ansatz. In Fig. 26 (right) the mother domain walls are painted in yellow and purple reflecting the $\mathbb{Z}_2^{(1)}$ charge: the yellow corresponds to $\phi \sim (1, 0, 0)$ while the purple indicates $\phi \sim (-1, 0, 0)$. The both connect two vacua $\phi \sim (0, 0, 1)$ in the upper bulk while $\phi \sim (0, 0, -1)$ in the lower bulk. Also, the daughter vortex strings are painted by orange and green reflecting the $\mathbb{Z}_2^{(2)}$ charge: the orange indicates $\phi \sim (0, 1, 0)$, and the green corresponds to $\phi \sim (0, -1, 0)$.

The field ϕ vanishes at the center of the monopole (the red blob). Though the distribution of ϕ is not a spherically symmetric hedgehog, the kink inside the daughter vortex can be regarded as a global monopole. To see this, let us consider a plane $y = 10$ in the right panel of Fig. 26. The field on the plane corresponds to a hemisphere with $\phi_2 > 0$ in the internal space (middle panel of Fig. 26). On the other hand, the field on a plane $y = -10$ corresponds to a hemisphere with $\phi_2 < 0$. Since these two hemispheres are smoothly connected on $y = 0$ on the boundary of the box, the field configuration wraps the quasi vacuum manifold S^2 representing a global monopole.

We show the numerical solutions of the monopole-string-wall composites for $\beta = k\pi/8$ with $k = 0, 1, \dots, 15$ in Fig. 27. All the solutions are obtained from the unique initial configuration $\phi \sim v\hat{r}$ by the relaxation scheme. Some of them are identical up to spatial rotations. Nevertheless we show all β because it is useful to see which direction the composite extends for a fixed β .

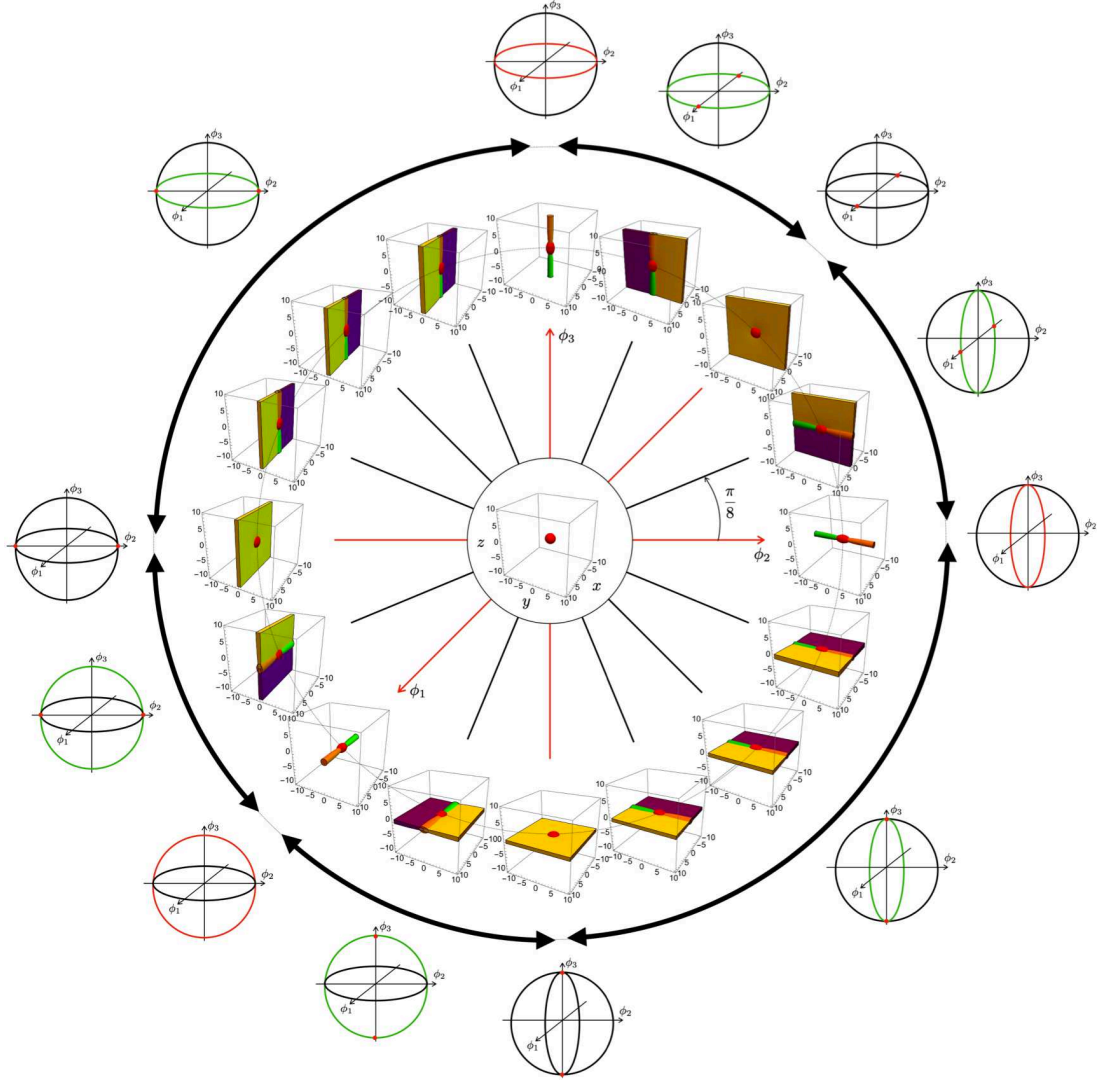


Figure 27: The monopole-string-wall composites for $\beta = k\pi/8$ ($k = 0, 1, \dots, 15$). The right-most figure having a monopole-string corresponds to $\beta = 0$ ($k = 0$). The others are placed counterclockwise by $\delta\beta = \pi/8$. The figure at the center shows the isolated global monopole for $\epsilon = 0$. The schematic pictures at the outer circle showing S^2 in the internal space indicates the true vacua in red color and quasi vacua in green.

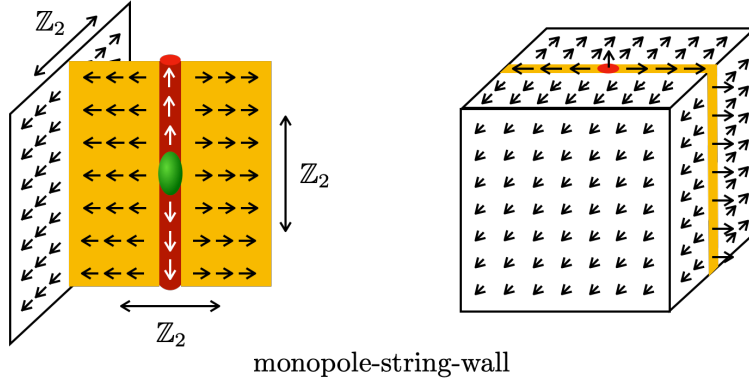


Figure 28: The composite of monopole-string-wall. The configuration of ϕ is shown by the small arrows.

The profile of ϕ is shown in the left panel of Fig. 28. The profile of ϕ on the boundary cube is shown in the right panel of Fig. 28. It is very different from the spherical hedgehog distribution of the usual monopole. However, indeed it can be continuously deformed into a spherical hedgehog, and therefore there should exist the monopole inside the cube.

We briefly present a result of dynamical simulation starting from a random and periodic initial configuration in Fig. 29.

As a local-soliton counterpart of this configuration, a composite soliton of domain wall, local vortex, and local monopole was constructed in Ref. [69] as a kink inside a non-Abelian sine-Gordon soliton [57, 58] inside a non-Abelian domain wall [59–61] (see also Ref. [32]). This configuration is also similar to a topological Nambu monopole in two-Higgs doublet model [80, 90, 91]. As a similar texture-type soliton, a Skymion as a kink inside a domain wall inside a domain wall was studied in Ref. [92] in which it is called a matryoshka Skymion.

5 Summary and discussion

In this work, we have studied various composite solitons of the global type appearing in the $O(2)$ and $O(3)$ linear sigma models $\phi = (\phi_1, \phi_2)$ and (ϕ_1, ϕ_2, ϕ_3) with perturbed ESB terms.

The $O(2)$ model with the ESB potential $V_N = \alpha(\phi_2)^N$ for $N = 0, 1, 2$ is identical to the axion model with the domain-wall number $N_{\text{DW}} = 1, 2$, admitting a composite of the global string and domain walls. In the $N = 0$ case, the topological global string exists as a stable soliton solution. In the $N = 1$ case, the $O(2)$ symmetry is explicitly broken to \mathbb{Z}_2 , the vacuum is a unique point, and there are no topologically nontrivial solitons. Nevertheless, as long as the ESB term is sufficiently small, there are non-topological composite solitons: a string attached by a domain wall. In the case of $N = 2$, there exists a topological composite soliton of the global string and the two domain walls. This is very well known but we have given another picture on the string-wall composite. From our viewpoint, the string-wall composite can be realized as an inner kink in the mother domain wall. The

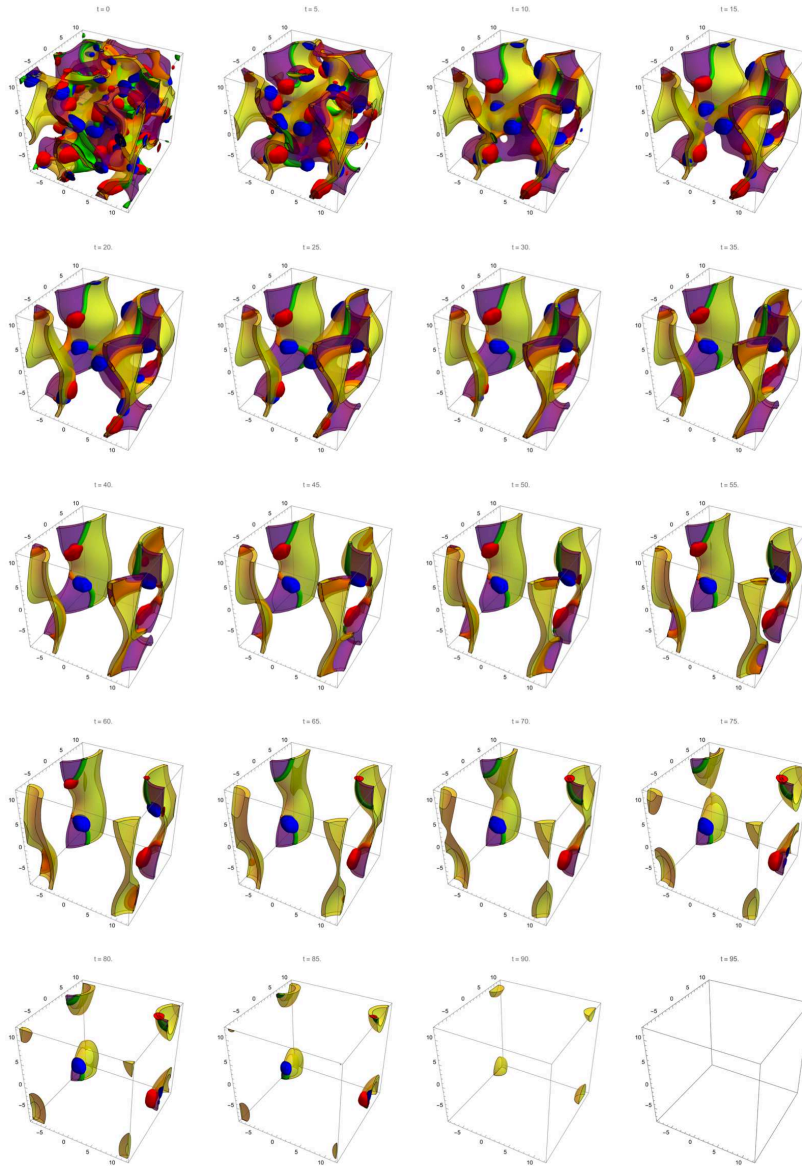


Figure 29: The dynamical simulation of the monopole-string-wall composite for $(v, \lambda, \alpha) = (1, 4, 1/4)$ and $\beta = -\pi/3$. The periodic boundary condition is imposed.

symmetry behind this is $G = \mathbb{Z}_2^{(1)} \times \mathbb{Z}_2^{(2)}$. The $\mathbb{Z}_2^{(2)}$ is spontaneously broken in the vacuum. This triggers the sequential spontaneous symmetry breaking and generations of the mother domain wall and daughter vortex as given in Eq. (2.15). The mother domain wall has a $\mathbb{Z}_2^{(1)}$ charge and when two mother domain walls with opposite $\mathbb{Z}_2^{(1)}$ charges join, an inner kink is produced at the junction line. It can be identified with a global vortex in the bulk

viewpoint.

Next, we have studied the $O(3)$ linear model with the small ESB potentials $V_N = \alpha(\phi_3)^N$ with $N = 0, 1, 2$. In the $N = 0$ case, the SSB is $G = O(3) \rightarrow H = O(2)$ giving rise to the global monopoles characterized by $\pi_2(G/H) \simeq \mathbb{Z}$. In the $N = 1$ case, we have $G = H = O(2)^{(12)}$. The vacuum is a unique point, and there are no topologically nontrivial solitons. Nevertheless, if the ESB potential is sufficiently weak, there is a non-topological composite of the global monopole attached by a global string. We have constructed the numerical solutions for the global monopole attached by the string, and a pair of the monopole and antimonopole confined by the string. In the $N = 2$ case, we have found that there are two branches corresponding to $\alpha > 0$ or $\alpha < 0$ (supposing small $|\alpha|$). The summary is given in Table 2. The symmetry of the Lagrangian is $G = O(2)^{(12)} \times \mathbb{Z}_2^{(3)}$ for both $\alpha > 0$ and $\alpha < 0$, which is spontaneously broken into $H = \mathbb{Z}_2^{(12)} \times \mathbb{Z}_2^{(3)}$ for $\alpha > 0$ and $H = O(2)^{(12)}$ for $\alpha < 0$. The SSB $G \rightarrow H$ gives rise to the $\mathbb{Z}_2^{(3)}$ charged string for $\alpha > 0$, and the $SO(2)^{(12)}$ charged domain wall for $\alpha < 0$ in the vacuum. The production of these topological defects triggers further SSB as given in Eqs. (3.15) and (3.21), resulting in the production of the monopoles inside the mother solitons.

The last composite soliton we have constructed in this paper is the composite of the monopole, string, and domain wall. This is the most generic solitonic configuration in the presence of the ESB potential V_2 of the quadratic terms of $\phi_{1,2,3}$ as Eq. (4.1). In general, the $O(3)$ symmetry is explicitly broken to $G = \mathbb{Z}_2 \times \mathbb{Z}_2 \times \mathbb{Z}_2$, and G is spontaneously broken to $H = \mathbb{Z}_2 \times \mathbb{Z}_2$ in the vacua. Then, the mother domain wall is generated, triggering the subsequent SSB of the remaining $\mathbb{Z}_2 \times \mathbb{Z}_2$ as Eq. (4.5). On the mother domain wall, the SSB $H \rightarrow \mathbb{Z}_2$ gives rise to the inner domain wall which is nothing but the daughter string from the bulk viewpoint. Furthermore, the SSB of the remaining \mathbb{Z}_2 takes place in the daughter string, resulting in the production of the inner kink, that can be identified with a granddaughter monopole from the bulk viewpoint.

Now, let us address several discussions and possible future directions. In the case of the $O(3)$ model with the quadratic potential $V = \alpha\phi_3^2$, the $O(2)^{(12)}$ symmetry is exact. If we couple a $U(1)$ gauge field to $U(1) \subset O(2)^{(12)}$, solitons become partially local solitons. In the case of $\alpha > 0$ discussed in Subsec. 3.4, strings become local ANO strings with Ising spins in their cores. However, a \mathbb{Z}_2 kink on a string remains as a global monopole in the bulk.¹In the case of $\alpha < 0$ discussed in Subsec. 3.5.1, a domain wall becomes a superconducting domain wall, since the $U(1)$ gauge symmetry is spontaneously broken around the domain wall. Consequently, a vortex on a domain wall becomes a local ANO vortex which is a global monopole in the bulk. This gives a field theoretical realization of a thin-film superconductor.

In addition, in the case of $\alpha < 0$, global monopoles become global vortices on a domain wall. It is known that the XY model in 2+1 dimensions exhibits the so-called Berezinskii-

¹In the limit of $\lambda \rightarrow \infty$, the model reduces to a gauged $O(3)$ nonlinear sigma model with an easy-plane potential. The model admits local string with an Ising spin, which carries a half-lump charge of $\pi_2(S^2) \simeq \mathbb{Z}$ [93–95]. In this limit, this lump charge becomes exact in contrast to the linear model for which the lump charge is only approximate. On the other hand, a kink on the string becomes singular in this limit.

Kosterlitz-Thouless (BKT) transition [96–99] at finite temperature, due to a creation of a pair of vortex and anti-vortex. In our case, such a BKT transition could occur on the domain wall. Such a transition on a soliton has not been studied before. While it is interesting on its own, from the bulk point of view it implies a novel phenomenon that a BKT-like transition by monopoles.

When one of degenerate vacua is lifted, domain walls become unstable as in Fig. 23. In such a case, a closed domain wall describes a bubble of the true vacua inside the false vacuum, which grows in time. Even in such a case, topological solitons such as monopoles can appear in the domain wall worldvolume as in Fig. 23. While the production of topological solitons by a collision of bubbles has been studied in the literature [100–104], topological solitons themselves on a bubble have not. The existence of such topological solitons may affect dynamics and evolution of bubbles in the early universe.

As discussed in this paper, the $O(3)$ model with an easy axis potential yields a domain-wall monopole described by a global vortex in the domain wall world-volume, which is an $O(2)$ model or the XY model. On the other hand, the domain wall has also a translational modulus, that we have not discussed in this paper. By using the both $U(1)$ and translational moduli, one can construct a D-brane soliton, a lump string ending on the domain wall, at least in the limit $\lambda \rightarrow \infty$ of a nonlinear sigma model [105–108]. This is in fact a global vortex in the domain wall world-volume. Since the both configurations are global vortices on the domain wall, one may wonder a relation between them. One can obtain a hint from Fig. 23. In the heavy limit of monopoles $\lambda \rightarrow \infty$, bending of the domain wall would become that of the D-brane soliton.

Acknowledgements

This work is supported in part by JSPS Grant-in-Aid for Scientific Research KAKENHI Grant No. JP22H01221 (M. E. and M. N.), Grant No. JP19K03839 (M. E.), Grant No. JP21J01117 (Y. H.), and Grant No. JP18H01217 (M. N.). The work of M. E. is also supported by the MEXT KAKENHI Grant-in-Aid for Scientific Research on Innovative Areas “Discrete Geometric Analysis for Materials Design” No. JP17H06462 from the MEXT of Japan. M.N. is also supported in part by the WPI program “Sustainability with Knotted Chiral Meta Matter (SKCM²)” at Hiroshima University.

A Classifying composite solitons

We classify composite solitons and present examples focusing on domain-wall vortex composites, monopole vortex composites, and monopole domain wall composites.

A.1 Classification

Before doing so, we first proposed that composite solitons can be classified into the following two types:

1. The SSB + ESB type,

2. The SSB + SSB (hierarchical SSBs) type.

The first type is focused in this paper. See also Ref. [32] for detailed explanations. In such a case, as explained in the main text, first, an SSB $G \rightarrow H$ occurs at high energy scale. Then, there appears a topological soliton that often spontaneously breaks a symmetry in the vacuum H to a subgroup K in the vicinity of the soliton. Such a soliton (called a mother soliton) carries moduli K/H corresponding to the locally happened SSB. Subsequently, in the original theory, a small ESB term is introduced at a low-energy scale that we can treat as a perturbation. Then, it induces a potential term on the moduli of the mother soliton, triggering a further SSB on the mother soliton (or lifting up some part of the moduli). This produces a daughter soliton inside the mother soliton.

The second type is not discussed in this paper but is also investigated in the literature, and so we mention it here. In this case, there are two scalar fields ϕ_1 and ϕ_2 belonging to irreducible representations of the symmetry group G . When these scalar fields develop VEVs in hierarchical energy scales, there occur successive SSBs $G \rightarrow H \rightarrow L$. The first (second) SSB occurs by the VEV of the first (second) fields ϕ_1 (ϕ_2). In this case, a daughter soliton $\pi_n(G/H)$ is created by the first SSB, and a mother soliton $\pi_m(H/L)$ with $m < n$ is created by the second SSB. Note that the total SSB is $G \rightarrow K$, and thus the daughter soliton is not stable when $\pi_n(G/L) = 0$ while the mother is not stable when $\pi_m(G/L) = 0$.

In the following, we summarize known examples for domain-wall vortex composites, monopole vortex composites, and monopole domain wall composites.

A.2 Domain-wall vortex composites

Domain-wall vortex composites can be further classified into (1) confined or (2) deconfined vortices depending on the number of domain walls attached to the vortex. A confined vortex is attached by a single domain wall. Thus, it is continuously pulled by the domain wall and so it is unstable. A deconfined vortex is attached by two (or more) domain walls with the same tension, and is stable. However, it can be confined with its anti-soliton, for which they are connected by two (or more) domain walls.

In the confined case, the wall is metastable and decays quantum mechanically by nucleation of holes bounded by a closed vortex string [70].

A.2.1 The SSB + ESB type

This type of configurations was first studied in Refs. [42, 43].

1. *Axion strings.* Axion strings with the domain wall number N_{DW} [44, 45]. The SSB is $U(1)_{\text{PQ}} \rightarrow \{1\}$ and the ESB is $U(1)_{\text{PQ}} \rightarrow \mathbb{Z}_{N_{\text{DW}}} (\mathbb{Z}_1 = \{1\})$. In the $N_{\text{DW}} = 1$ case (the confined case), one axion string is attached by one sine-Gordon soliton and is unstable. In the general N_{DW} case (the deconfined case), one axion string is attached by N_{DW} sine-Gordon domain walls of the same tension and is stable. In this case, the axion string can be described by a kink inside a domain wall as shown in this paper. In either case, a string and anti-string are connected by N_{DW} domain walls. There are many variations. One recent example is an axionic Alice string [109, 110].

The SSB is $U(1)_{\text{PQ}} \times SU(2) \rightarrow (\mathbb{Z}_4)_{\text{PQ}+(2,3)} \times U(1)_1$ and the ESB is $U(1)_{\text{PQ}} \rightarrow \mathbb{Z}_2$. Although one axion string is attached by two domain walls ($N_{\text{DW}} = 2$), it decays into two axionic Alice strings each of which is attached by one domain wall (the Lazarides-Shafi mechanism [111]).

2. *Two-Higgs doublet models (2HDMs)*. In this model, there are non-Abelian fractional Z -strings [112–114]. In addition to the standard electroweak symmetry breaking $U(1)_Y \times SU(2)_W \rightarrow U(1)_{\text{EM}}$, the relative phase $U(1)_a$ between two Higgs doublets is also spontaneously broken: The SSB is $U(1)_a \times U(1)_Y \times SU(2)_W \rightarrow U(1)_{\text{EM}}$ and the ESB is $U(1)_a \rightarrow \{1\}$ (or $\{\mathbb{Z}_2\}$), depending on the potential. One non-Abelian fractional string is attached by one (or two) domain walls (depending on the interaction), because of an ESB term of relative phase $U(1)_a$. A single $U(1)_a$ string is attached by two (or four) domain walls, $N_{\text{DW}} = 2(4)$, and decays into two non-Abelian fractional strings, each of which is attached by one (or two) domain walls [113, 114]. If the number is two, the composite is stable. On the other hand, a single Z -string can be decomposed into a pair of two non-Abelian fractional Z -strings connected by one (or two) domain wall(s), constituting a vortex molecule [115].
3. *Chiral symmetry breaking in QCD*. The SSB is that of chiral symmetry breaking $SU(3)_L \times SU(3)_R \times U(1)_A \rightarrow SU(3)_{L+R} \times \mathbb{Z}_3$ and the ESB is $U(1)_A \rightarrow \mathbb{Z}_3$ [116]. One axial string winding around the axial $U(1)_A$ symmetry is attached by three chiral domain walls ($N_{\text{DW}} = 3$) because of an explicit $U(1)_A$ symmetry breaking by anomaly [117]. It is unstable to decay into three non-Abelian global vortices each of which is attached by one chiral domain wall [13, 118, 119].
4. *High density QCD*. In high density limit of QCD, the ground state is the color-flavor locked (CFL) phase exhibiting color superconductivity [120]. It admits non-Abelian semi-superfluid vortices [13, 121–124]. A single non-Abelian semi-superfluid vortex can be decomposed into a pair of chiral non-Abelian vortices connected by one (or two) non-Abelian chiral domain wall(s), depending on the interaction [125]. A single chiral non-Abelian vortex is attached by one (or two) non-Abelian chiral domain wall(s) [125].
5. *Supersymmetric theories*. A wall in a wall as a string in supersymmetric theories [48, 126–128]. If composite solitons are BPS, then a vortex is attached by two domain walls and they are stable. In particular in the model in Ref. [48], when a single ANO string is absorbed into a domain wall, it splits into two half-quantized strings. This situation is the same with chiral p -wave superconductors (the item 9, below).
6. *Domain-wall Skyrmions in field theory*. Domain-wall Skyrmions exist in the $U(1)$ gauge theory coupled with two complex scalar fields, or the $\mathbb{C}P^1$ model ($O(3)$ non-linear sigma model) with the easy-axis potential. The SSB is $SU(2) \rightarrow U(1)$ and the ESB is $SU(2) \rightarrow U(1)$. A domain wall connects vacua with a VEV of only one of ϕ_1 and ϕ_2 . A vortex in the bulk is absorbed into the wall and becomes a

sine-Gordon soliton inside the wall [49]. In strong gauge coupling, the model reduces to the $\mathbb{C}P^1$ model. A $\mathbb{C}P^1$ lump (baby Skyrmion) is absorbed into a $\mathbb{C}P^1$ wall and can be described as a sine-Gordon soliton in the domain wall [49, 50] (see also Refs. [71–75]). This can be generalized to the $\mathbb{C}P^{N-1}$ model, for which the SSB is $SU(N) \rightarrow SU(N-1) \times U(1)$ and the ESB is $SU(N) \rightarrow U(1)^{N-1}$. The $\mathbb{C}P^{N-1}$ model admits N vacua and $N-1$ parallel domain walls [129–133]. Then, $\mathbb{C}P^{N-1}$ lumps absorbed into $\mathbb{C}P^{N-1}$ domain walls can be described by $U(1)^{N-1}$ coupled sine-Gordon solitons in the domain walls [52]. Non-Abelian vortices [53–56] absorbed into a non-Abelian domain wall [59–61] can be described as non-Abelian sine-Gordon solitons [57, 58] in the domain-wall effective theory which is a $U(N)$ chiral Lagrangian with a pion mass [51, 69].

7. *Condensed matter example 1: Domain-wall Skyrmions in chiral magnets* [34–38] (see also [39]). This can be realized by adding the Dzyaloshinskii-Moriya interaction to the field theoretical $\mathbb{C}P^1$ domain-wall Skyrmions mentioned above (the item 6). Previously, a Bloch line in a Bloch wall in magnets was well known [134, 135].
8. *Condensed matter example 2: Two-component miscible BECs [136–143] and two-gap superconductors [144–149]*. There are two complex scalar fields ϕ_1 and ϕ_2 describing condensates of two atoms of BECs or gap functions of superconductors. In either case, the SSB pattern is: $U(1)_1 \times U(1)_2 \simeq [U(1)_g \times U(1)_r]/\mathbb{Z}_2 \rightarrow \{1\}$ and the ESB is $U(1)_r \rightarrow \{1\}$, where the $U(1)_g$ is the overall phase rotation, which is gauged for superconductors but not for BECs. The ESB term is $\phi_1^* \phi_2 + \text{c.c.}$ called the Josephson interaction for superconductors, or Rabi interaction for BECs. Either of ϕ_1 and ϕ_2 can have a fractionally quantized vortex attached by a sine-Gordon soliton, like axion strings. A vortex winding around ϕ_1 and the one around ϕ_2 are connected by a sine-Gordon soliton, constituting a vortex molecule. Generalizations to N -components were also studied for BECs [150, 151] and superconductors [152]. The extension to more general charge assignments introduces various types of vortex molecules [153].
9. *Condensed matter example 3: Chiral p -wave superconductors*. Similar to two-gap superconductors, there are two gap functions (complex scalar fields) ϕ_1 and ϕ_2 . However, the ESB term in this case is $\phi_1^{*2} \phi_2^2 + \text{c.c.}$, in contrast to the conventional Josephson term $\phi_1^* \phi_2 + \text{c.c.}$ for two-gap superconductors. The ground states are either $(\phi_1, \phi_2) \sim (1, 0)$ or $(0, 1)$. The SSB is $U(1)_1 \times U(1)_2 \simeq [U(1)_g \times U(1)_r]/\mathbb{Z}_2 \rightarrow U(1)_1 = U(1)_{g-r}$ at $(\phi_1, \phi_2) \sim (1, 0)$ or $U(1)_2 = U(1)_{g+r}$ at $(\phi_1, \phi_2) \sim (0, 1)$, where $U(1)_g$ is the overall gauge transformation and $U(1)_r$ is a relative phase rotation. The ESB is $U(1)_r \rightarrow \mathbb{Z}_2$. A chiral domain wall exists connecting the two ground states. A half-quantum vortex can stably exist on the chiral domain wall [154, 155], which can be identified with a kink (sine-Gordon soliton with a half (π) period) inside the domain wall. This situation is close to the above item 6 in which the kink is a sine-Gordon soliton with 2π period. When a singly quantized vortex in the bulk is absorbed into the domain wall, it splits into two half-quantized vortices. This situation is the same with supersymmetric theory [48]. Apart from the domain wall, in one region, a singly quantized

vortex winding around $U(1)_g$ once is split into two half-quantized vortices connected by two domain walls constituting a vortex molecule [156, 157]. The other ground state appears inside the region between the domain walls.

10. *Condensed matter example 3: 3P_2 neutron superfluids.* A singly quantized vortex is split into two half-quantized non-Abelian vortices connected by one or two solitons [158–160] as the case of chiral p -wave superconductors.
11. *Condensed matter example 4: ${}^3\text{He}$ superfluids.* A spin-mass vortex is confined by a soliton in the B-phase, and a half-quantum vortex is confined by a soliton in polar and polar-distorted A phases [21, 40, 41, 161, 162]. A Mermin-Ho vortex within a domain wall exists [21].

A.2.2 The SSB + SSB type

1. *Wall-vortex composites in GUTs* [42, 43]. The relevant sequential SSBs are $SO(10) \rightarrow SU(4)_c \times SU(2)_R \times SU(2)_L \times \mathbb{Z}_2^C \rightarrow SU(3)_c \times SU(2)_L \times U(1)_Y$, in which \mathbb{Z}_2^C corresponds to the charge conjugation. The symmetry $SU(4)_c \times SU(2)_R \times SU(2)_L$ is the same as that of the Pati-Salam model [163]. At the first symmetry breaking, the \mathbb{Z}_2 string appears due to $\pi_1(SO(10)/SU(4)_c \times SU(2)_R \times SU(2)_L \times \mathbb{Z}_2^C) \simeq \pi_0(\mathbb{Z}_2) = \mathbb{Z}_2$. The second breaking gives rise to the domain wall separating two vacua which are interchanged by the charge conjugation. Since \mathbb{Z}_2^C is embedded in the continuous $SO(10)$ symmetry, the domain wall is not topologically stable but is bounded by the \mathbb{Z}_2 strings. The domain walls collapse before they dominate the energy of the universe, so that there is no domain wall problem.
2. *The Georgi-Machacek model.* The sequential SSBs are $U(1)_Y \times SU(2)_W \rightarrow \mathbb{Z}_2 \times U(1)_{EM} \rightarrow U(1)_{EM}$ [164]. The first SSB due to VEVs of three $SU(2)$ triplet Higgs fields produces a \mathbb{Z}_2 string, and the second SSB due to a VEV of an $SU(2)$ doublet Higgs field gives a domain wall attached to the string.
3. *Alice strings attached by domain walls.* The sequential SSBs are $U(1) \times SU(2) \rightarrow \mathbb{Z}_4 \times U(1) \rightarrow \{1\}$ [165, 166]. The first SSB due to the complex triplet representation $\mathbf{3}$ of $SU(2)$ yields a (BPS) Alice strings [167, 168], and the second SSB occurring due to the fundamental representation of $SU(2)$ gives a domain wall attached to each Alice string [165, 166]. However, the existence of solitons at the second SSB does not rely on the usual homotopy arguments, but on a nontrivial Aharonov-Bohm phase. Such a soliton is called a Aharonov-Bohm defect.
4. *Two-flavor dense QCD.* The sequential SSBs are $U(1)_B \times SU(3)_C \rightarrow \mathbb{Z}_6 \times SO(3) \rightarrow \mathbb{Z}_3$. The first SSB due to the representation $\mathbf{6}$ (a 3×3 anti-symmetric tensor) of $SU(3)$ yields a non-Abelian Alice strings [169, 170], and the second SSB occurring due to the anti-fundamental representation $\mathbf{\bar{3}}$ of $SU(3)$ gives solitons (Aharonov-Bohm defects) attached to the Alice strings [171]. Thus, non-Abelian Alice string are confined by solitons to constitute “mesonic or baryonic molecules”.

A.2.3 The modified XY model

The third type which is rather nontrivial is the modified XY model [172] or its Goldstone model extension [173, 174]. In a certain parameter region, two hierarchical SSBs occur $U(1) \rightarrow \mathbb{Z}_2 \rightarrow \{1\}$. In numerical simulations, a two-step phase transition was found. In the first step, vortices are created (BKT-type transition) and in the second step domain walls connecting them (Ising-type transition) are created [173].

A.3 Vortex monopole composites

A.3.1 The SSB + ESB type

When a monopole is attached by two (or more) vortex strings of the same tension, the configuration is stable. In this case, it is often the case that a monopole can be regarded as a kink on a vortex string.

1. *1/4 BPS vortex-monopoles in supersymmetric gauge theory.* A $U(N)$ gauge theory with N fundamental Higgs scalar fields with a common $U(1)$ charge admits a 't Hooft-Polyakov type monopole attached by two non-Abelian vortex strings of the same tension [64]. The SSB is $U(N)_C \times SU(N)_F \rightarrow SU(N)_{C+F}$ and the ESB is $SU(N)_F \rightarrow U(1)^{N-1}$. The SSB without ESB yields a non-Abelian vortex carrying $\mathbb{C}P^{N-1}$ moduli [53–56], and the ESB induces a potential on the moduli. The monopole can be realized as a $\mathbb{C}P^{N-1}$ kink inside the non-Abelian vortex world-sheet. In a supersymmetric extension, these are 1/4 BPS states and are nonperturbatively stable.² Such a vortex monopole configuration yields the correspondence between quantum effects in the two dimensional $\mathbb{C}P^{N-1}$ model and four dimensional gauge theory [65, 66]. Non-Abelian monopoles on multiple non-Abelian vortices can be also realized [67]. The cases of SO, USp gauge groups were studied in Ref. [68].
2. *Topological Nambu monopole in 2HDMs* [80, 90, 91].

The SSB is $SU(2)_W \times SU(2)_{\text{cust.}} \times U(1)_a \rightarrow U(1)_{\text{em}} \times SU(2)_{\text{cust.}}$ when $\theta_W = 0$. Here $SU(2)_{\text{cust.}}$ is called the Higgs custodial symmetry. Turning on $\theta_W \neq 0$ or the ESB interaction in the Higgs potential, the original symmetry is explicitly broken into $SU(2)_W \times U(1)_Y \times \mathbb{Z}_2^{\text{CP}} \times U(1)_a$, which is spontaneously broken into $U(1)_{\text{em}} \times \mathbb{Z}_2^{\text{CP}}$. The SSB without ESB yields a non-Abelian vortex carrying $\mathbb{C}P^1$ moduli, and the ESB induces a potential on the moduli. In contrast to a Nambu monopole in Standard Model(SM) which is attached by one Z -string as mentioned in Sec. A.3.3, there is a topological Nambu monopole in 2HDMs attached by the two non-Abelian topological Z -strings [80, 90, 91]. The \mathbb{Z}_2^{CP} symmetry ensures the degeneracy of the tensions of the two Z -strings. If \mathbb{Z}_2^{CP} is also explicitly broken, the monopole is confined and is unstable [80]. Otherwise the monopole is stable [90]. Although the two Z -strings correspond to two minima of the lifted potential of the $\mathbb{C}P^1$ moduli, this

²These can be obtained from vortex instantons (instanton immersed into a vortex) [66, 175, 176] by the Scherk-Schwarz dimensional reduction [177] or an S^1 compactification with a twisted boundary condition [175].

monopole connecting the strings cannot be regarded as a kink on a string in the sense that magnetic fluxes spread out almost spherically but not confined. In spite of the trivial second homotopy group of the vacuum, the monopole has a non-trivial $U(1)_{\text{em}}$ bundle [91].

A texture version is Skyrmions on a vortex string: vortex Skyrmions realized as sine-Gordon kinks inside a vortex string in a Skyrme model with a BEC-inspired potential [81, 178] or a simpler potential [82, 179].

A.3.2 The SSB + SSB type

1. *Confinement phase of QCD.* Quarks are confined by color electric flux tubes in QCD, giving rise to a confinement. As a dual superconductor description, monopoles are confined by color magnetic flux tubes or vortices [180–182], where a monopole and anti-monopole is connected by a color magnetic flux tube.

The generalization of this vortex-monopole composite to supersymmetric QCD was proposed to study the confinement problem [183–187] in which hierarchical SSBs was studied: $SU(N+1) \times SU(N)_F \rightarrow U(N)_C \times SU(N)_F \rightarrow SU(N)_{C+F}$. In the first SSB a 't Hooft-Polyakov monopole is created, and in the second SSB it is attached by a non-Abelian vortex string.

2. *High density QCD.* In high density QCD, a monopole and anti-monopole are confined by non-Abelian vortex strings [188, 189], explaining a quark-hadron continuity or duality [189].
3. *Grand unified theory(GUT).* There is a cosmological monopole problem in GUTs: monopoles are created at GUT phase transition from a unified gauge group G to that of the standard model but no monopoles are observed [190–192]. To avoid this problem, it was proposed that in a certain period of early universe, the electric magnetic $U(1)$ symmetry was spontaneously broken. $G = SU(5), SO(10) \rightarrow SU(3) \times SU(2) \times U(1) \rightarrow SU(3) \times SU(2)$. Thus all (anti-)monopoles are confined to enhance pair annihilations of monopole and anti-monopole (the Langacker-Pi mechanism [193]).
4. *Beads on a string.* Monopoles on a string exist in an $SU(2)$ gauge theory coupled to two adjoint real Higgs scalar fields [194–197]. In this case, hierarchical symmetry breakings are considered as $SU(2) \rightarrow U(1) \rightarrow \mathbb{Z}_2$: in the first breaking a monopole is created, and in the second breaking \mathbb{Z}_2 strings attached to the monopole are created. This composite is sometimes called a necklace. This can be regarded as a kink on a string. The gauge kinetic mixing with the SM $U(1)_{\text{em}}$ field was discussed in Refs. [198, 199]. See Refs. [200, 201] for similar objects.
5. *Alice-string monopole composites.* Alice-string monopole composites are considered [166]. One monopole is confined but two monopoles are not.

6. *Condensed matter example 1: Chiral liquid crystals and chiral magnets* [28–30, 202]. A toron is a pair of monopole and anti-monopole connected by lump (baby Skyrmion) string.
7. *Condensed matter example 2: ${}^3\text{He}$ superfluids* [21]. This is called a nexus soliton.

A.3.3 Exception

Nambu monopole in the Standard Model (SM) [203–205]. The fact that the vacuum manifold of the SM is S^3 leads to no stable monopole nor strings ($\pi_1(S^3) = \pi_2(S^3) = \{1\}$). However, a monopole attached by a single Z -string, called the Nambu monopole, exists and has a non-zero magnetic $U(1)_{\text{em}}$ flux. In contrast to the Nambu monopole in 2HDMs, the monopole in the SM cannot be stable but is confined. In addition, the monopole cannot have any non-trivial $U(1)_{\text{em}}$ bundle around it because $U(1)_{\text{em}}$ cannot be defined at the core of the Z -string [91].

A.4 Domain-wall monopoles

A.4.1 The SSB + ESB type

Compared with vortex monopoles, there are not many studies for domain-wall monopoles³ except for the following examples.

1. *Local monopoles in a non-Abelian domain wall.* $SU(N)$ 't Hooft-Polyakov monopoles are $U(1)^{N-1}$ global vortices [69] inside a non-Abelian domain wall [59–61].⁴ A global analogue of this composite is studied in the main text of this paper. A texture version of this composite configuration is a domain-wall Skyrmions where Skyrmions are realized as lumps inside the domain wall [33, 58, 87, 88] (see also Ref.[89]).

A.4.2 The SSB + SSB type

As far as we know, there are no examples of this type.

B $N = 2$ axion string-wall composite: An effective Lagrangian approach

In this appendix, we show the validity of the ansatz in Eq. (3.16) for a vortex-monopole composite, i. e. a kink inside a vortex, in the $O(2)$ model ($N = 2$) from the view point of the moduli approximation [210, 211]. We consider the two component scalar fields $\phi = (\phi_1, \phi_2)$ with the Lagrangian (2.1) with the additional potential (2.2) for $N = 2$:

$$\mathcal{L}_2 = \frac{1}{2}(\partial_\mu \phi)^2 - \frac{\lambda}{4}(\phi^2 - v^2)^2 + \tilde{\alpha}(\phi_2)^2. \quad (\text{B.1})$$

³There is an example of unstable composite of a domain wall and monopole in a GUT. The SSB is $SU(5) \times \mathbb{Z}_2 \rightarrow [SU(3)_C \times SU(2)_L \times U(1)_Y]/\mathbb{Z}_6$ with a global symmetry \mathbb{Z}_2 . A domain wall and monopoles coexist. However, after the monopoles are absorbed into the domain wall, they are unstable to decay [206–208]. This was proposed as a monopole eraser to solve the cosmological monopole problem.

⁴These can be obtained from domain-wall instantons [60, 69, 209] by the Scherk-Schwarz dimensional reduction [177] or an S^1 compactification with a twisted boundary condition.

We assume $\tilde{\alpha} > 0$ hereafter (in the main text we have used $\alpha = -\tilde{\alpha}$), and the weak coupling regime is

$$\frac{\lambda v^4}{4} \gg \tilde{\alpha} v^2. \quad (\text{B.2})$$

The vacua can be obtained by solving

$$\frac{\delta V}{\delta \phi_1} = \lambda \phi_1 (\phi^2 - v^2) = 0, \quad \frac{\delta V}{\delta \phi_2} = \lambda \phi_2 (\phi^2 - v^2) - 2\tilde{\alpha} \phi_2 = 0. \quad (\text{B.3})$$

There are two solutions

$$\phi_1 = 0, \quad \phi_2 = \pm v \sqrt{1 + \frac{2\tilde{\alpha}}{\lambda v^2}}. \quad (\text{B.4})$$

Let us perturb ϕ around one of the vacua as

$$\phi_1 = v \delta_1, \quad \phi_2 = v \sqrt{1 + \frac{2\tilde{\alpha}}{\lambda v^2}} + v \delta_2. \quad (\text{B.5})$$

Plugging these into the potential and keeping only quadratic terms of $\delta_{1,2}$, we have

$$\begin{aligned} V &= \frac{\lambda}{4} \left[v^2 \delta_1^2 + v^2 \left(\sqrt{1 + \frac{2\tilde{\alpha}}{\lambda v^2}} + \delta_2 \right)^2 - v^2 \right]^2 - \tilde{\alpha} v^2 \left(\sqrt{1 + \frac{2\tilde{\alpha}}{\lambda v^2}} + \delta_2 \right)^2 \\ &= \frac{\lambda v^4}{4} \left[\delta_1^2 + 1 + \frac{2\tilde{\alpha}}{\lambda v^2} + 2\sqrt{1 + \frac{2\tilde{\alpha}}{\lambda v^2}} \delta_2 + \delta_2^2 - 1 \right]^2 - \tilde{\alpha} v^2 \left(1 + \frac{2\tilde{\alpha}}{\lambda v^2} + 2\sqrt{1 + \frac{2\tilde{\alpha}}{\lambda v^2}} \delta_2 + \delta_2^2 \right) \\ &= \frac{\lambda v^4}{4} \left[\frac{2\tilde{\alpha}}{\lambda v^2} + 2\sqrt{1 + \frac{2\tilde{\alpha}}{\lambda v^2}} \delta_2 + \delta_1^2 + \delta_2^2 \right]^2 - \tilde{\alpha} v^2 \left(1 + \frac{2\tilde{\alpha}}{\lambda v^2} + 2\sqrt{1 + \frac{2\tilde{\alpha}}{\lambda v^2}} \delta_2 + \delta_2^2 \right) \\ &\simeq \frac{\lambda v^4}{4} \left[\left(\frac{2\tilde{\alpha}}{\lambda v^2} \right)^2 + 2 \frac{2\tilde{\alpha}}{\lambda v^2} 2\sqrt{1 + \frac{2\tilde{\alpha}}{\lambda v^2}} \delta_2 + 2 \frac{2\tilde{\alpha}}{\lambda v^2} (\delta_1^2 + \delta_2^2) + 4 \left(1 + \frac{2\tilde{\alpha}}{\lambda v^2} \right) \delta_2^2 \right] \\ &\quad - \tilde{\alpha} v^2 \left(1 + \frac{2\tilde{\alpha}}{\lambda v^2} + 2\sqrt{1 + \frac{2\tilde{\alpha}}{\lambda v^2}} \delta_2 + \delta_2^2 \right) \\ &\simeq \frac{\lambda v^4}{4} \left[2 \frac{2\tilde{\alpha}}{\lambda v^2} (\delta_1^2 + \delta_2^2) + 4 \left(1 + \frac{2\tilde{\alpha}}{\lambda v^2} \right) \delta_2^2 \right] - \tilde{\alpha} v^2 \delta_2^2 \\ &\simeq \tilde{\alpha} v^2 \delta_1^2 + \lambda v^4 \left(1 + \frac{2\tilde{\alpha}}{\lambda v^2} \right) \delta_2^2. \end{aligned} \quad (\text{B.6})$$

Hence, there are two typical masses

$$m_1 = \sqrt{2\tilde{\alpha}}, \quad m_2 = \sqrt{2\lambda \left(1 + \frac{2\tilde{\alpha}}{\lambda v^2} \right)} v \simeq \sqrt{2\lambda} v, \quad (\text{B.7})$$

where m_1 is the mass of the pseudo-NG mode while m_2 is that of the Higgs mode. The weak coupling regime requires

$$m_1 \ll m_2. \quad (\text{B.8})$$

The $\mathbb{Z}_2^{(2)}$ is spontaneously broken in the above vacua, and it gives rise to a mother domain wall. In order to estimate energy scales, let us consider the $\mathbb{Z}_2^{(1)}$ charged mother domain wall by fixing the amplitude $|\phi| = v$ as

$$\phi = v(\pm \cos \Theta, \sin \Theta), \quad (\text{B.9})$$

the \pm signature is responsible for the $\mathbb{Z}_2^{(1)}$ charge. Then, the Lagrangian reduces to the sine-Gordon model with a half period as

$$\mathcal{L}_2 = \frac{v^2}{2} \partial_\mu \Theta \partial^\mu \Theta - v^2 \tilde{\alpha} \sin^2 \Theta. \quad (\text{B.10})$$

The mother domain wall solution can be approximated by a sine-Gordon soliton with a half period

$$\Theta_0(x) = 2 \arctan e^{m_1 x} + \frac{\pi}{2}, \quad (\text{B.11})$$

with the wall width m_1^{-1} . Then, the tension (energy per unit area) of the mother domain wall can be approximated by

$$\sigma = 2v^2 m_1. \quad (\text{B.12})$$

The mother domain wall is produced at the mass scale v , but its tension $v^2 m_1$ is much smaller than the typical scale v^3 .

As soon as the mother domain wall is generated, it breaks the $\mathbb{Z}_2^{(1)}$ symmetry, and a daughter domain wall can be produced in general. To estimate the energy scales, let us next take the product ansatz

$$\phi = v(\varphi(y) \cos \Theta_0(x), \sin \Theta_0(x)), \quad (\text{B.13})$$

where y is the world-volume coordinates of the mother domain wall. Plugging this into the Lagrangian and integrate it over x , we get the effective Lagrangian

$$L_2 = \int dx \mathcal{L}_2 = \frac{v^2}{m_1} \partial_{\mu'} \varphi \partial^{\mu'} \varphi - \frac{\lambda v^4}{3m_1} (\varphi^2 - 1)^2 - \frac{m_1 v^2}{3} \varphi^2, \quad (\text{B.14})$$

where $\mu' = 0, 2, 3$. There is a $\mathbb{Z}_2^{(1)}$ symmetry and it is spontaneously broken in the vacua $\varphi = \pm 1$ of the effective Lagrangian (B.14). The inner kink is obtained as

$$\varphi \simeq \frac{\sqrt{m_2^2 - m_1^2}}{m_2} \tanh \left(\frac{\sqrt{m_2^2 - m_1^2}}{\sqrt{6}} y \right), \quad (\text{B.15})$$

and its tension (energy per unit length) is given by

$$\mu \simeq \frac{4\sqrt{2} (m_2^2 - m_1^2)^{\frac{3}{2}}}{3\sqrt{3} m_1 \lambda} \simeq \frac{4\sqrt{2} m_2^3}{3\sqrt{3} \lambda m_1} = \frac{8\sqrt{2} m_2}{3\sqrt{3} m_1} v^2. \quad (\text{B.16})$$

Thus, the inner kink, generated at the same instant as the mother domain wall produced at the energy scale v , has the tension $\mu \simeq (m_2/m_1)v^2$ and the width is $\sqrt{6}m_2^{-1}$. This inner kink is nothing but a vortex from the bulk point of view, as discussed in the main text. We thus have obtained the ansatz in Eq. (3.16).

References

- [1] R. Rajaraman, *Solitons and Instantons: An Introduction to Solitons and Instantons in Quantum Field Theory*. North-Holland Personal Library, 1987.
- [2] N. S. Manton and P. Sutcliffe, *Topological solitons*, Cambridge Monographs on Mathematical Physics. Cambridge University Press, 2004, [10.1017/CBO9780511617034](https://doi.org/10.1017/CBO9780511617034).
- [3] Y. M. Shnir, *Magnetic Monopoles*, Text and Monographs in Physics. Springer, Berlin/Heidelberg, 2005, [10.1007/3-540-29082-6](https://doi.org/10.1007/3-540-29082-6).
- [4] T. Vachaspati, *Kinks and domain walls: An introduction to classical and quantum solitons*. Cambridge University Press, 4, 2010, [10.1017/CBO9780511535192](https://doi.org/10.1017/CBO9780511535192).
- [5] M. Dunajski, *Solitons, instantons, and twistors*, Oxford Graduate Texts In Mathematics. Oxford University Press, U.S.A., 2010.
- [6] E. J. Weinberg, *Classical solutions in quantum field theory: Solitons and Instantons in High Energy Physics*, Cambridge Monographs on Mathematical Physics. Cambridge University Press, 9, 2012, [10.1017/CBO9781139017787](https://doi.org/10.1017/CBO9781139017787).
- [7] Y. M. Shnir, *Topological and Non-Topological Solitons in Scalar Field Theories*. Cambridge University Press, 7, 2018, [10.1017/9781108555623](https://doi.org/10.1017/9781108555623).
- [8] D. Tong, *TASI lectures on solitons: Instantons, monopoles, vortices and kinks*, in *Theoretical Advanced Study Institute in Elementary Particle Physics: Many Dimensions of String Theory*, 6, 2005, [hep-th/0509216](https://arxiv.org/abs/hep-th/0509216).
- [9] D. Tong, *Quantum Vortex Strings: A Review*, *Annals Phys.* **324** (2009) 30 [[0809.5060](https://arxiv.org/abs/0809.5060)].
- [10] M. Eto, Y. Isozumi, M. Nitta, K. Ohashi and N. Sakai, *Solitons in the Higgs phase: The Moduli matrix approach*, *J. Phys. A* **39** (2006) R315 [[hep-th/0602170](https://arxiv.org/abs/hep-th/0602170)].
- [11] M. Shifman and A. Yung, *Supersymmetric Solitons and How They Help Us Understand Non-Abelian Gauge Theories*, *Rev. Mod. Phys.* **79** (2007) 1139 [[hep-th/0703267](https://arxiv.org/abs/hep-th/0703267)].
- [12] M. Shifman and A. Yung, *Supersymmetric solitons*, Cambridge Monographs on Mathematical Physics. Cambridge University Press, 5, 2009, [10.1017/CBO9780511575693](https://doi.org/10.1017/CBO9780511575693).
- [13] M. Eto, Y. Hirono, M. Nitta and S. Yasui, *Vortices and Other Topological Solitons in Dense Quark Matter*, *PTEP* **2014** (2014) 012D01 [[1308.1535](https://arxiv.org/abs/1308.1535)].
- [14] T. W. B. Kibble, *Topology of Cosmic Domains and Strings*, *J. Phys. A* **9** (1976) 1387.
- [15] T. W. B. Kibble, *Some Implications of a Cosmological Phase Transition*, *Phys. Rept.* **67** (1980) 183.
- [16] A. Vilenkin, *Cosmic Strings and Domain Walls*, *Phys. Rept.* **121** (1985) 263.
- [17] M. Hindmarsh and T. Kibble, *Cosmic strings*, *Rept. Prog. Phys.* **58** (1995) 477 [[hep-ph/9411342](https://arxiv.org/abs/hep-ph/9411342)].
- [18] T. Vachaspati, L. Pogosian and D. Steer, *Cosmic Strings*, *Scholarpedia* **10** (2015) 31682 [[1506.04039](https://arxiv.org/abs/1506.04039)].
- [19] A. Vilenkin and E. S. Shellard, *Cosmic Strings and Other Topological Defects*. Cambridge University Press, 7, 2000.
- [20] N. D. Mermin, *The topological theory of defects in ordered media*, *Rev. Mod. Phys.* **51** (1979) 591.

- [21] G. E. Volovik, *The Universe in a helium droplet*, International Series of Monographs on Physics. Oxford Scholarship Online, 2009, [10.1093/acprof:oso/9780199564842.001.0001](https://doi.org/10.1093/acprof:oso/9780199564842.001.0001).
- [22] B. V. Svistunov, E. S. Babaev and N. V. Prokof'ev, *Superfluid States of Matter*, Cambridge Monographs on Mathematical Physics. CRC Press, 2015, [10.1201/b18346](https://doi.org/10.1201/b18346).
- [23] A. V. Ustinov, *Solitons in Josephson Junctions: Physics of Magnetic Fluxons in Superconducting Junctions and Arrays*. Wiley-VCH, 2015.
- [24] Z. F. Ezawa, *Quantum Hall Effects Recent Theoretical and Experimental Developments, 3rd Edition*. World Scientific, 2013, [10.1142/8210](https://doi.org/10.1142/8210).
- [25] Y. Kawaguchi and M. Ueda, *Spinor Bose-Einstein condensates*, *Phys. Rept.* **520** (2012) 253.
- [26] L. Pismen, *Vortices in Nonlinear Fields: From Liquid Crystals to Superfluids, from Non-Equilibrium Patterns to Cosmic Strings*, International Series of Monographs on Physics. Clarendon Press, 1999.
- [27] Y. M. Bunkov and H. Godfrin, *Topological Defects and the Non-Equilibrium Dynamics of Symmetry Breaking Phase Transitions (NATO Science Series)*. Springer, Dordrecht, 2000, [10.1007/978-94-011-4106-2](https://doi.org/10.1007/978-94-011-4106-2).
- [28] G. P. Alexander, B. G.-g. Chen, E. A. Matsumoto and R. D. Kamien, *Colloquium: Disclination loops, point defects, and all that in nematic liquid crystals*, *Rev. Mod. Phys.* **84** (2012) 497.
- [29] I. I. Smalyukh, *Review: knots and other new topological effects in liquid crystals and colloids*, *Rept. Prog. Phys.* **83** (2020) 106601.
- [30] J.-S. Wu and I. I. Smalyukh, *Hopfions, heliknotons, skyrmions, torons and both abelian and nonabelian vortices in chiral liquid crystals*. Taylor & Francis, 2022, [10.1080/21680396.2022.2040058](https://doi.org/10.1080/21680396.2022.2040058).
- [31] S. Shankar, A. Souslov, M. J. Bowick, M. C. Marchetti and V. Vitelli, *Topological active matter*, *Nature Reviews Physics* **4** (2022) 380.
- [32] M. Nitta, *Relations among topological solitons*, *Phys. Rev. D* **105** (2022) 105006 [[2202.03929](https://arxiv.org/abs/2202.03929)].
- [33] M. Eto, K. Nishimura and M. Nitta, *How baryons appear in low-energy QCD: Domain-wall Skyrmion phase in strong magnetic fields*, [2304.02940](https://arxiv.org/abs/2304.02940).
- [34] R. Cheng, M. Li, A. Sapkota, A. Rai, A. Pokhrel, T. Mewes et al., *Magnetic domain wall skyrmions*, *Phys. Rev. B* **99** (2019) 184412.
- [35] S. Lepadatu, *Emergence of transient domain wall skyrmions after ultrafast demagnetization*, *Phys. Rev. B* **102** (2020) 094402.
- [36] T. Nagase et al., *Observation of domain wall bimerons in chiral magnets*, *Nature Commun.* **12** (2021) 3490 [[2004.06976](https://arxiv.org/abs/2004.06976)].
- [37] K. Yang, K. Nagase and Y. Hirayama *et.al.*, *Wigner solids of domain wall skyrmions*, *Nat Commun* **12** (2021) 6006.
- [38] C. Ross and M. Nitta, *Domain-wall skyrmions in chiral magnets*, *Phys. Rev. B* **107** (2023) 024422 [[2205.11417](https://arxiv.org/abs/2205.11417)].
- [39] S. K. Kim and Y. Tserkovnyak, *Magnetic Domain Walls as Hosts of Spin Superfluids and Generators of Skyrmions*, *Phys. Rev. Lett.* **119** (2017) 047202 [[1701.08273](https://arxiv.org/abs/1701.08273)].

- [40] G. E. Volovik, *Composite topological objects in topological superfluids*, *J. Exp. Theor. Phys.* **131** (2020) 11 [[1912.05962](#)].
- [41] G. E. Volovik and K. Zhang, *String monopoles, string walls, vortex skyrmions, and nexus objects in the polar distorted B phase of ^3He* , *Phys. Rev. Res.* **2** (2020) 023263 [[2002.07578](#)].
- [42] T. W. B. Kibble, G. Lazarides and Q. Shafi, *Walls Bounded by Strings*, *Phys. Rev. D* **26** (1982) 435.
- [43] A. E. Everett and A. Vilenkin, *Left-right Symmetric Theories and Vacuum Domain Walls and Strings*, *Nucl. Phys. B* **207** (1982) 43.
- [44] A. Vilenkin and A. E. Everett, *Cosmic Strings and Domain Walls in Models with Goldstone and PseudoGoldstone Bosons*, *Phys. Rev. Lett.* **48** (1982) 1867.
- [45] M. Kawasaki and K. Nakayama, *Axions: Theory and Cosmological Role*, *Ann. Rev. Nucl. Part. Sci.* **63** (2013) 69 [[1301.1123](#)].
- [46] A. A. Abrikosov, *On the Magnetic properties of superconductors of the second group*, *Sov. Phys. JETP* **5** (1957) 1174.
- [47] H. B. Nielsen and P. Olesen, *Vortex Line Models for Dual Strings*, *Nucl. Phys. B* **61** (1973) 45.
- [48] R. Auzzi, M. Shifman and A. Yung, *Domain Lines as Fractional Strings*, *Phys. Rev. D* **74** (2006) 045007 [[hep-th/0606060](#)].
- [49] M. Nitta, *Josephson vortices and the Atiyah-Manton construction*, *Phys. Rev. D* **86** (2012) 125004 [[1207.6958](#)].
- [50] M. Kobayashi and M. Nitta, *Sine-Gordon kinks on a domain wall ring*, *Phys. Rev. D* **87** (2013) 085003 [[1302.0989](#)].
- [51] M. Nitta, *Josephson junction of non-Abelian superconductors and non-Abelian Josephson vortices*, *Nucl. Phys. B* **899** (2015) 78 [[1502.02525](#)].
- [52] T. Fujimori, H. Iida and M. Nitta, *Field theoretical model of multilayered Josephson junction and dynamics of Josephson vortices*, *Phys. Rev. B* **94** (2016) 104504 [[1604.08103](#)].
- [53] A. Hanany and D. Tong, *Vortices, instantons and branes*, *JHEP* **07** (2003) 037 [[hep-th/0306150](#)].
- [54] R. Auzzi, S. Bolognesi, J. Evslin, K. Konishi and A. Yung, *NonAbelian superconductors: Vortices and confinement in $N=2$ SQCD*, *Nucl. Phys. B* **673** (2003) 187 [[hep-th/0307287](#)].
- [55] M. Eto, Y. Isozumi, M. Nitta, K. Ohashi and N. Sakai, *Moduli space of non-Abelian vortices*, *Phys. Rev. Lett.* **96** (2006) 161601 [[hep-th/0511088](#)].
- [56] M. Eto, K. Konishi, G. Marmorini, M. Nitta, K. Ohashi, W. Vinci et al., *Non-Abelian Vortices of Higher Winding Numbers*, *Phys. Rev. D* **74** (2006) 065021 [[hep-th/0607070](#)].
- [57] M. Nitta, *Non-Abelian Sine-Gordon Solitons*, *Nucl. Phys. B* **895** (2015) 288 [[1412.8276](#)].
- [58] M. Eto and M. Nitta, *Non-Abelian Sine-Gordon Solitons: Correspondence between $SU(N)$ Skyrmions and $\mathbb{C}P^{N-1}$ Lumps*, *Phys. Rev. D* **91** (2015) 085044 [[1501.07038](#)].
- [59] M. Shifman and A. Yung, *Localization of nonAbelian gauge fields on domain walls at weak coupling (D-brane prototypes II)*, *Phys. Rev. D* **70** (2004) 025013 [[hep-th/0312257](#)].

- [60] M. Eto, M. Nitta, K. Ohashi and D. Tong, *Skyrmions from instantons inside domain walls*, *Phys. Rev. Lett.* **95** (2005) 252003 [[hep-th/0508130](#)].
- [61] M. Eto, T. Fujimori, M. Nitta, K. Ohashi and N. Sakai, *Domain walls with non-Abelian clouds*, *Phys. Rev. D* **77** (2008) 125008 [[0802.3135](#)].
- [62] G. 't Hooft, *Magnetic Monopoles in Unified Gauge Theories*, *Nucl. Phys. B* **79** (1974) 276.
- [63] A. M. Polyakov, *Particle Spectrum in Quantum Field Theory*, *JETP Lett.* **20** (1974) 194.
- [64] D. Tong, *Monopoles in the higgs phase*, *Phys. Rev. D* **69** (2004) 065003 [[hep-th/0307302](#)].
- [65] M. Shifman and A. Yung, *NonAbelian string junctions as confined monopoles*, *Phys. Rev. D* **70** (2004) 045004 [[hep-th/0403149](#)].
- [66] A. Hanany and D. Tong, *Vortex strings and four-dimensional gauge dynamics*, *JHEP* **04** (2004) 066 [[hep-th/0403158](#)].
- [67] M. Nitta and W. Vinci, *Non-Abelian Monopoles in the Higgs Phase*, *Nucl. Phys. B* **848** (2011) 121 [[1012.4057](#)].
- [68] M. Eto, T. Fujimori, S. B. Gudnason, Y. Jiang, K. Konishi, M. Nitta et al., *Vortices and Monopoles in Mass-deformed SO and USp Gauge Theories*, *JHEP* **12** (2011) 017 [[1108.6124](#)].
- [69] M. Nitta, *Josephson instantons and Josephson monopoles in a non-Abelian Josephson junction*, *Phys. Rev. D* **92** (2015) 045010 [[1503.02060](#)].
- [70] J. Preskill and A. Vilenkin, *Decay of metastable topological defects*, *Phys. Rev. D* **47** (1993) 2324 [[hep-ph/9209210](#)].
- [71] P. M. Sutcliffe, *Sine-Gordon solitons from CP(1) instantons*, *Phys. Lett. B* **283** (1992) 85.
- [72] G. N. Stratopoulos and W. J. Zakrzewski, *Approximate Sine-Gordon solitons*, *Z. Phys. C* **59** (1993) 307.
- [73] A. E. Kudryavtsev, B. M. A. G. Piette and W. J. Zakrzewski, *Skyrmions and domain walls in (2+1)-dimensions*, *Nonlinearity* **11** (1998) 783 [[hep-th/9709187](#)].
- [74] P. Jennings and P. Sutcliffe, *The dynamics of domain wall Skyrmions*, *J. Phys. A* **46** (2013) 465401 [[1305.2869](#)].
- [75] V. Bychkov, M. Kreshchuk and E. Kurianovych, *Strings and skyrmions on domain walls*, *Int. J. Mod. Phys. A* **33** (2018) 1850111 [[1603.06310](#)].
- [76] M. Eto and M. Nitta, *Quantum nucleation of topological solitons*, *JHEP* **09** (2022) 077 [[2207.00211](#)].
- [77] J. Jaykka and M. Speight, *Easy plane baby skyrmions*, *Phys. Rev. D* **82** (2010) 125030 [[1010.2217](#)].
- [78] M. Kobayashi and M. Nitta, *Fractional vortex molecules and vortex polygons in a baby Skyrme model*, *Phys. Rev. D* **87** (2013) 125013 [[1307.0242](#)].
- [79] M. Kobayashi and M. Nitta, *Vortex polygons and their stabilities in Bose-Einstein condensates and field theory*, *J. Low Temp. Phys.* **175** (2014) 208 [[1307.1345](#)].
- [80] M. Eto, Y. Hamada, M. Kurachi and M. Nitta, *Dynamics of Nambu monopole in two Higgs doublet models. Cosmological Monopole Collider*, *JHEP* **07** (2020) 004 [[2003.08772](#)].

- [81] S. B. Gudnason and M. Nitta, *Incarnations of Skyrmions*, *Phys. Rev. D* **90** (2014) 085007 [[1407.7210](#)].
- [82] S. B. Gudnason and M. Nitta, *Skyrmions confined as beads on a vortex ring*, *Phys. Rev. D* **94** (2016) 025008 [[1606.00336](#)].
- [83] E. R. C. Abraham and P. K. Townsend, *Q kinks*, *Phys. Lett. B* **291** (1992) 85.
- [84] E. R. C. Abraham and P. K. Townsend, *More on Q kinks: A (1+1)-dimensional analog of dyons*, *Phys. Lett. B* **295** (1992) 225.
- [85] M. Arai, M. Naganuma, M. Nitta and N. Sakai, *Manifest supersymmetry for BPS walls in $N=2$ nonlinear sigma models*, *Nucl. Phys. B* **652** (2003) 35 [[hep-th/0211103](#)].
- [86] M. Arai, M. Naganuma, M. Nitta and N. Sakai, *BPS wall in $N=2$ SUSY nonlinear sigma model with Eguchi-Hanson manifold*, [hep-th/0302028](#).
- [87] M. Nitta, *Correspondence between Skyrmions in 2+1 and 3+1 Dimensions*, *Phys. Rev. D* **87** (2013) 025013 [[1210.2233](#)].
- [88] S. B. Gudnason and M. Nitta, *Domain wall Skyrmions*, *Phys. Rev. D* **89** (2014) 085022 [[1403.1245](#)].
- [89] A. E. Kudryavtsev, B. M. A. G. Piette and W. J. Zakrzewski, *On the interactions of skyrmions with domain walls*, *Phys. Rev. D* **61** (2000) 025016 [[hep-th/9907197](#)].
- [90] M. Eto, Y. Hamada, M. Kurachi and M. Nitta, *Topological Nambu monopole in two Higgs doublet models*, *Phys. Lett. B* **802** (2020) 135220 [[1904.09269](#)].
- [91] M. Eto, Y. Hamada and M. Nitta, *Topological structure of a Nambu monopole in two-Higgs-doublet models: Fiber bundle, Dirac's quantization, and a dyon*, *Phys. Rev. D* **102** (2020) 105018 [[2007.15587](#)].
- [92] M. Nitta, *Matryoshka Skyrmions*, *Nucl. Phys. B* **872** (2013) 62 [[1211.4916](#)].
- [93] B. J. Schroers, *Bogomolny solitons in a gauged $O(3)$ sigma model*, *Phys. Lett. B* **356** (1995) 291 [[hep-th/9506004](#)].
- [94] B. J. Schroers, *The Spectrum of Bogomol'nyi solitons in gauged linear sigma models*, *Nucl. Phys. B* **475** (1996) 440 [[hep-th/9603101](#)].
- [95] M. Nitta and W. Vinci, *Decomposing Instantons in Two Dimensions*, *J. Phys. A* **45** (2012) 175401 [[1108.5742](#)].
- [96] V. L. Berezinsky, *Destruction of long range order in one-dimensional and two-dimensional systems having a continuous symmetry group. I. Classical systems*, *Sov. Phys. JETP* **32** (1971) 493.
- [97] V. L. Berezinsky, *Destruction of long range order in one-dimensional and two-dimensional systems having a continuous symmetry group. II. Quantum systems*, *Sov. Phys. JETP* **34** (1972) 610.
- [98] J. M. Kosterlitz and D. J. Thouless, *Ordering, metastability and phase transitions in two-dimensional systems*, *J. Phys. C* **5** (1972) L124.
- [99] J. M. Kosterlitz and D. J. Thouless, *Ordering, metastability and phase transitions in two-dimensional systems*, *J. Phys. C* **6** (1973) 1181.
- [100] S. W. Hawking, I. G. Moss and J. M. Stewart, *Bubble Collisions in the Very Early Universe*, *Phys. Rev. D* **26** (1982) 2681.

- [101] A. M. Srivastava, *Numerical simulation of bubble collision and formation of vortices*, *Phys. Rev. D* **45** (1992) 3304.
- [102] A. M. Srivastava, *Numerical simulation of dynamical production of vortices by critical and subcritical bubbles*, *Phys. Rev. D* **46** (1992) 1353.
- [103] S. Chakravarty and A. M. Srivastava, *Vortex production in a first order phase transition at finite temperature*, *Nucl. Phys. B* **406** (1993) 795 [[hep-ph/9209246](#)].
- [104] E. J. Copeland and P. M. Saffin, *Bubble collisions in Abelian gauge theories and the geodesic rule*, *Phys. Rev. D* **54** (1996) 6088 [[hep-ph/9604231](#)].
- [105] J. P. Gauntlett, R. Portugues, D. Tong and P. K. Townsend, *D-brane solitons in supersymmetric sigma models*, *Phys. Rev. D* **63** (2001) 085002 [[hep-th/0008221](#)].
- [106] M. Shifman and A. Yung, *Domain walls and flux tubes in N=2 SQCD: D-brane prototypes*, *Phys. Rev. D* **67** (2003) 125007 [[hep-th/0212293](#)].
- [107] Y. Isozumi, M. Nitta, K. Ohashi and N. Sakai, *All exact solutions of a 1/4 Bogomol'nyi-Prasad-Sommerfield equation*, *Phys. Rev. D* **71** (2005) 065018 [[hep-th/0405129](#)].
- [108] M. Eto, T. Fujimori, T. Nagashima, M. Nitta, K. Ohashi and N. Sakai, *Dynamics of Strings between Walls*, *Phys. Rev. D* **79** (2009) 045015 [[0810.3495](#)].
- [109] R. Sato, F. Takahashi and M. Yamada, *Unified Origin of Axion and Monopole Dark Matter, and Solution to the Domain-wall Problem*, *Phys. Rev. D* **98** (2018) 043535 [[1805.10533](#)].
- [110] C. Chatterjee, T. Higaki and M. Nitta, *Note on a solution to domain wall problem with the Lazarides-Shafi mechanism in axion dark matter models*, *Phys. Rev. D* **101** (2020) 075026 [[1903.11753](#)].
- [111] G. Lazarides and Q. Shafi, *Axion Models with No Domain Wall Problem*, *Phys. Lett. B* **115** (1982) 21.
- [112] G. R. Dvali and G. Senjanovic, *Topologically stable electroweak flux tubes*, *Phys. Rev. Lett.* **71** (1993) 2376 [[hep-ph/9305278](#)].
- [113] M. Eto, M. Kurachi and M. Nitta, *Constraints on two Higgs doublet models from domain walls*, *Phys. Lett. B* **785** (2018) 447 [[1803.04662](#)].
- [114] M. Eto, M. Kurachi and M. Nitta, *Non-Abelian strings and domain walls in two Higgs doublet models*, *JHEP* **08** (2018) 195 [[1805.07015](#)].
- [115] M. Eto, Y. Hamada and M. Nitta, *Stable Z-strings with topological polarization in two Higgs doublet model*, **2111.13345**.
- [116] M. Eto, E. Nakano and M. Nitta, *Non-Abelian Global Vortices*, *Nucl. Phys. B* **821** (2009) 129 [[0903.1528](#)].
- [117] A. P. Balachandran and S. Dikal, *Topological string defect formation during the chiral phase transition*, *Int. J. Mod. Phys. A* **17** (2002) 1149 [[hep-ph/0108086](#)].
- [118] A. P. Balachandran and S. Dikal, *NonAbelian topological strings and metastable states in linear sigma model*, *Phys. Rev. D* **66** (2002) 034018 [[hep-ph/0204262](#)].
- [119] M. Eto, Y. Hirono and M. Nitta, *Domain Walls and Vortices in Chiral Symmetry Breaking*, *PTEP* **2014** (2014) 033B01 [[1309.4559](#)].

- [120] M. G. Alford, A. Schmitt, K. Rajagopal and T. Schäfer, *Color superconductivity in dense quark matter*, *Rev. Mod. Phys.* **80** (2008) 1455 [[0709.4635](#)].
- [121] A. P. Balachandran, S. Digal and T. Matsuura, *Semi-superfluid strings in high density QCD*, *Phys. Rev. D* **73** (2006) 074009 [[hep-ph/0509276](#)].
- [122] E. Nakano, M. Nitta and T. Matsuura, *Non-Abelian strings in high density QCD: Zero modes and interactions*, *Phys. Rev. D* **78** (2008) 045002 [[0708.4096](#)].
- [123] M. Eto and M. Nitta, *Color Magnetic Flux Tubes in Dense QCD*, *Phys. Rev. D* **80** (2009) 125007 [[0907.1278](#)].
- [124] M. Eto, M. Nitta and N. Yamamoto, *Instabilities of Non-Abelian Vortices in Dense QCD*, *Phys. Rev. Lett.* **104** (2010) 161601 [[0912.1352](#)].
- [125] M. Eto and M. Nitta, *Chiral non-Abelian vortices and their confinement in three flavor dense QCD*, *Phys. Rev. D* **104** (2021) 094052 [[2103.13011](#)].
- [126] A. Ritz, M. Shifman and A. Vainshtein, *Enhanced worldvolume supersymmetry and intersecting domain walls in $N=1$ SQCD*, *Phys. Rev. D* **70** (2004) 095003 [[hep-th/0405175](#)].
- [127] M. Eto, Y. Isozumi, M. Nitta and K. Ohashi, *$1/2$, $1/4$ and $1/8$ BPS equations in SUSY Yang-Mills-Higgs systems: Field theoretical brane configurations*, *Nucl. Phys. B* **752** (2006) 140 [[hep-th/0506257](#)].
- [128] S. Bolognesi, *Strings inside walls in $N=1$ super Yang-Mills*, *J. Phys. A* **42** (2009) 195404 [[0710.5198](#)].
- [129] J. P. Gauntlett, D. Tong and P. K. Townsend, *Multidomain walls in massive supersymmetric sigma models*, *Phys. Rev. D* **64** (2001) 025010 [[hep-th/0012178](#)].
- [130] D. Tong, *The Moduli space of BPS domain walls*, *Phys. Rev. D* **66** (2002) 025013 [[hep-th/0202012](#)].
- [131] Y. Isozumi, M. Nitta, K. Ohashi and N. Sakai, *Construction of non-Abelian walls and their complete moduli space*, *Phys. Rev. Lett.* **93** (2004) 161601 [[hep-th/0404198](#)].
- [132] Y. Isozumi, M. Nitta, K. Ohashi and N. Sakai, *Non-Abelian walls in supersymmetric gauge theories*, *Phys. Rev. D* **70** (2004) 125014 [[hep-th/0405194](#)].
- [133] M. Eto, Y. Isozumi, M. Nitta, K. Ohashi, K. Ohta and N. Sakai, *D-brane construction for non-Abelian walls*, *Phys. Rev. D* **71** (2005) 125006 [[hep-th/0412024](#)].
- [134] C. W. Chen, *Magnetism and metallurgy of soft magnetic materials*. Dover Pubns, 1977.
- [135] A. P. Malozemoff and J. C. Slonczewski, *Magnetic domain walls in bubble materials*. 1979.
- [136] D. T. Son and M. A. Stephanov, *Domain walls in two-component Bose-Einstein condensates*, *Phys. Rev. A* **65** (2002) 063621 [[cond-mat/0103451](#)].
- [137] K. Kasamatsu, M. Tsubota and M. Ueda, *Vortex molecules in coherently coupled two-component Bose-Einstein condensates*, *Phys. Rev. Lett.* **93** (2004) 250406 [[cond-mat/0406150](#)].
- [138] K. Kasamatsu, M. Tsubota and M. Ueda, *Vortices in multicomponent Bose-Einstein condensates*, *Int. J. Mod. Phys. B* **19** (2005) 1835 [[cond-mat/0505546](#)].
- [139] M. Cipriani and M. Nitta, *Crossover between integer and fractional vortex lattices in*

- coherently coupled two-component Bose-Einstein condensates*, *Phys. Rev. Lett.* **111** (2013) 170401 [[1303.2592](#)].
- [140] M. Tylutki, L. P. Pitaevskii, A. Recati and S. Stringari, *Confinement and precession of vortex pairs in coherently coupled Bose-Einstein condensates*, *Phys. Rev. A* **93** (2016) 043623 [[1601.03695](#)].
- [141] M. Eto and M. Nitta, *Confinement of half-quantized vortices in coherently coupled Bose-Einstein condensates: Simulating quark confinement in a QCD-like theory*, *Phys. Rev. A* **97** (2018) 023613 [[1702.04892](#)].
- [142] M. Kobayashi, M. Eto and M. Nitta, *Berezinskii-Kosterlitz-Thouless Transition of Two-Component Bose Mixtures with Intercomponent Josephson Coupling*, *Phys. Rev. Lett.* **123** (2019) 075303 [[1802.08763](#)].
- [143] M. Eto, K. Ikeno and M. Nitta, *Collision dynamics and reactions of fractional vortex molecules in coherently coupled Bose-Einstein condensates*, *Phys. Rev. Res.* **2** (2020) 033373 [[1912.09014](#)].
- [144] E. Babaev, *Vortices carrying an arbitrary fraction of magnetic flux quantum in two gap superconductors*, *Phys. Rev. Lett.* **89** (2002) 067001 [[cond-mat/0111192](#)].
- [145] J. Goryo, S. Soma and H. Matsukawa, *Deconfinement of vortices with continuously variable fractions of the unit flux quanta in two-gap superconductors*, *Europhysics Letters* **80** (2007) 17002.
- [146] A. Crisan, Y. Tanaka, D. D. Shivagan, A. Iyo, L. Cosereanu, K. Tokiwa et al., *Anomalous ac susceptibility response of $(\text{Cu,C})\text{Ba}_2\text{Ca}_2\text{Cu}_3\text{O}_y$: Experimental indication of two-component vortex matter in multi-layered cuprate superconductors*, *Japanese Journal of Applied Physics* **46** (2007) L451.
- [147] Y. Tanaka, A. Crisan, D. D. Shivagan, A. Iyo, K. Tokiwa and T. Watanabe, *Interpretation of abnormal ac loss peak based on vortex-molecule model for a multicomponent cuprate superconductor*, *Japanese Journal of Applied Physics* **46** (2007) 134.
- [148] A. Crisan, A. Iyo, Y. Tanaka, H. Matsuhata, D. D. Shivagan, P. M. Shirage et al., *Magnetically coupled pancake vortex molecules in $\text{HgBa}_2\text{Ca}_{n-1}\text{Cu}_n\text{O}_y$ ($n \geq 6$)*, *Phys. Rev. B* **77** (2008) 144518.
- [149] Y. Tanaka, H. Yamamori, T. Yanagisawa, T. Nishio and S. Arisawa, *Voltage-less alternating current (ac) josephson effect in two-band superconductors*, *Physica C: Superconductivity and its Applications* **538** (2017) 6.
- [150] M. Eto and M. Nitta, *Vortex trimer in three-component Bose-Einstein condensates*, *Phys. Rev. A* **85** (2012) 053645 [[1201.0343](#)].
- [151] M. Eto and M. Nitta, *Vortex graphs as N -omers and $CP(N-1)$ Skyrmions in N -component Bose-Einstein condensates*, *EPL* **103** (2013) 60006 [[1303.6048](#)].
- [152] M. Nitta, M. Eto, T. Fujimori and K. Ohashi, *Baryonic Bound State of Vortices in Multicomponent Superconductors*, *J. Phys. Soc. Jap.* **81** (2012) 084711 [[1011.2552](#)].
- [153] C. Chatterjee, S. B. Gudnason and M. Nitta, *Chemical bonds of two vortex species with a generalized Josephson term and arbitrary charges*, *JHEP* **04** (2020) 109 [[1912.02685](#)].
- [154] M. Sigrist and D. F. Agterberg, *The role of domain walls on the vortex creep dynamics in unconventional superconductors*, *Progress of Theoretical Physics* **102** (1999) 965–981.

- [155] S. B. Etter, W. Huang and M. Sigrist, *Half-quantum vortices on c-axis domain walls in chiral p-wave superconductors*, *New Journal of Physics* **22** (2020) 093038.
- [156] J. Garaud and E. Babaev, *Skyrmionic state and stable half-quantum vortices in chiral p-wave superconductors*, *Phys. Rev. B* **86** (2012) 060514.
- [157] J. Garaud and E. Babaev, *Properties of skyrmions and multi-quanta vortices in chiral p-wave superconductors*, *Scientific Reports* **5** (2015) 17540.
- [158] Y. Masaki, T. Mizushima and M. Nitta, *Non-Abelian Half-Quantum Vortices in 3P_2 Topological Superfluids*, [2107.02448](#).
- [159] M. Kobayashi and M. Nitta, *Core structures of vortices in Ginzburg-Landau theory for neutron 3P_2 superfluids*, *Phys. Rev. C* **105** (2022) 035807 [[2203.09300](#)].
- [160] M. Kobayashi and M. Nitta, *Proximity effects of vortices in neutron $3P_2$ superfluids in neutron stars: Vortex core transitions and covalent bonding of vortex molecules*, *Phys. Rev. C* **107** (2023) 045801 [[2209.07205](#)].
- [161] S. Autti, V. V. Dmitriev, J. T. Mäkinen, A. A. Soldatov, G. E. Volovik, A. N. Yudin et al., *Observation of half-quantum vortices in topological superfluid ^3He* , *Phys. Rev. Lett.* **117** (2016) 255301.
- [162] J. T. Makinen, K. Zhang and V. B. Eltsov, *Vortex-bound solitons in topological superfluid ^3He* , *Journal of Physics Condensed Matter* .
- [163] J. C. Pati and A. Salam, *Lepton Number as the Fourth Color*, *Phys. Rev. D* **10** (1974) 275.
- [164] C. Chatterjee, M. Kurachi and M. Nitta, *Topological Defects in the Georgi-Machacek Model*, *Phys. Rev. D* **97** (2018) 115010 [[1801.10469](#)].
- [165] C. Chatterjee and M. Nitta, *Aharonov-Bohm defects*, *Phys. Rev. D* **101** (2020) 085002 [[1905.01884](#)].
- [166] M. Nitta, *Confinement and moduli locking of Alice strings and monopoles*, *JHEP* **03** (2021) 276 [[2011.14396](#)].
- [167] C. Chatterjee and M. Nitta, *BPS Alice strings*, *JHEP* **09** (2017) 046 [[1703.08971](#)].
- [168] C. Chatterjee and M. Nitta, *The effective action of a BPS Alice string*, *Eur. Phys. J. C* **77** (2017) 809 [[1706.10212](#)].
- [169] Y. Fujimoto and M. Nitta, *Non-Abelian Alice strings in two-flavor dense QCD*, *Phys. Rev. D* **103** (2021) 054002 [[2011.09947](#)].
- [170] Y. Fujimoto and M. Nitta, *Vortices penetrating two-flavor quark-hadron continuity*, *Phys. Rev. D* **103** (2021) 114003 [[2102.12928](#)].
- [171] Y. Fujimoto and M. Nitta, *Topological confinement of vortices in two-flavor dense QCD*, *JHEP* **09** (2021) 192 [[2103.15185](#)].
- [172] D. B. Carpenter and J. T. Chalker, *The phase diagram of a generalised xy model*, *Journal of Physics: Condensed Matter* **1** (1989) 4907.
- [173] M. Kobayashi, G. Fejős, C. Chatterjee and M. Nitta, *Vortex confinement transitions in the modified Goldstone model*, *Phys. Rev. Res.* **2** (2020) 013081 [[1908.11087](#)].
- [174] M. Kobayashi and M. Nitta, *\mathbb{Z}_n modified XY and Goldstone models and vortex confinement transition*, *Phys. Rev. D* **101** (2020) 085003 [[1912.09456](#)].

- [175] M. Eto, Y. Isozumi, M. Nitta, K. Ohashi and N. Sakai, *Instantons in the Higgs phase*, *Phys. Rev. D* **72** (2005) 025011 [[hep-th/0412048](#)].
- [176] T. Fujimori, M. Nitta, K. Ohta, N. Sakai and M. Yamazaki, *Intersecting Solitons, Amoeba and Tropical Geometry*, *Phys. Rev. D* **78** (2008) 105004 [[0805.1194](#)].
- [177] J. Scherk and J. H. Schwarz, *How to Get Masses from Extra Dimensions*, *Nucl. Phys. B* **153** (1979) 61.
- [178] S. B. Gudnason and M. Nitta, *Baryonic torii: Toroidal baryons in a generalized Skyrme model*, *Phys. Rev. D* **91** (2015) 045027 [[1410.8407](#)].
- [179] M. Nitta, *Fractional instantons and bions in the principal chiral model on $\mathbb{R}^2 \times S^1$ with twisted boundary conditions*, *JHEP* **08** (2015) 063 [[1503.06336](#)].
- [180] Y. Nambu, *Strings, Monopoles and Gauge Fields*, *Phys. Rev. D* **10** (1974) 4262.
- [181] S. Mandelstam, *Vortices and Quark Confinement in Nonabelian Gauge Theories*, *Phys. Lett. B* **53** (1975) 476.
- [182] S. Mandelstam, *Vortices and Quark Confinement in Nonabelian Gauge Theories*, *Phys. Rept.* **23** (1976) 245.
- [183] R. Auzzi, S. Bolognesi, J. Evslin and K. Konishi, *NonAbelian monopoles and the vortices that confine them*, *Nucl. Phys. B* **686** (2004) 119 [[hep-th/0312233](#)].
- [184] R. Auzzi, S. Bolognesi and J. Evslin, *Monopoles can be confined by 0, 1 or 2 vortices*, *JHEP* **02** (2005) 046 [[hep-th/0411074](#)].
- [185] M. Eto, L. Ferretti, K. Konishi, G. Marmorini, M. Nitta, K. Ohashi et al., *Non-Abelian duality from vortex moduli: A Dual model of color-confinement*, *Nucl. Phys. B* **780** (2007) 161 [[hep-th/0611313](#)].
- [186] M. Cipriani, D. Dorigoni, S. B. Gudnason, K. Konishi and A. Michelini, *Non-Abelian monopole-vortex complex*, *Phys. Rev. D* **84** (2011) 045024 [[1106.4214](#)].
- [187] C. Chatterjee and K. Konishi, *Monopole-vortex complex at large distances and nonAbelian duality*, *JHEP* **09** (2014) 039 [[1406.5639](#)].
- [188] A. Gorsky, M. Shifman and A. Yung, *Confined Magnetic Monopoles in Dense QCD*, *Phys. Rev. D* **83** (2011) 085027 [[1101.1120](#)].
- [189] M. Eto, M. Nitta and N. Yamamoto, *Confined Monopoles Induced by Quantum Effects in Dense QCD*, *Phys. Rev. D* **83** (2011) 085005 [[1101.2574](#)].
- [190] C. P. Dokos and T. N. Tomaras, *Monopoles and Dyons in the SU(5) Model*, *Phys. Rev. D* **21** (1980) 2940.
- [191] G. Lazarides and Q. Shafi, *The Fate of Primordial Magnetic Monopoles*, *Phys. Lett.* **94B** (1980) 149.
- [192] J. Preskill, *Cosmological Production of Superheavy Magnetic Monopoles*, *Phys. Rev. Lett.* **43** (1979) 1365.
- [193] P. Langacker and S.-Y. Pi, *Magnetic Monopoles in Grand Unified Theories*, *Phys. Rev. Lett.* **45** (1980) 1.
- [194] M. Hindmarsh and T. W. B. Kibble, *BEADS ON STRINGS*, *Phys. Rev. Lett.* **55** (1985) 2398.

- [195] Y. Ng, T. W. B. Kibble and T. Vachaspati, *Formation of Non-Abelian Monopoles Connected by Strings*, *Phys. Rev. D* **78** (2008) 046001 [[0806.0155](#)].
- [196] T. W. B. Kibble and T. Vachaspati, *Monopoles on strings*, *J. Phys. G* **42** (2015) 094002 [[1506.02022](#)].
- [197] M. Hindmarsh, K. Rummukainen and D. J. Weir, *Numerical simulations of necklaces in $SU(2)$ gauge-Higgs field theory*, *Phys. Rev. D* **95** (2017) 063520 [[1611.08456](#)].
- [198] T. Hiramatsu, M. Ibe, M. Suzuki and S. Yamaguchi, *Gauge kinetic mixing and dark topological defects*, *JHEP* **12** (2021) 122 [[2109.12771](#)].
- [199] A. Chitose and M. Ibe, *More on Dark Topological Defects*, [2303.10861](#).
- [200] B. Kleihaus, J. Kunz and Y. Shnir, *Monopole anti-monopole chains*, *Phys. Lett. B* **570** (2003) 237 [[hep-th/0307110](#)].
- [201] B. Kleihaus, J. Kunz and Y. Shnir, *Monopoles, antimonopoles and vortex rings*, *Phys. Rev. D* **68** (2003) 101701 [[hep-th/0307215](#)].
- [202] P. Ackerman and I. Smalyukh, *Diversity of knot solitons in liquid crystals manifested by linking of preimages in torons and hopfions*, *Phys. Rev. X* **7** (2017) 011006.
- [203] Y. Nambu, *String-Like Configurations in the Weinberg-Salam Theory*, *Nucl. Phys. B* **130** (1977) 505.
- [204] A. Achucarro and T. Vachaspati, *Semilocal and electroweak strings*, *Phys. Rept.* **327** (2000) 347 [[hep-ph/9904229](#)].
- [205] M. Eto, K. Konishi, M. Nitta and Y. Ookouchi, *Brane Realization of Nambu Monopoles and Electroweak Strings*, *Phys. Rev. D* **87** (2013) 045006 [[1211.2971](#)].
- [206] G. R. Dvali, H. Liu and T. Vachaspati, *Sweeping away the monopole problem*, *Phys. Rev. Lett.* **80** (1998) 2281 [[hep-ph/9710301](#)].
- [207] L. Pogosian and T. Vachaspati, *Interaction of magnetic monopoles and domain walls*, *Phys. Rev. D* **62** (2000) 105005 [[hep-ph/9909543](#)].
- [208] M. Brush, L. Pogosian and T. Vachaspati, *Magnetic monopole—domain wall collisions*, *Phys. Rev. D* **92** (2015) 045008 [[1505.08170](#)].
- [209] M. Nitta, *Incarnations of Instantons*, *Nucl. Phys. B* **885** (2014) 493 [[1311.2718](#)].
- [210] N. S. Manton, *A Remark on the Scattering of BPS Monopoles*, *Phys. Lett. B* **110** (1982) 54.
- [211] M. Eto, Y. Isozumi, M. Nitta, K. Ohashi and N. Sakai, *Manifestly supersymmetric effective Lagrangians on BPS solitons*, *Phys. Rev. D* **73** (2006) 125008 [[hep-th/0602289](#)].